ABSTRACT

Title of Thesis: EFFECTS OF SEA LEVEL RISE ON TIDAL MARSHES

Jennifer Holly Bryan, Master of Science, 2014

Thesis directed by: Assistant Professor Lora Harris
University of Maryland Center for Environmental Science

There is growing concern regarding the potentially negative impacts of sea level rise (SLR) on tidal wetlands in the Mid-Atlantic region of the United States. In Chapter one, I investigate the phenotypic plasticity and biomechanical properties of *Zizania aquatica* under experimental inundation treatments. At lower elevations and higher inundation designed to simulate SLR, *Zizania aquatica* did indeed respond with phenotypic changes such as increased height and stem thickness, and decreased stem density, areal aboveground biomass, and modulus of elasticity.

In Chapter two, I investigate the nitrogen removal role of Chesapeake Bay tidal wetlands under current and simulated long-term SLR. I also examine nitrogen removal at smaller scales in Maryland, comparing restoration goals for nitrogen loading reductions with the loss of nitrogen removal services expected by 2025. Tidal wetlands are expected to decrease in the Bay and Maryland and associated loss of nitrogen removal services may affect attainment of restoration goals.

EFFECTS OF SEA LEVEL RISE ON TIDAL MARSHES

by

Jennifer Holly Bryan

Thesis submitted to the Faculty of the Graduate School of the
University of Maryland, College Park in partial fulfillment
of the requirements for the degree of
Master of Science
2014

Advisory Committee:

Assistant Professor Lora Harris, Chair
Associate Professor Andrew Baldwin
Professor Michael Kemp
Assistant Professor Nathaniel B. Weston

PREFACE

Chapter one is a complete manuscript, which will be submitted shortly to Estuaries and Coasts with co-authors Dr. Lora Harris and Dr. Nathaniel Weston. Chapter two is a contribution to a larger collaborative effort in which we investigate changes in Chesapeake Bay tidal marshes due to long-term SLR and the impact of these changes on nitrogen, carbon, and phosphorus removal services. Collaborators will build upon my Chesapeake Bay SLR and nitrogen removal analyses to expand the study beyond nitrogen.

To Chris and Sophie

ACKNOWLEGEMENTS

This thesis would not have been possible without the support of many people. Many thanks to my advisor, Dr. Lora Harris, who read through my numerous revisions, provided much needed reality checks and was always there to offer encouragement and assistance. Also, thanks to my committee members, Dr. Andrew Baldwin, Dr. Michael Kemp, and Dr. Nathaniel Weston who offered guidance and support. I would particularly like to thank Dr. Weston, who provided me with the opportunity to conduct my thesis research at his long-term research site. Thanks to University of Maryland, Maryland Sea Grant, and the National Estuarine Research Reserve, without which I would not have had the financial means to complete my thesis. I am also grateful to the Harris Lab and volunteers who provided essential help in the marsh during long, hot summer days. And, finally, thanks to my husband and daughter who endured this long process with me, always offering support and love.

TABLE OF CONTENTS

CHAPTER 1:
MORPHOLOGICAL CHANGES AND BIOMECHANICAL PROPERTIES OF ZIZANIA AQUATICA UNDER EXPERIMENTAL INUNDATION TREATMENTS

ABSTRACT

Data documenting the effect of sea level rise on tidal fresh and oligohaline marshes are scarce. A theory has been developed from studies in salt marsh ecosystems that a dynamic equilibrium between vegetation and sediment capture enables many marsh platforms to respond and adjust to current rates of rise. However, these hypotheses have not been tested in freshwater tidal ecosystems. Here, I present results from experiments manipulating inundation regimes for an annual grass species, *Zizania aquatica* in an oligohaline marsh. Tested hypotheses focus on the phenotypic plasticity and biomechanical properties of *Z. aquatica* experiencing increasing tidal inundation. *Zizania aquatica* responded to increased inundation treatments with phenotypic change such as increased stem height and diameter, and decreased stem density, areal aboveground biomass, and modulus of elasticity. This work evaluates whether conceptual models regarding the plasticity of vegetation measured in salt marshes apply to freshwater communities. These preliminary data suggest oligohaline and tidal fresh marshes will have very different responses to sea level rise when compared to salt marshes.

INTRODUCTION

Tidal marshes provide important ecosystem services such as flood mitigation, nutrient cycling, sediment trapping, carbon sequestration, and wildlife habitat (Barbier et al. 2011). Potential consequences of accelerated sea level rise, such as changes in plant community structure, reduced diversity and species richness, and an overall loss of coastal wetlands, has raised concerns about how coastal wetlands will respond to accelerated sea level rise. The global average rate of sea level rise is about 1.7 mm yr^{-1} (Titus et al. 2009), which is anticipated to accelerate and cause increased inundation of low elevation tidal plant communities (Morris 2007a). Prolonged inundation, either by frequency or duration, can be harmful to plant diversity. Baldwin et al. (2001) demonstrated that 3 to 10 cm of flooding negatively affected seedling recruitment and growth for many tidal freshwater marsh plant species and lowered overall diversity.

Tidal fresh and oligohaline wetlands are characterized by periodic inundation by low salinity (0-5) water as a result of tides. Conversely, salt marshes have an annual salinity range of 18-30 (Odum 1988). Low salinity tidal fresh and oligohaline marshes support a diverse plant community, often with multiple dominant species of annuals and perennials (Odum 1988). This may enable greater resilience to sea level rise in tidal fresh marshes, because multiple species may be able to fill the same niche. Conversely, salt marshes tend to have low plant species diversity, and the low marsh is typically dominated by a single species, *Spartina alterniflora*, which is adapted to high salt stress (Odum 1988). High rates of net primary production and greater allocation of resources to

aboveground biomass production is common in tidal fresh and oligohaline marshes (Odum 1988). In contrast, salt marshes tend to have lower net primary production and allocate more resources to belowground biomass production and mechanisms of avoidance and adaptation, such as processes of exclusion and extrusion of salts and toxins (e.g. sulfide; Odum 1988).

Decomposition rates are high in tidal fresh marshes because the plants have high nitrogen content and are composed of more labile materials (Odum 1988). Therefore, tidal fresh marshes are more likely to require large amounts of inorganic sediments for marsh vertical accretion with increasing rates of sea level rise, since low marsh annual vegetation allocates more energy to aboveground biomass production and peat accumulation is low due to high decomposition rates. Fortunately, these marshes are typically not limited by sediment supply due to their proximity to sediment sources (Pasternack and Brush 2001). In contrast, salt marshes have low decomposition rates, and, consequently, high rates of peat accumulation, since the plants have lower nitrogen content and more recalcitrant materials, such as lignin and cellulose (Odum 1988). Salt marshes are more dependent upon in-situ organic sediment supplies such as plant litter and belowground biomass production for vertical sediment accretion. Furthermore, salt marshes are likely to be inorganic sediment supply limited, since they are nearby marine sediments with low organic carbon content (Odum 1988).

There is growing concern about how accelerated sea level rise will affect tidal wetland communities in general and how the effects will vary between salt and tidal fresh wetland systems. Vegetation influences marsh hydrodynamics,

which in turn influences sedimentation. Morris et al. (2002) proposed that tidal wetland vegetation has evolved to withstand hydrodynamic forces while creating physical structure that influences sediment capture and marsh platform accretion, thereby shifting marsh elevation toward a dynamic equilibrium with mean sea level. In salt marshes, the dominant marsh grass is *Spartina alterniflora*, which generally exists at elevations supraoptimal to plant growth, such that increased flooding results in an increase in productivity (Morris et al. 2002). Plant biomass, density, height, and structure influence wave and current attenuation in salt marsh plant canopies (Leonard et al. 1995b). Emergent plant vegetation causes water velocity patterns that vary inversely with canopy drag (Yang 1998, Lightbody and Nepf 2006). Bottom current velocity also decreases when stems are present, which in turn contributes to sedimentation by diminishing particle resuspension and increasing particle capture by vegetation (López and Garcia 1998).

In salt marshes, sedimentation rates positively correlate with marsh plant community density and productivity (Morris et al. 2002). Indeed, the water flooding marshes contains less suspended sediment than water overlying open mud flats (Yang 1998). Salt marshes studied by Morris et al. (2002) have shown higher annual growth during periods of high sea level. Increased inundation in salt marshes results in increased plant production and provides greater opportunity for the marsh to accrete sediment vertically and move toward a dynamic equilibrium between marsh accretion and sea level. However, beyond a certain, unknown, rate of sea level rise, the marsh may be unable to accrete sufficiently to keep pace with rising water (Warren and Niering 1993, Kirwan and Temmerman 2009). This

disconnect, between the rate of sea level rise and sedimentation, may result in the conversion of tidal marsh to open water (Morris et al. 2002, Kirwan et al. 2010b). Marshes receiving high concentrations of suspended sediments are better able to increase marsh surface elevation and maintain stability against increasing sea level rise than are marshes with low suspended sediment concentrations (Morris et al. 2002, Kirwan et al. 2010a).

High stem density can increase sedimentation processes (Leonard et al. 1995a); however, morphological changes may occur in tandem with higher densities that can impede this process (Harley and Bertness 1996). For instance, Harley and Bertness (1996) found crowded plants allocated more growth to aboveground biomass, growing taller and thinner, in an effort to better compete for light with their close neighbors. As a result, the crowded plants grew closer to their maximum critical height and, consequently, had a tendency to break more easily (Harley and Bertness 1996). The study of plant biomechanical properties, as pioneered by Niklas (1991, 1992, 1994), has yielded several valuable morphological indicators in plants that are hallmarks of phenotypic plasticity. For example, the ratio of the critical buckling height of a plant, or the maximum height a plant can reach prior to failing under its own weight, to actual height is a measure of the factor of safety, or the structural capacity of a plant to withstand forces (e.g. wind, current, etc.; Niklas 1994). In the same experiment, Harley and Bertness (1996) evaluated the plastic response of plants in plots they had thinned to reduce competition with neighbors. They found plants in the thinned plots responded with thicker stems, a feature the authors hypothesized provided added

stability in the water column (Harley and Bertness 1996). Indeed, many plants respond plastically to the surrounding environment; however, there is often a cost associated with this phenotypic plasticity (Anten et al. 2005). The plant must allocate a disproportionate amount of resources to the phenotypic change that is necessary to survive in the surrounding environment (Niklas 1992, Anten 2005), such as more resources allocated to stem height at the expense of stem stability.

Tidal fresh and oligohaline marshes have not been studied as extensively as salt marshes; much less is known about whether similar feedbacks among inundation, sediment capture, and plant structure apply to these ecosystems. To begin to evaluate these feedbacks, I chose an annual grass species, *Zizania aquatica* var. *aquatica* (southern wild rice), which is common in the low marsh zone of tidal fresh and oligohaline marshes in the mid-Atlantic region. *Zizania aquatica* germination begins in late April and flowering occurs from mid-July through early September, with most seed dispersal occurring in late August by wind and rainstorms (Whigham and Simpson 1977). Baldwin et al. (2001) suggested that increased water levels and decreased sediment supply may cause reduced survival in species that reproduce by seedling recruitment. As a low marsh annual that colonizes the marsh platform via seedling recruitment, *Z. aquatica* may be at greater risk from relative sea level rise; the rate of which is approximately 3.5 mm yr^{-1} in the mid-Atlantic region, which is higher than the global average (Titus et al. 2009). Whigham and Simpson (1977) found *Z. aquatica* allocates more resources to belowground biomass during its seedling phase, but, over the life cycle of this plant, more resources go toward

aboveground biomass. As a result, plants stems may become top heavy and suffer greater mortality during summer storms (Whigham and Simpson 1977). *Zizania aquatica* may be at greater risk of stem failure under sea level rise as indicated by changes in mechanical properties such as the modulus of elasticity (a measure of stem stiffness or resistance to deformation; Niklas 1991, 1994).

I evaluated the phenotypic response of *Z. aquatica* under experimental inundation treatments to determine whether feedbacks between vegetation and inundation are similar to those found in salt marshes. Findings from these experiments inform our understanding of the potential vulnerability of tidal fresh and oligohaline wetlands to increasing sea level rise. I investigated plant phenotypic response of *Z. aquatica* to increased inundation to determine whether *Z. aquatica* will have increased productivity, accompanied by changes in density, height, diameter, and modulus of elasticity. In particular, I expected that *Z. aquatica* experiencing increased inundation would respond with increased productivity, as was seen with *S. alterniflora* salt marshes (Morris et al. 2002). This change in production was expected to accompany an increase in stem density (shoots per meter squared) and stem height and a decrease in stem diameter and modulus of elasticity.

METHODS

Study Site and Experimental Design:

I conducted experiments in a marsh located along the upper Delaware River near Salem, New Jersey, USA (Figure 1). Vegetation at the site is dominated by a nearly monotypic stand of *Z. aquatica*. The site is oligohaline, with an average salinity of about 2.2. The mean tidal range at the portion of the river near the study site is about 1.7 meters (NOAA 2014).

I conducted the experiment using a single "marsh organ", modified from an earlier design developed by Morris (2004) that has been used extensively in studies of wetland inundation (Kirwan and Guntenspergen 2012, Kirwan et al. 2012, Langley et al. 2013, Morris 2007b). This modified marsh organ is a large wooden structure consisting of steps, with each step representing a different elevation (Figure 2). The purpose of the marsh organ is to assess the phenotypic response of vegetation exposed to increasing inundation, a proxy for sea level rise, which was sampled in June and August 2012 and July 2013. This has been an active research site with a *Z. aquatica* marsh organ present since 2010; however, the focus of this work is on data collected during 2012. The marsh organ contains five steps, each holding 4-5 five-gallon buckets (replicates) filled with intact sediment cores taken from the adjacent marsh in 2010 (Figure 3). There was a 10 cm difference between each step. Vegetation from the native seed bank contained in the intact sediment cores was allowed to naturally colonize the buckets. Consequently, *Z. aquatica* exclusively colonized and regenerated throughout the experiment from the marsh sediment cores in the marsh organ

buckets. In the experiment, the lowest elevation was most inundated and, conversely, the highest elevation was least inundated. The second highest elevation best represented elevations where *Z. aquatica* grows in the adjacent marsh.

Water level data loggers (Schumberger CTD diver) recorded water depth as a measure of inundation at the marsh organ. The logger was fastened to a pole in the creek next to the marsh organ at 0.3 meters below the lowest marsh organ step. The logger data for the marsh organ was georeferenced using a Real Time Kinematic GPS to the North American Vertical Datum (NAVD) to determine the flooding depth for each elevation on the organ and all depth data were corrected to total depth.

Biomass:

In order to evaluate the productivity of *Z. aquatica* in response to increasing inundation, I destructively harvested *Z. aquatica* from the adjacent marsh to develop a regression equation with stem length, with which I estimated biomass in the marsh organ at each sampling event. Plant stems were cut at the sediment surface and morphological measurements were taken prior to placing the plants in labeled brown paper bags for drying. All biomass samples were dried to constant weight in a drying oven at 60^{o}C. I developed an equation (Eq. 1, R^2 = 0.67) based upon these destructively harvested data (Figure 4) to estimate plant weight in the marsh organ for each sampling event based upon measured plant height.

$$\text{Weight} = 2.16*10^{-4}\,(\text{Height})^2 - 4.47*10^{-3}\,(\text{Height}) - 8.86*10^{-1} \qquad \text{Eq.1}$$

The marsh organ was visited on two occasions during the summer of 2012 in order to collect morphology and density measurements. Aboveground biomass could not be harvested directly from the marsh organ during the growing season, as this would have altered the ongoing density and morphological measurements. Additionally, aboveground biomass was not harvested at the end of the growing season as this experiment was conducted in tandem with another research study at the marsh organ. As a result, aboveground biomass was estimated for each sampling event, using Equation 1. Aboveground biomass was estimated for each experimental unit (i.e. bucket) by substituting the average stem length for "height" in Equation 1, which was then averaged for each inundation step. These mean values were then normalized to the bucket area (i.e. 0.07 m^2) and the stem density for each bucket, to compute biomass as grams dry weight per square meter.

Morphology:

To adequately describe the morphological response of *Z. aquatica* to changed inundation in the marsh organ experiment, I took marsh organ measurements and collected *Z. aquatica* samples from the adjacent marsh on June 21, 2012 and August 6, 2012, following the protocol described by Morris (2007b). During these sampling events, I counted the number of stems in each bucket and took morphological measurements (e.g. stem height and diameter). Plant height (cm) was measured using a Lufkin Red End folding two-meter stick, and basal stem diameter (mm) was measured using vernier calipers close to the sediment

surface. Due to the higher plant density within the buckets at the highest elevation, a subsample of ten plants was measured.

In 2013, I was able to revisit the marsh organ to collect morphological, biomechanical, and biomass measurements. I harvested *Z. aquatica* from the Salem marsh organ on July 19, 2013. At this sampling event, I recorded stem density and removed all stems from the buckets. Stems were cut with clippers at the sediment surface and transported within PVC pipes to the lab for processing. Upon reaching the lab, the *Z. aquatica* stems were placed in buckets of tap water to maintain turgor until plant measurements commenced.

In addition to the basic morphological measurements described above, I measured and recorded length to the center of mass on the stem, and diameter at this center of mass. To determine the center of mass, or the load application site (*P*), the apical portion of the stem was increasingly moved off the edge of a flat table until the stem fulcrum balanced on the table edge. I later tested this measurement by cutting and weighing the basal and apical portions of the stems and comparing dry weights.

Biomechanical Characteristics:

To determine the biomechanical response of *Z. aquatica* subjected to increasing inundation, I conducted measurements to determine the modulus of elasticity (*E*) and second moment of area (*I*) of *Z. aquatica* plant stems. Collectively, these measurements provide a quantitative assessment of the ability of *Z. aquatica* stems to resist deformation when forces are applied. These measurements inform our understanding of the material properties (*E*), such as

stiffness, and morphology (*I*) of the plant stems, which may lead to the vulnerability of *Z. aquatica* to mechanical stress due to converging physical forces of wind or tide (Niklas 1992). I used the following equation to compute *E* (Eq. 2), where *P* is the load application site, located at the center of gravity determined for each individual stem, *b* is the length from the base of *P*, δ is the stem deflection, and *I* is the second moment of area (Eq. 3).

Equation 3 is given for computing the second moment of area of a hollow stem. The variables R and r are the inner and outer radii (Figure 5).

$$E = Pb^3/3\delta I \quad \text{(Eq. 2, Niklas 1992)}$$

$$I = (\pi/4)*(R^4 - r^4) \quad \text{(Eq. 3, Niklas 1992)}$$

I conducted these biomechanical measurements using the experimental framework developed by Niklas (1992) shown in Figure 6, in which the plant stem is cantilevered at a 90° angle. The basal portion of the stem was inserted into floral foam, which I clamped to a heavy stand. I measured vertical stem deflections (δ) with load applied to a point (*P*) on the stem. To perform load measurements, a 500 mL plastic beaker was connected to the stem load application site (*b*) and successively filled with deionized (DI) water while changes in stem deflection were measured. The stem deflection was determined based on what distance the apical portion of the stem reached on the level-adjusted meter stick that was vertically clamped to a second stand.

Prior to the first load application, I measured the initial location of the apical portion of the plant using a level to eliminate the effect of the force of gravity. The next deflection measurement was taken using the force of gravity,

with the mass of the stem itself acting alone. Following these initial measurements, the pre-weighed load constant (i.e. beaker) was applied to the stem at the load application site (i.e. center of gravity for the individual stem), and DI water was added in known increments (20 mL, for *Z. aquatica*) to the load constant using a calibrated 5 mL Fisherbrand Finnpipette. Following each load application, I measured the deflection by determining the change in height of the apical end of the stem along the meter stick. Each stem had 3-5 weights and deflections measured. Once the deflection measurements were complete, the final step was to cut the stem where the load was applied (*b*) and measure the inner and outer radii (Figure 5). Following data collection, the second moment of area was calculated (Eq. 3) and used as input for the modulus of elasticity equation (Eq. 2). After *E* was computed, the frequency distribution patterns of *E* were examined to assess normality and, consequently, whether the experiments were performed properly. Upon determination that *E* was normally distributed for each *Z aquatica* stem measured, an average *E* was computed for each stem. Finally, I developed a regression model (Eq. 4; $R^2 = 0.85$) in order to estimate the modulus of elasticity for *Z. aquatica* in 2012.

$$E = 3*10^{10} (\text{Diameter}) - 4*10^{8} \quad \text{(Eq. 4)}$$

Statistical Analyses:

Statistical analyses and regression equations were performed with the free statistical software R studio (R Core Team 2013). I performed one-way Analysis of Variance (ANOVA) to determine whether differences existed among the experimental inundation treatments in the marsh organ. I assessed whether the

data met assumptions of homogeneity of variances (car package; Fox and Weisberg 2011) and normality of residuals (nortest package; Gross and Ligges 2012). When these data did not meet the assumptions for homogeneity of variances and normality, rather than perform a transformation of these data, I used the White Correction ANOVA (car package; Fox and Weisberg 2011). Tukey's post hoc comparisons were conducted using the multcomp package (Hothorn et al. 2008). Box and whisker plots, showing the median of the sample and the upper and lower quartiles were produced in R studio. Differences were deemed to be significant at the 0.05 level.

RESULTS

Z. aquatica production varied strongly as a function of elevation and, consequently, inundation treatments. In June 2012, aboveground areal biomass was different (p <0.05) among elevations, with biomass significantly greater at the highest elevation (0.17 m NAVD) compared to the lowest elevations -0.2 and -0.33 m (Figure 7a). By August, there remained a significant difference (p < 0.0001) for aboveground areal biomass among elevations, with the highest elevation having significantly greater biomass compared to all the remaining, lower elevation steps (Figure 7b).

In contrast to areal aboveground biomass, individual plant weight was not significantly different (Figure 8a) among elevation treatments in June. However, by August, weight followed a parabolic relationship with elevation and was significantly different (p < 0.005; Figure 8b). In August, individual plants growing at the lower elevations (-0.07 and -0.2 m, NAVD) had greater weight compared to the highest elevation (Figure 8b).

Stem density was different among elevations for both June (p <0.001; Figure 9a) and August (p <0.001; Figure 9b), with stem density being significantly greater at the highest elevation compared to the remaining elevations. By August the stem density at the highest elevation had decreased to a median of about 35 plants per bucket (Figure 9b) from about 60 in June (Figure 9a). June stem length was significantly different (p = 0.037), though likely due to the high variability in length, especially at the lowest elevation (-0.33 m NAVD), however, post hoc tests did not indicate significant differences in stem length

among elevations (Figure 10a). By August, stem length was different among elevations ($p < 0.001$) and exhibited a parabolic relationship similar to that seen with individual plant weight (Figure 10b), with the tallest stems found at elevations -0.07 and -0.2 m NAVD. Stem diameter was different among elevations ($p = 0.036$) in June, with significant differences among the highest elevation and elevations 0.04 and -0.2 m NAVD (Figure 11a). In August, stem diameter was again different among elevations ($p = 0.020$), with the lower elevations having greater stem diameters compared to the highest elevation (Figure 11b). Finally, in June, *Z. aquatica* exhibited a difference among elevations for modulus of elasticity ($p = 0.035$), with lower *E* at elevations 0.04 and -0.2 m NAVD compared to the highest elevation (Figure 12a). By August, this difference among elevations was more pronounced and all lower elevations, compared to the highest elevation, showed lower *E*, or decreased stem stiffness ($p < 0.0001$; Figure 12b).

DISCUSSION

In this study, *Z. aquatica* showed changes in productivity, morphology, and biomechanical properties in response to flooding regime throughout the 2012 growing season. In June, different plant responses to elevations occurred, such as significantly lower aboveground biomass (Figure 7a), stem density (Figure 9a), and modulus of elasticity (Figure 12a) in the lower elevations compared to the highest elevation. Moreover, I saw significantly greater stem diameter (Figure 11a) for *Z. aquatica* growing in the lower elevations compared to the highest elevation; however, I did not observe significant differences between individual plant weight (Figure 8a) and stem length (Figure 10a) in June. The plant response to flooding was more pronounced in August, with significant differences in all measured phenotypic response variables with depth (Figures 7b-12b). These data illustrate the phenotypic plasticity exhibited by *Z. aquatica* throughout this experiment. As the plant response to the experimental treatment is greatest by the end of the growing season, the focus from here will be on the August 2012 data.

In salt marshes, Morris et al. (2002) found that *Spartina alterniflora* undergoes a change in production, moving toward supraoptimal growth when flooded. I had expected a similar response in *Z. aquatica*; an increase in areal aboveground biomass with increasing inundation. However, *Z. aquatica* responded instead with a significant decrease in areal aboveground biomass at lower elevations receiving increased flooding (Figure 7b). While areal biomass was greatest at the highest elevation receiving the least amount of inundation (0.17 m NAVD), the individual plant weight was significantly greater at the

middle (-0.07 m NAVD) and second lowest (-0.2 m NAVD) elevation (Figure 8b). I found no effect of elevation on plant weight until -0.07 m NAVD, and there appears to be a threshold below -0.2 m NAVD where individual plant weight decreases with flooding. At the ecosystem scale, I had expected that tidal marshes had evolved resilience to withstand changes in inundation, regardless of estuarine salinity regime or plant community. However, given the difference between *Z. aquatica* and *S. alterniflora* responses to flooding, this expectation may be incorrect. For example, due to the biogeochemical conditions present in salt marshes, *S. alterniflora* must allocate more resources to salt tolerance and belowground biomass production, which means fewer resources are available for aboveground growth (Odum 1988). In contrast, *Z. aquatica* allocates more resources to aboveground, rather than belowground, production in order to compete for light in a diverse plant community. As a result of this competition to grow taller than neighboring plants, *Z. aquatica* tends to have reduced stem stability. While both species make tradeoffs to survive, the phenotypic response of each species to the surrounding environmental conditions produces markedly different results.

It is worthwhile to consider the variables that contributed to these results, which differ from my initial productivity hypothesis. I hypothesized that higher stem density would accompany greater aboveground biomass in the lower elevations receiving greater inundation, as was found in *S. alterniflora* salt marshes (Morris et al. 2002). In contrast, I found the highest elevation, which received the least inundation, had the greatest areal aboveground biomass and

significantly higher stem density (Figure 9b). This result is likely to do greater seed germination rate under less flooded conditions, as was seen in Baldwin et al. (2001). While biomass and density did not respond as expected, *Z. aquatica* was significantly taller in the lower elevation plots as was expected, specifically in the middle (-0.07 m NAVD) and second lowest (-0.2 m NAVD) elevation (Figure 10b), which contributed to the significantly higher individual plant weight (Figure 8b) at these elevations. Thinner stem diameter was expected to accompany the taller *Z. aquatica* stems at the lower elevations; however, I found a significantly greater stem thickness for *Z. aquatica* growing at the lower elevations (Figure 11b).

These stem density, height, and diameter results differ from those reported by Harley and Bertness (1996) for several salt marsh species. Harley and Bertness (1996) found that plants growing densely tended to grow taller with thinner stems to more effectively compete with neighboring plants for light; whereas, plants growing less densely tended to be shorter with thicker stems to increase stability in the water column. My results show that densely populated *Z. aquatica* plants at higher elevations were significantly shorter with thinner stems; less densely populated plants were significantly taller with thicker stems. *Zizania aquatica* also showed decreased stem stiffness (i.e. increased elasticity) at the lower elevations. According to Niklas (1994), mechanical theory predicts that plant stem diameter and stiffness tend to increase with an increase in stem height, so that taller plants tend to have thicker, stiffer stems when compared to shorter plants.

Zizania aquatica investigated at this site does not fit this model, as taller, thicker stems had decreased stem stiffness at the lower elevations.

Finally, I investigated the modulus of elasticity of *Z. aquatica* stems experiencing increased inundation. I found, as expected, that taller *Z. aquatica* growing in the lower elevations had significantly lower modulus of elasticity, or decreased stem stiffness (Figure 12b). The average August modulus of elasticity result for *Z. aquatica* was $1.59*10^8$ kg $m^{-1}s^{-2}$. This value is within the same order of magnitude as other modulus of elasticity results reported in literature. For ease of comparison with the results from this study, the following modulus of elasticity literature values have been converted to kg m^{-1} s^{-2}. For instance, Harley and Bertness (1996) found *S. alterniflora* had an average modulus of elasticity value of $5.32*10^8$ kg $m^{-1}s^{-2}$, which is comparable to my results. Furthermore, Niklas (1995) reported modulus of elasticity values for many herbaceous stems, including *Juncus spp*. ($3.21*10^8$ kg $m^{-1}s^{-2}$), which is also comparable to *Z. aquatica* values.

When a plant species is subjected to an altered environment, survival depends upon the ability of the plant to respond plastically, with phenotypic enhancements, to better tolerate the altered conditions (Puijalon et al. 2007). The phenotypic plastic response of plants to altered environmental conditions may require tradeoffs, such as thicker, rather than taller, stems to stabilize the plant against mechanical failure (Niklas 1992). *Zizania aquatica* exhibited a range of phenotypic responses to the manipulated inundation levels, including taller, thicker stems with decreased density, biomass, and modulus of elasticity at lower

elevations. The ability of *Z. aquatica* to respond with phenotypic plasticity to decreased elevation, and consequently, increased inundation, is apparent in the morphological changes observed between June and August 2012. While *Z. aquatica* did show the capacity for phenotypic plasticity, the question remains whether the species has a large enough range in its plastic response to persist under these conditions with accelerated rise.

The mid-Atlantic region of the United States has a relative sea level rise rate of about 3.5 mm yr^{-1} (Titus et al. 2009). It has been suggested that a relative sea level rise rate of about 2 mm yr^{-1} will cause many wetlands to become stressed, and many wetlands may convert to open water under an accelerated rate of 7 mm yr^{-1} (Titus et al. 2009). Current theories of wetland response to these changes describe vegetation as regulating the marsh elevation toward equilibrium with sea level rise up to some rate of sea level rise at which a threshold is reached (Morris et al 2002, Mudd et al. 2009). If sea level rises too rapidly, the marsh may not be able to maintain the amount of sediment and organic matter accretion necessary to survive. Vegetation will either succumb to inundation or possibly undergo a landward range shift, if there are no barriers to migration.

The rate of sea level rise a marsh can endure is largely a function of sediment availability. While tidal fresh and oligohaline marshes tend to have a sufficient supply of sediments from upland terrestrial sources (Boumans et al. 2002, Pasternack and Brush 2001), the productivity, morphological, and biomechanical response of *Z. aquatica* stems to increased inundation point to the potential vulnerability of this species. Taller stems are typically accompanied by

higher stem density in other plant species where the relationship has been observed (Niklas 1992, Harley and Bertness 1996, Anten et al. 2005); that was not the case in this study. Besides providing the disadvantage of competition, higher stem density provides the advantage of structural support (Harley and Bertness 1996) and buffering from hydrodynamic and wind forces, which will be greatest for the tallest plant stems (Anten et al. 2005). In this experiment, stems were thicker and more elastic, as well as taller, in the lower elevations, suggesting a phenotypic response with the potential to stabilize the stems under increased inundation and with lower stem densities.

While *Z. aquatica* stems experiencing increased inundation did exhibit stabilizing phenotypic responses, these responses were accompanied by significantly reduced stem density (Figures 9a and 9b), which suggests the potential vulnerability of *Z. aquatica* to increased flooding. Baldwin et al. (2001) investigated the response of several tidal freshwater marsh species to increasing inundation and found seedling recruitment and germination was inhibited by increased inundation, particularly when flooding occurred early in the growing season. Greater flooding early in the growing season had a greater influence on seedling recruitment of annual species in particular, which were found in lower abundance for the remainder of the year (Baldwin et al. 2001). *Zizania aquatica* growing in the marsh organ represent a naturally regenerating stand, with seedling recruitment from the initial intact marsh sediment cores repopulating the marsh organ each year. These *Z. aquatica* density data (Figure 9b) suggest seedling recruitment is reduced under increased flooding conditions, as was seen in

Baldwin et al. (2001) with other tidal freshwater marsh plants. Moreover, the reduced density of *Z. aquatica* growing under conditions of increased flooding suggests that the loss of stems could lead to a reduction in sediment capture potential by low marsh vegetation and, therefore, increased erosion of the marsh platform. This will likely reduce the ability of the marsh to accrete enough sediment to keep up with accelerated sea level rise.

Another potential vulnerability for *Z. aquatica*, is associated with the stems growing taller under increasing inundation (Figures 10a and 10b). *Zizania aquatica* growing in situ in the marsh has a tendency to become top heavy and succumb to stem failure during late summer storms (Whigham and Simpson 1977). Under conditions of accelerated sea level rise, stem failure may occur earlier in the growing season, due to the phenotypic responses reported here, which could lead to a loss of seed stock if failure occurs prior to seed production. The cumulative effect of these potential vulnerabilities (i.e. taller, less dense stems) could lead to reduced seedling recruitment over time with increasing sea level rise (Baldwin et al. 2001), which could contribute to a loss of species richness (Baldwin et al. 1996) and possible conversion to open water in portions of the low marsh if landward migration is not possible. Given the intense pressure on coastal systems from urban encroachment, which limits landward migration of tidal marshes with sea level rise, it is likely that these marshes will not fare well with increasing sea level rise.

In conducting the manipulated inundation experiments with *Z. aquatica*, I made several necessary assumptions. The marsh organ design, with each step

representing a decrease in elevation and, therefore, an increase in flooding, approximates how *Z. aquatica* will respond to increasing inundation as a proxy for sea level rise. The experimental units (i.e. buckets) in which *Z. aquatica* grew in these inundation experiments did not provide the exact conditions seen in the natural marsh. For instance, these experimental units have the potential to restrict the ability of *Z. aquatica* to spread out vertically (shoots) and horizontally (roots). However, this does not appear to have influenced my results. I saw that elevation and, consequently, inundation affects shoot density (Figure 9b), which suggests the experimental units did not restrict shoot growth. Furthermore, *Z. aquatica* tends to allocate more resources to aboveground rather than belowground growth (Whigham and Simpson 1977). Although belowground growth was not specifically investigated in this study, given findings from other research conducted with Z. aquatica (Whigham and Simpson 1977), it seems likely that the experimental units did not restrict root growth.

The *Z. aquatica* marsh organ community was shaped by interacting biological factors, such as seedling recruitment and intraspecific competition, in addition to inundation effects on plant growth and physiology. While this work did not consider the complexities associated with species interactions in the diverse plant community of the tidal freshwater marsh, it adds to our understanding of the autoecology of an important species, providing a framework for future efforts to document the impacts of inundation on other freshwater tidal plant species in this ecosystem. Furthermore, salinity intrusion into the marsh, which may also be a factor influencing tidal freshwater marshes with increasing

sea level rise, was not addressed in this simple study of the interaction between *Z. aquatica* and increasing inundation. An increase in salinity accompanied by an increase in flooding, could further compound seedling recruitment and germination in tidal freshwater marshes. Baldwin et al. (1996) found reduced species richness, seedling recruitment, and germination for many oligohaline species with a salinity increase greater than 4. Furthermore, Weston et al. (2006) found salt-water intrusion into tidal freshwater marshes triggers microbial decomposition of organic matter, which could hinder marsh ability to vertically accrete and keep pace with sea level rise.

Further study would be useful to discover interactions amongst a more diverse plant community, the effects of reduced *Z. aquatica* stem density on sediment capture, and on the species' susceptibility to hydrodynamic forces with reduced stem density and increased inundation. Finally, future study might also consider salinity intrusion, which may be a factor influencing tidal fresh and oligohaline marshes with increasing sea level rise.

FIGURES

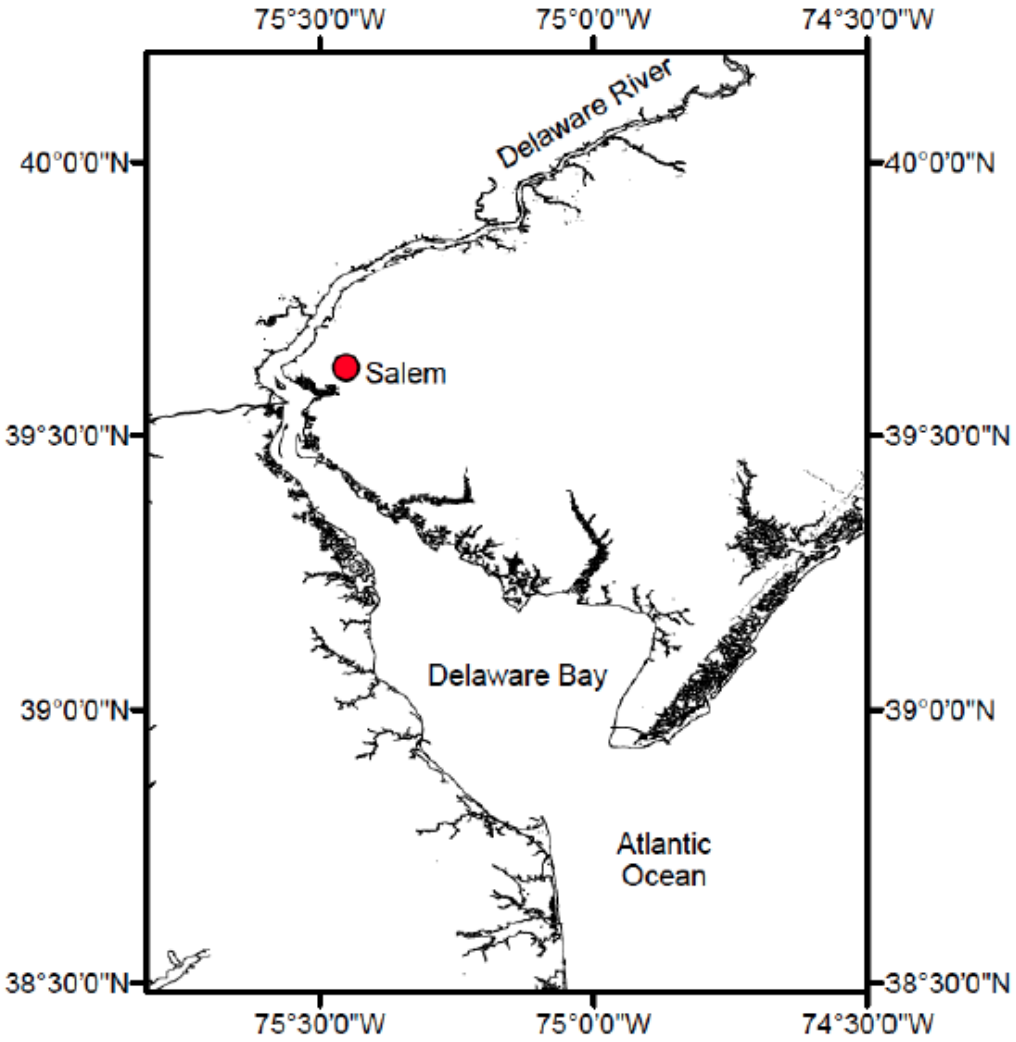

Figure 1 Site map showing location along the Delaware River.

Figure 2 Photograph of marsh organ with *Zizania aquatica* in a small tidal creek. Photo from Dr. Nathaniel Weston.

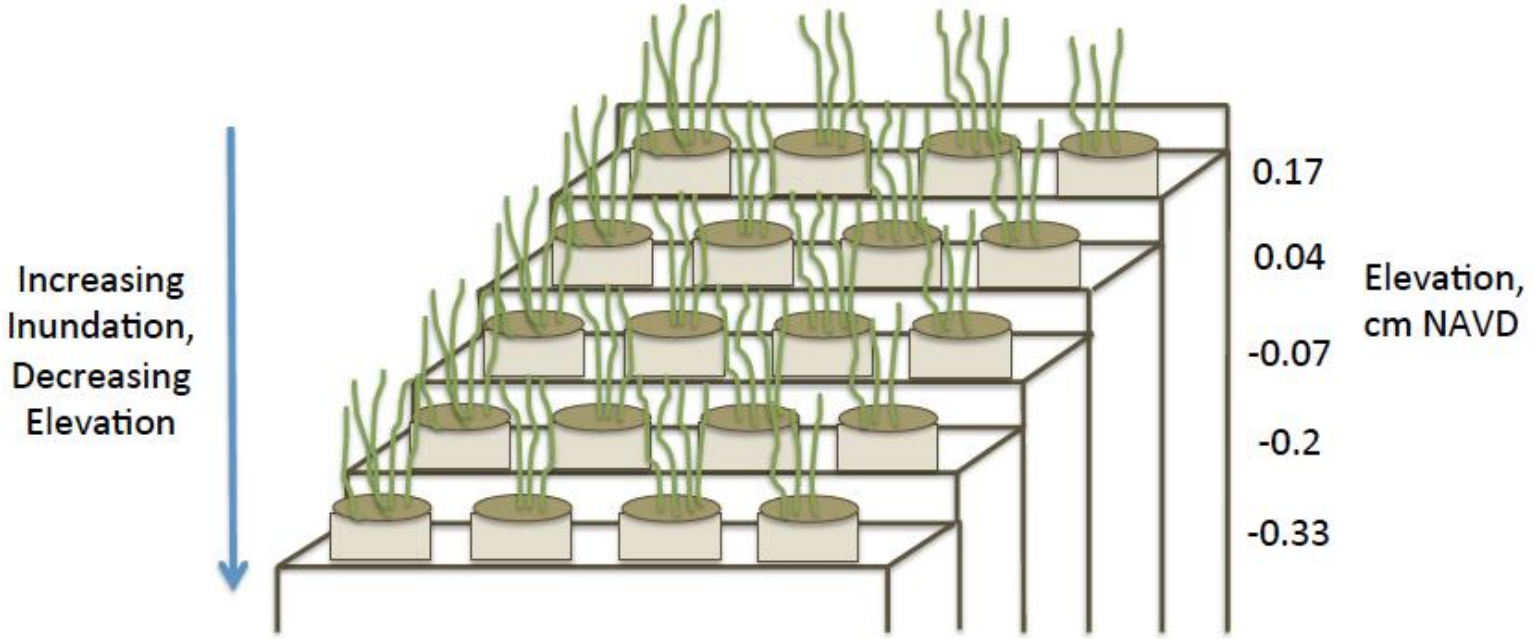

Figure 3 Marsh organ cartoon showing experimental design and change in elevation for each step.

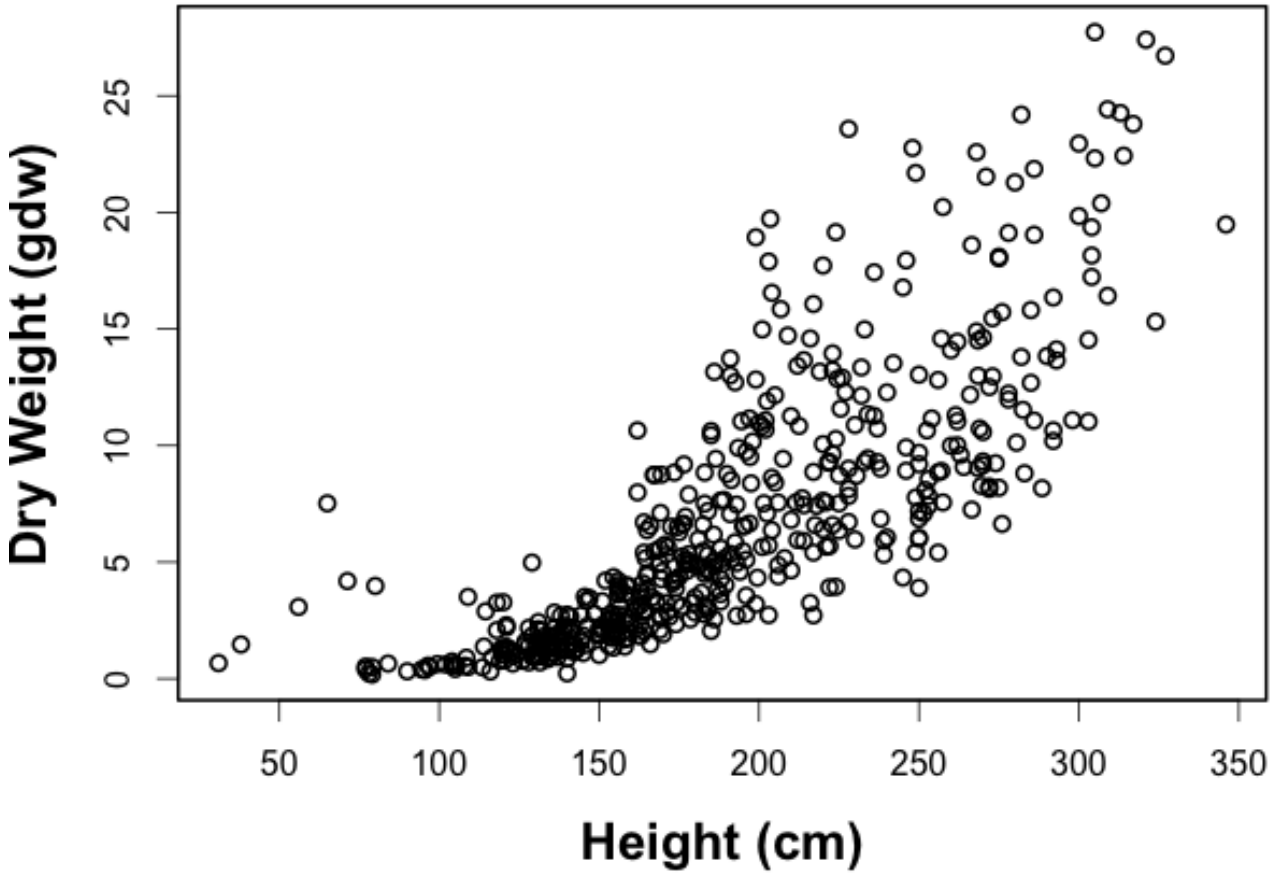

Figure 4 Destructive harvest data for *Z. aquatica* used to develop the following regression equation: Weight = $2.16*10^{-4}$ $(Height)^2 - 4.47*10^{-3}$ $(Height) - 8.86*10^{-1}$ ($R^2 = 0.67$; p value: <0.001; df = 502).

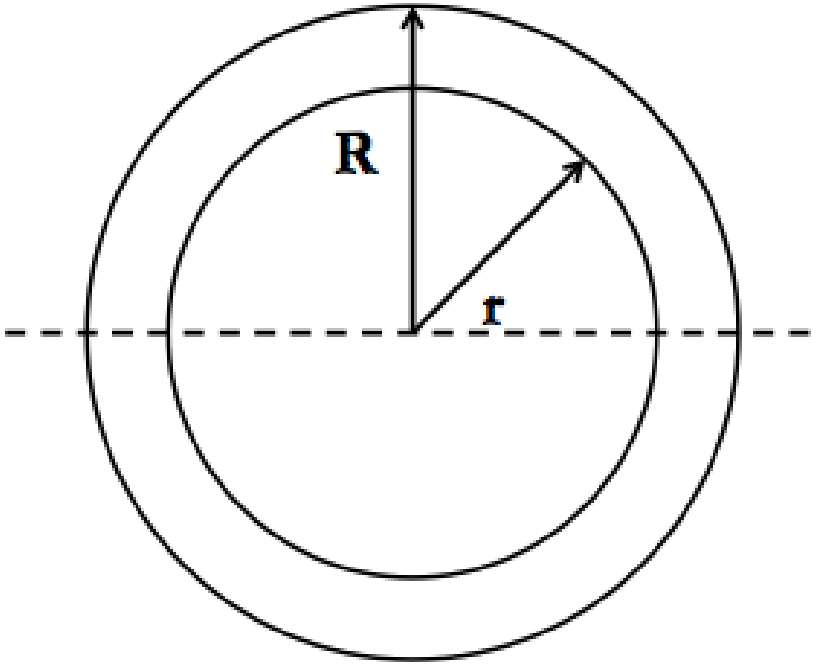

Figure 5 Diagram illustrating the inner and outer radii measurements required for the second moment of area (*I*) calculation.

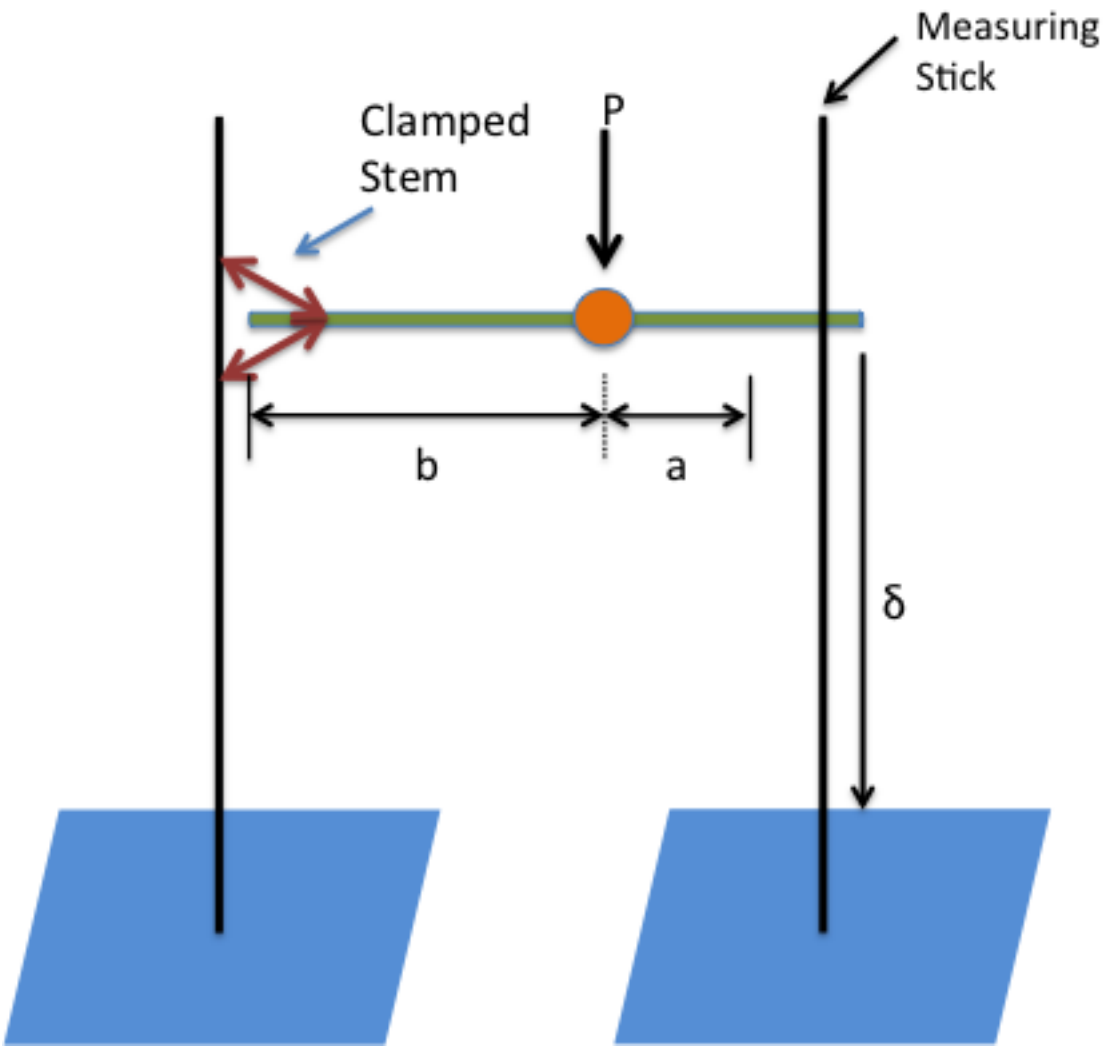

Figure 6 Cartoon illustrating the experimental framework used for the determining the modulus of elasticity (*E*), where *P* is the point on the stem where the load is applied, *b* is the length from the base of the stem to the point where the load is applied, and *a* is the apical portion of the plant.

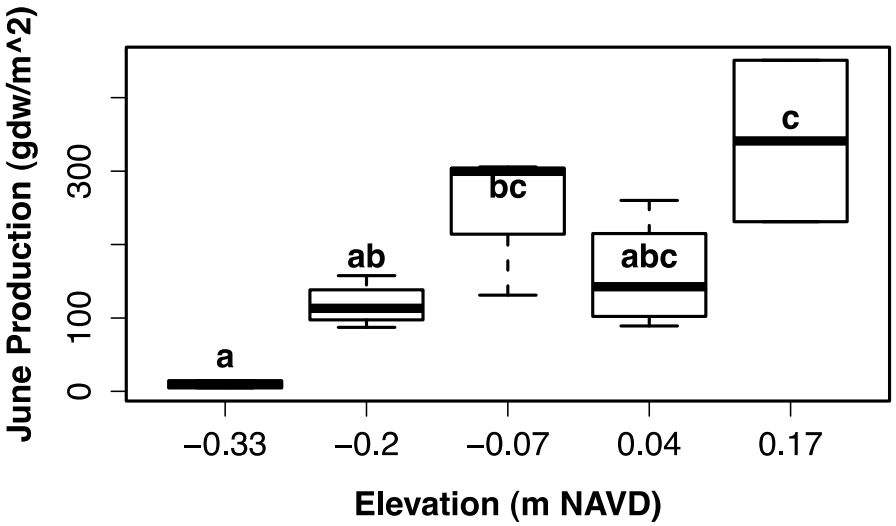

(a)

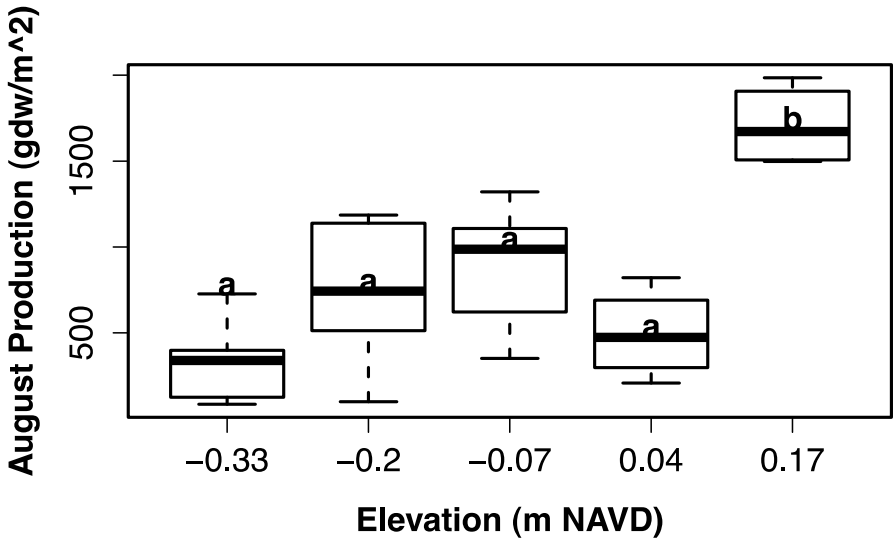

(b)

Figure 7 *Zizania aquatica* areal aboveground biomass in response to increasing inundation (decreasing elevation) treatments in June (a) and August (b) 2012. Each box whisker plot represents the median, upper and lower quartiles, and the range of the data (4-5 buckets) for the given elevation. Inundation increases with changes to elevation from 0.17 m NAVD to -0.33 m NAVD. Letters represent statistically significant Tukey differences among elevations with a significance level of 0.05. Aboveground biomass was calculated from a quadratic equation (Weight = $2.16*10^{-4}$ (Height)^2 – $4.47*10^{-3}$ (Height) – $8.86*10^{-1}$; R^2 = 0.67) based upon destructive harvest data. Statistics for June (n = ~5 replicates per row, p value = 0.0067, F value = 6.4) and August (n = ~5, p value = 0.00015, F value =10.5).

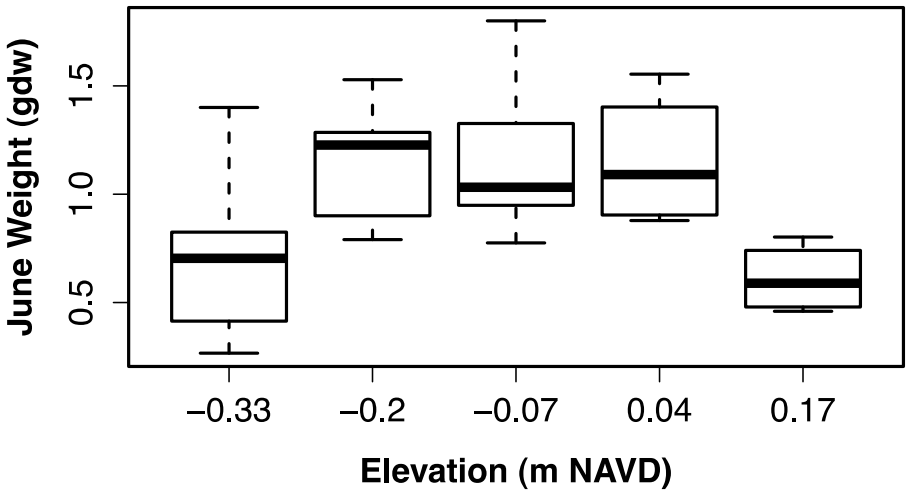

(a)

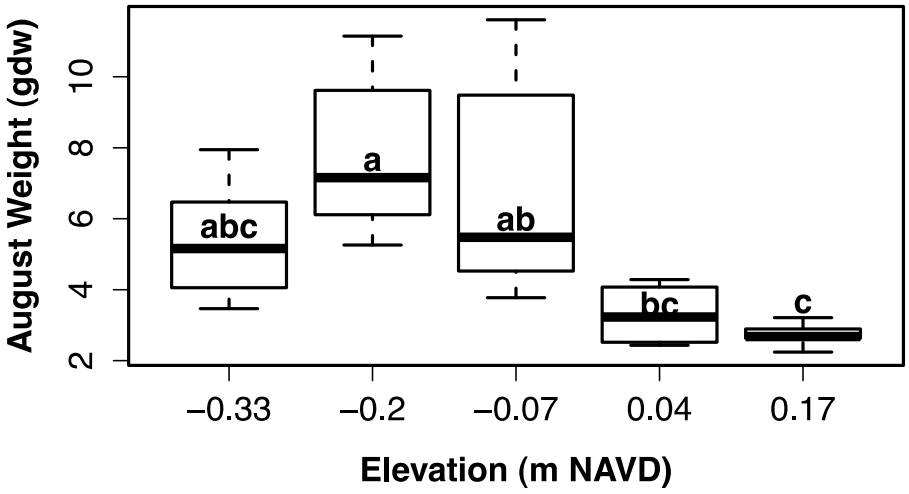

(b)

Figure 8 *Zizania aquatica* individual plant weight in response to increasing inundation (with decreasing elevation) treatments in June (a) and August (b) 2012. Each box whisker plot represents the median, upper and lower quartiles, and the range of the data (4-5 buckets) for the given elevation. Inundation increases with changes to elevation from 0.17 m NAVD to -0.33 m NAVD. Letters represent statistically significant Tukey differences among elevations with a significance level of 0.05. Statistics for June (p value = 0.058, F value = 2.8) and August (p value = 0.005, F value =5.3).

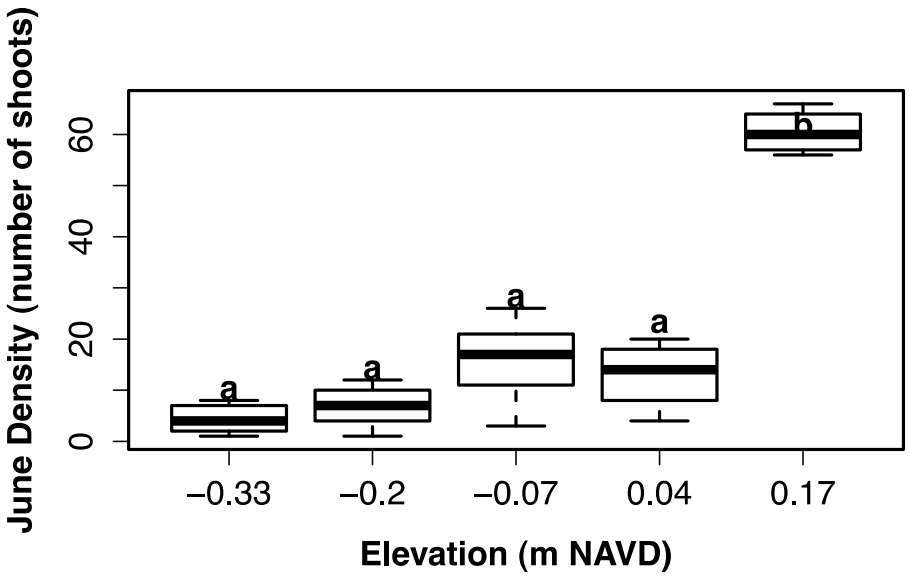

(a)

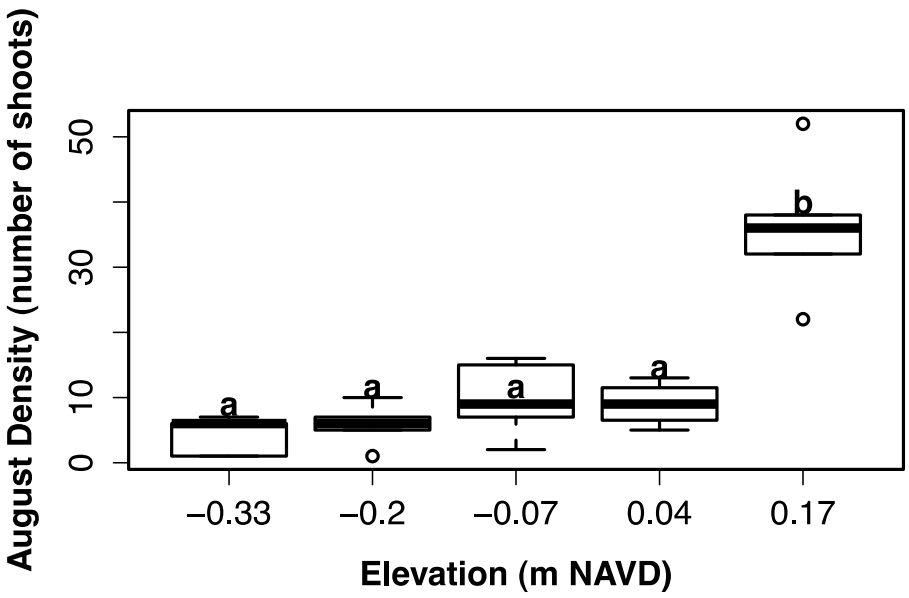

(b)

Figure 9 *Zizania aquatica* stem density in response to increasing inundation (with decreasing elevation) treatments in June (a) and August (b) 2012. Each box whisker plot represents the median, upper and lower quartiles, and the range of the data (4-5 buckets) for the given elevation. Inundation increases with changes to elevation from 0.17 m NAVD to -0.33 m NAVD. Letters represent statistically significant Tukey differences among elevations with a significance level of 0.05. Statistics for June (p value = < 0.001 F value =63.1) and August (p value = < 0.001, F value =22.5).

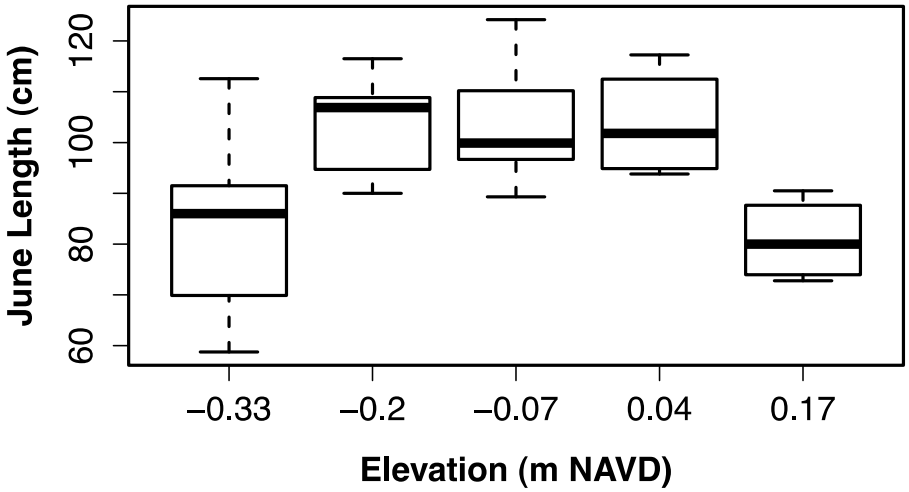

(a)

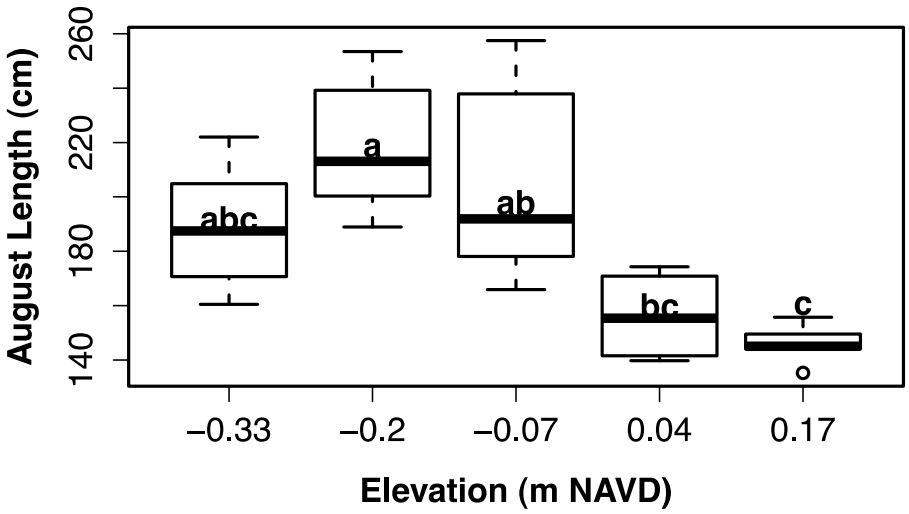

(b)

Figure 10 *Zizania aquatica* stem length in response to increasing inundation (with decreasing elevation) treatments in June (a) and August (b) 2012. Each box whisker plot represents the median, upper and lower quartiles, and the range of the data (4-5 buckets) for the given elevation. Inundation increases with changes to elevation from 0.17 m NAVD to -0.33 m NAVD. Letters represent statistically significant Tukey differences among elevations with a significance level of 0.05. Statistics for June (p value = 0.036, F value = 3.2) and August (p value < 0.001, F value =7.1).

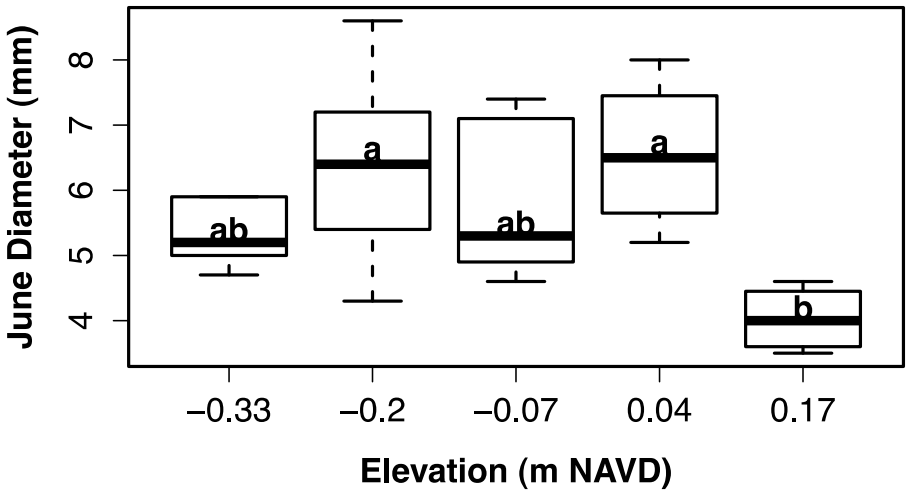

(a)

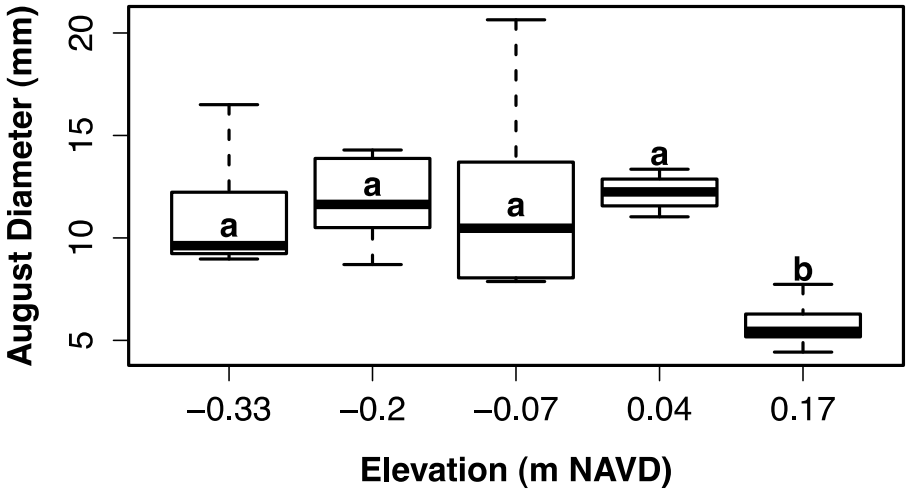

(b)

Figure 11 *Zizania aquatica* stem diameter in response to increasing inundation (with decreasing elevation) treatments in June (a) and August (b) 2012. Each box whisker plot represents the median, upper and lower quartiles, and the range of the data (4-5 buckets) for the given elevation. Inundation increases with changes to elevation from 0.17 m NAVD to -0.33 m NAVD. Letters represent statistically significant Tukey differences among elevations with a significance level of 0.05. Statistics for June (p value = 0.036, F value = 3.2) and August (p value = 0.019, F value = 3.8).

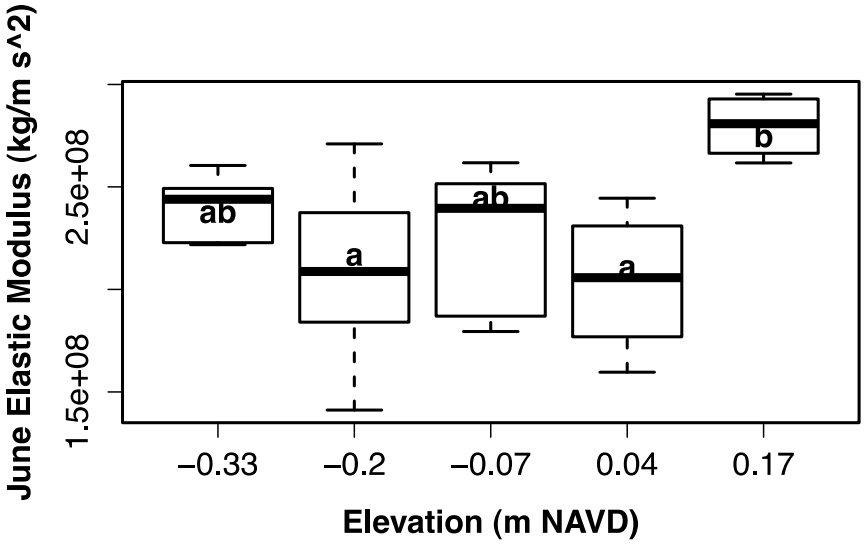

(a)

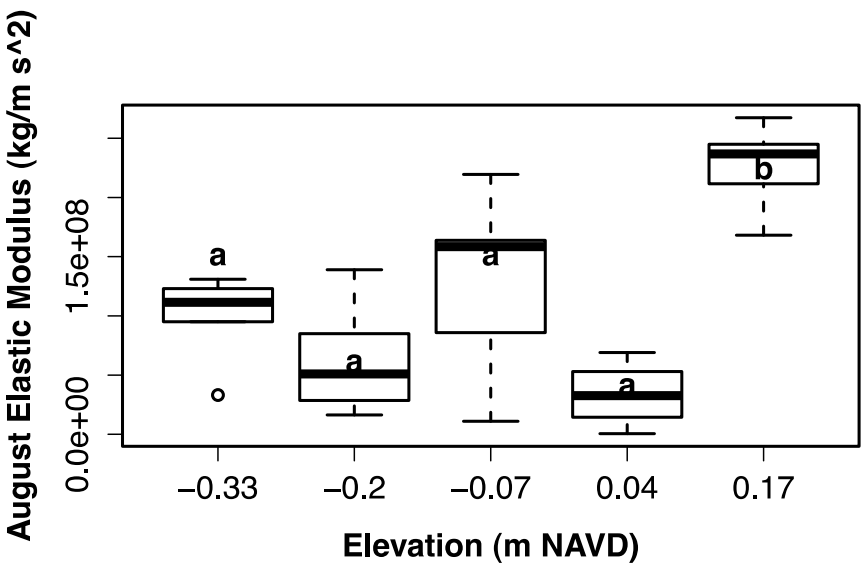

(b)

Figure 12 *Zizania aquatica* stem modulus of elasticity in response to increasing inundation (with decreasing elevation) treatments in June (a) and August (b) 2012. Each box whisker plot represents the median, upper and lower quartiles, and the range of the data (4-5 buckets) for the given elevation. Inundation increases with changes to elevation from 0.17 m NAVD to -0.33 m NAVD. Letters represent statistically significant Tukey differences among elevations with a significance level of 0.05. Elasticity was calculated from a regression equation (Elasticity = $3*10^{10}$ (Diameter) – $4*10^{8}$; R^2=0.85) based upon results from the biomechanical measurements taken in 2013. Statistics for June (p value = 0.035, F value =3.3) and August (p value = < 0.001, F value = 9.8).

CHAPTER TWO:
THE FUTURE ROLE OF CHESAPEAKE BAY TIDAL WETLANDS AS NITROGEN SINKS AND SOURCES UNDER PROJECTED SEA LEVEL RISE

ABSTRACT

There is increasing concern that sea level rise (SLR) could negatively impact the Chesapeake Bay through the loss of wetlands. Wetlands act as nutrient sinks through burial or, in the case of nitrogen, transformation to di-nitrogen gas through denitrification. Upon degradation and submergence, wetlands may act as a source, rather than a sink, of nutrients. Projected changes to these ecosystems under SLR were not considered when total maximum daily loads (TMDLs) were instituted for the Chesapeake Bay, which has implications for restoration efforts. I obtained estimates of current and projected areal wetland coverage for the Chesapeake Bay under various SLR scenarios and calculated denitrification and nitrogen burial rates for Chesapeake Bay tidal wetlands under these scenarios for the years 2025, 2050, 2075, and 2100. In addition to presenting these large-scale results for the Chesapeake Bay, I describe two case studies at increasingly finer scales, comparing 2025 projected TMDL nitrogen loadings to nitrogen removal by tidal wetlands undergoing projected SLR for five Maryland major basins and 22 Calvert county watersheds. My work will inform resource managers, at several scales, of the areas with increased vulnerability to accelerated SLR, which may have the potential to negatively impact Bay restoration goals associated with decreased nitrogen loadings.

INTRODUCTION

Chesapeake Bay Tidal Wetlands:

The Chesapeake Bay estuary is relatively shallow with broad shoals and extensive flats, which gradually slope toward a deeper channel. Bay hydrology is driven by tides, which influence the presence of tidal wetlands ranging from tidal freshwater marshes and swamps, to brackish and salt marshes. The salinity in the Bay varies from oligohaline (< 0.5-2; Odum 1988) in tidal freshwater marshes to mesohaline (1-10; Lippson and Lippson 2006) in brackish marshes to polyhaline (18-30; Odum 1988) in salt marshes. According to Baldwin et al. (2012), tidal wetlands cover an area of about 160,000 ha in the Chesapeake Bay.

Ecosystem services ensue from the flow of materials and energy from the natural environment, which either directly or indirectly benefit humans (Costanza et al. 1997). Wetlands provide many ecosystem services, such as filtration of toxins and pollutants, the uptake and transformation of nutrients, floodwater attenuation, groundwater recharge, water quality improvement, habitat, and recreation opportunities (Costanza et al. 1997). Wetlands are advantageously situated in the landscape to intercept nutrients and pollutants from upland terrestrial sources before they reach estuaries and coastal environments, where the increased nutrient loading can lead to eutrophication. Increasing awareness of the inherent benefits of wetlands, whether natural, restored, or constructed, has led to the managed use of wetlands for trapping nutrients exported from agricultural lands (Hansson et al. 2005) or wastewater effluent to improve water quality.

These ecologically important services are often not given much consideration in policy decisions (Costanza et al. 1997).

Of specific interest for this study, Chesapeake Bay tidal wetlands provide nitrogen removal services (e.g. denitrification and nitrogen burial), which are important wetland processes that effectively reduce the flow of nitrogen reaching estuarine and coastal environments (White and Howes 1994). Nitrogen loss from the wetland may occur as denitrification or anaerobic ammonium oxidation both of which result in the conversion of nitrate to di-nitrogen gas to the atmosphere. In the case of denitrification, this process occurs as coupled nitrification-denitrification where there are both oxic and anoxic sediment conditions available either spatially or temporally. The process of anaerobic ammonium oxidation (anammox) also releases di-nitrogen gas to the atmosphere. However, in the Chesapeake Bay, anammox is not considered a primary loss pathway for nitrogen (Rich et al. 2008). Nitrate may be converted to ammonium via dissimilatory nitrate reduction to ammonium (DNRA), a process that doesn't remove reactive nitrogen from the system, and then stored in marsh sediments before eventually being exported from the wetland to coastal marine environments (Koop-Jakobsen and Giblin 2010). However, the focus of this study is specific to denitrification, the nitrogen loss process that appears to be most prevalent in coastal sediments (Kemp et al. 1990, Hussein and Rabenhorst 2002, Kellogg et al. 2013). Nitrogen burial occurs when nitrogen, largely recalcitrant, accumulates as a result of sedimentation and is stored in tidal wetland soils.

Not all tidal wetlands are created equal when it comes to providing nitrogen removal services. Indeed, oligohaline (low salinity) marshes in the Chesapeake Bay are estimated to remove 2-3 times as much nitrogen as mesohaline (high salinity) marshes and are much more extensive in their coverage (Boynton et al. 1995). For instance, tidal freshwater wetlands tend to have high rates of denitrification (14.7 g m^{-2} yr^{-1}; Greene 2005) and N burial (23.4 g m^{-2} yr^{-1}; Merrill and Cornwell 2000) compared to salt marshes (0.6 g m^{-2} yr^{-1} and 3.6-5.2 g m^{-2} yr^{-1}, respectively; Thomas and Christian 2001). Nitrogen removal rates in brackish marshes fall in between tidal freshwater and salt marshes, with denitrification rates of about 7.36 g m^{-2} yr^{-1} (Kemp 2006) and burial rates of about 13.6 g m^{-2} yr^{-1} (Merrill and Cornwell 2000).

Climate Change and SLR:

Sea level rise (SLR) is an outcome of climate change that could negatively impact the Chesapeake Bay through the loss of tidal wetlands. Indeed, this has already occurred in the Bay, with many wetlands showing signs of decline, particularly along the Eastern shore (Kearney et al. 2002). Marsh stability depends upon complex, often nonlinear, feedbacks between SLR, marsh vertical accretion, and marsh vegetation (Morris et al. 2002, Mudd et al. 2010). Tidal wetlands have a high potential for adjusting to SLR, since an increase in inundation is likely to increase sediment deposition and, consequently, marsh vertical accretion (Leonard et al. 1995, Reed 1995, Kirwan et al. 2010). However, if tidal marshes are unable to vertically accrete sediments sufficiently they will surpass a threshold for adaptability to SLR beyond which marsh erosion will

occur. According to Kirwan et al. (2010), marshes that have exceeded a SLR threshold will likely become submerged and erode within 30-40 years. Eroding marshes act as sources, rather than sinks, of nutrients, sediments, and organic matter (Boynton et al. 2008).

When considering the potential impact of SLR on Chesapeake Bay tidal wetlands, it is necessary to consider climate and hydrological processes. The cumulative effect of these processes combined with SLR may create a more substantial impact on tidal wetlands than SLR considered in isolation. Global climate models show much uncertainty and variation in their projections, though there is a broad consensus in the expected trends. Generally, annual mean temperatures will continue to increase in the 21st century (Hayhoe 2007), possibly by about 2-5^{o}C (Najjar et al. 2010). Additionally, global climate models predict an increase in winter and spring mean precipitation and an increase in extreme events such as heat waves, storms, and droughts (Hayhoe et al. 2007, Najjar et al. 2010). In tandem with the predicted changes in precipitation and temperature, it is expected that there will be an increase in winter and spring streamflow and a decrease in summer streamflow (Hayhoe et al. 2007, Najjar et al. 2010). The combination of increased drought, evapotranspiration, and reduced summer streamflow may lead to a seasonal increase in Bay salinity, particularly in the upper and mid Bay. As riverine inputs decrease in the summer, tidal fresh and brackish marshes will likely be stressed by an increase in salinity.

Mechanisms of global SLR include processes such as glacial ice melting and thermal expansion of oceans since the last glaciation. Geographical and

temporal variation from the global SLR rate is often due to processes such as regional long-term land subsidence from post-glacial rebound and annual/decadal fluctuations in atmospheric circulation (e.g. North Atlantic Oscillation) and precipitation patterns (Barbosa and Silva 2009). Similar to global climate models, there is much uncertainty regarding future SLR projections; however, it is generally agreed that SLR will continue to accelerate throughout the 21st century. Assuming a constant accelerated rate of SLR as seen in the 20th century, Church and White (2006) predict that global sea level will rise to ~ 0.28 - 0.34m by 2100. Rahmstorf (2007) developed a semi-empirical model, based upon the relationship between historic global SLR and mean surface temperatures, to predict higher increase in the global mean sea level (0.5m - 1.4m) by 2100 given a temperature increase between 1.4 and 5.8^{o}C. The Church and White (2006) global SLR prediction have come to be considered conservative, and, in comparison, the Rahmstorf (2007) projection is considered to be more likely (Najjar et al. 2010).

The global rate of SLR is estimated to be about 1.5-2 mm yr^{-1} (Church and White 2006, Titus et al. 2009), whereas the regional estimate for the Chesapeake Bay is between 3 mm yr-^{1} (Reed et al. 2008, Barbosa and Silva 2009) and 3.5 mm yr^{-1} (Titus et al. 2009). Long-term tide gauge data indicates there has been an increasing SLR trend for the Chesapeake Bay during the past century (Barbosa and Silva 2009, Titus et al. 2009, Najjar et al. 2010). Najjar et al. (2000) predicted mean SLR in the Mid-Atlantic region will increase by ~ 0.19 m by 2030 and 0.66 m by 2095. More recently, Boesch et al. (2013), predict accelerated SLR rates of ~ 0.43 m by 2050 and 1.1m by 2100 for the tidal waters of Maryland.

Total Maximum Daily Loads:

The U.S. Clean Water Act of 1972 required the establishment of Total Maximum Daily Loads (TMDLs) for impaired waters in an effort to improve water quality standards. The Chesapeake Bay is listed as an impaired waterbody. Executive Order 13508, signed by President Obama, in 2009, recognized the Chesapeake Bay as a national treasure worthy of restoration and protection (EO 2009). As a result, TMDLs were developed by the U.S. Environmental Protection Agency (EPA) to set limits on nutrient (nitrogen and phosphorus) and sediment pollution in the Bay and its tributaries. These pollution control measures are required to be in place by 2025. Watershed Implementation Plans (WIPs) were developed on the state level to determine how individual states within the Chesapeake Bay watershed will meet the required pollution allocations. At the county level in Maryland, progress toward meeting the water quality goals and implementation of TMDLs is reevaluated every two years.

Despite anticipated changes in climate over the next century, we are just beginning to modify management actions to take into account the interactive effects of climate change on pollutant delivery. Nutrient and sediment delivery are expected to increase in the Chesapeake Bay region due to climate and land use changes that will likely result in greater runoff (Reed et al. 2008, Najjar et al. 2010). At the same time, SLR will continue to affect the areas occupied by tidally influenced marshes. Healthy, accreting tidal marshes serve as sinks for nitrogen, effectively acting as "ecosystem-scale kidneys" (Boynton et al. 2008). Tidal marshes in the Patuxent River were found to remove up to 30% of the total

nitrogen imported into the marsh (Boynton et al. 2008). In comparison, eroding marshes that are unable to accrete enough sediments to keep pace with SLR, as seen along the Eastern Shore of Maryland in the Chesapeake Bay (Ward et al. 1998, Stevenson et al. 2002), have a diminished capacity for nitrogen removal services and may act as a source of nitrogen via erosion of buried nitrogen, rather than a sink, as they continue to become submerged with accelerated SLR. Loss of wetlands due to climate change will further reduce nitrogen removal capacity at the same time nitrogen loading is increasing.

Objectives:

I seek to answer the following research questions: (1) What role do tidal wetlands play in nitrogen removal in relation to current nitrogen loads? (2) How will projections of SLR that include changes to wetland area affect loading goals set by the TMDLs? (3) How does spatial scale affect our understanding of these questions from Bay-wide, to basin scale, to 12-digit watersheds? I expect these analyses will provide evidence of a potential increase in nitrogen exported from tidal wetlands (released from burial) and a decrease in denitrification as tidal wetlands submerge and erode. Furthermore, I expect to find that TMDLs may not be adequate to meet restoration goals, as planned, since they do not account for wetland N removal services.

METHODS

Chesapeake Bay tidal wetlands provide important nitrogen removal services. In an effort to highlight the importance of these wetlands and the potential threat accelerated SLR presents to these systems, I provide estimates of areal tidal wetland coverage using SLAMM projections for various SLR scenarios and estimate nitrogen removal for these scenarios to assess future changes in N removal services for tidal wetlands in the Bay. In addition to a large-scale examination of tidal wetlands in the entirety of the Chesapeake Bay, this study includes similar analyses at increasingly smaller scales. Restoration goals for nitrogen loadings by 2025 for five major basins in Maryland that are targeted for Phase II of the Watershed Implementation Plan for the Chesapeake Bay TMDL (MDE 2012) are explored in comparison to SLR projections. Because these basin-scale WIPs are informed by local efforts by county and municipal governments, Phase II of the WIP for Maryland as developed in Calvert County was also explored as a case study to examine how changes to tidal wetlands might impact restoration efforts in the coastal plain. The Calvert County WIP has been designed for target loads in 2020 (MDE 2012).

Sea Level Affecting Marsh Model:

The role of tidal wetlands in mitigating nutrient loads through burial and denitrification warrants further investigation using tools that can link watershed activities to wetland ecosystem processes while also considering the impacts of SLR and changes in hydrology. The aim of this work is to provide broad predictions of altered nitrogen removal rates by marshes using previously reported

results from a SLR model capable of simulating the response of tidal wetlands to long term accelerated SLR projections. The Sea Level Affecting Marshes Model (SLAMM; Park et al. 1989; Clough and Park 2008; http://www.warrenpinnacle.com/prof/SLAMM) was applied to the Chesapeake Bay region in a project funded by the National Wildlife Federation (NWF; Glick et al. 2008). The resulting Bay dataset of predicted wetland coverage under various SLR scenarios is available to the public.

SLAMM is an ecosystem-based model that indirectly considers hydrodynamics and sediment loads when simulating wetland response to long-term SLR (Fagherazzi et al. 2012). SLAMM indirectly calculates these parameters and does not include mechanistic formulations, so it is incapable of simulating feedback mechanisms; however, the simplicity of the model has facilitated its widespread application due to fast run-times and ease of use (Fagherazzi et al. 2012). SLAMM version 5.0 is a cell based (30 m x 30 m) model that easily integrates with raster-based GIS data, incorporating major processes affecting wetland fate such as accretion, erosion and inundation as well as an algorithm to model saltwater intrusion (Glick et al. 2008, Clough and Park 2008). Land categories used in SLAMM are derived from USFWS National Wetland Inventory (NWI) categories (Glick et al. 2008, Clough and Park 2008). Technical detail describing SLAMM 5.0.2 model processes, assumptions, equations, and land categories, are thoroughly detailed by Clough and Park (2008).

SLR projections used in this SLAMM dataset are based on the emission scenarios A1 and B1 from the Intergovernmental Panel on Climate Change

(IPCC) Special Report on Emissions Scenario (SRES) Fourth Assessment Report (Glick et al. 2008, Craft et al. 2009). Within these scenarios (i.e. A1 and B1) there are several groups, (e.g. A1B, A1F1, and B1), which represent various levels of economic growth, global population, and technological efficiencies. Emissions scenarios are thoroughly detailed by IPCC (2007). The dataset included simulations for the following SRES scenarios and groups: B1 mean (0.31 m of SLR by 2100), A1B mean (0.39 m), A1FI mean (0.49 m), A1B max (0.69 m) (Clough and Park 2008). In addition to the SRES scenarios, there were three additional SLR scenarios (i.e. 1.0 m, 1.5 m, and 2.0 m) included in the dataset (Clough and Park 2008). Simulations were based on incremental time steps of 25 years, which cover the period between the years 2000-2100. In addition, a reference (1996) simulation was run to enable comparisons and to validate the model. The model simulations were developed using USGS digital elevation model data, NOAA tidal data, and USFWS National Wetland Inventory data inputs, all of which are publicly available. For more details on model inputs, please see the NWF Technical report (Glick et al. 2008).

Dataset Acquisition:

In order to evaluate changes in tidal wetland area and loss of nitrogen removal services with long-term SLR, I exported Chesapeake Bay SLAMM zipfiles from Data Basin (2013). Data Basin is a science-based, free and open access site developed by the Conservation Biology Institute to support the scientific community via shared datasets. The Chesapeake Bay SLAMM files were originally created for a study that simulated SLR response of coastal

habitats, such as marshes and beaches, in the entire Chesapeake and Delaware Bay region (Glick et al. 2008).

Scenario Selection:

Chesapeake Bay

The original geographic information system (GIS) files exported from Data Basin included multiple IPCC SRES scenarios, and a broader spatial scale that included Delaware Bay and the Delmarva Coastal Bay complex. Therefore, it was necessary to narrow the dataset both spatially and to SLR projections appropriate for this analysis. The model simulations I chose for my Chesapeake Bay tidal wetlands study were based upon the estimated global and local SLR rates. There is a general consensus that global SLR projections for the 21st century have been previously underestimated (0.28 – 0.34 m; Church and White 2006) and will more than likely be in the range of 0.5 - 1.4 m (Rahmstorf 2007, Najjar et al. 2010). The SLR trend for the Mid-Atlantic region tends to be comparatively higher than the global SLR rate (Titus et al. 2009, Sallenger et al. 2012). By 2100, Maryland SLR rates are projected to range between 0.7 - 1.7 m (Boesch et al. 2013). These combined factors provided the basis for selecting the model simulations based upon SRES A1B max (0.69 m), 1.0 m, and 1.5 m rise by the end of the 21st century.

Maryland Basins

The five Maryland basins selected for inclusion in this study drain into the Bay and have tidally-influenced wetlands at their coastal margins. These basins are the Eastern Shore, Western Shore, Susquehanna, Patuxent, and Potomac

(Figure 1). The SLR scenarios used in the basin study were SRES A1B max and 1.0 m by 2100. The criteria for scenario selection was two-fold, based upon the restoration goals for the Maryland portion of the Bay and the projected rate of SLR for Maryland. The restoration goals include reductions in nitrogen loading for the entire Maryland basin and each individual basin by 2025 (EPA 2010, MDE 2012). Therefore, I narrowed my focus to 2025 SLR projections to assess changes in tidal wetland area and nitrogen removal services in the basins in comparison to the 2025 restoration goals.

Boesch et al. (2013) predict a SLR of about 0.43 m by 2050 for Maryland. Assuming the predicted SLR accumulates in a linear fashion during the given period, in half the time (i.e. 2025), the SLR will be about 0.22 m. Additionally, the SRES A1B max SLR scenario (0.69 m), appears to increase in a near-linear fashion over the next 100 years (Figure in: Najjar et al. 2010). I used this as a guideline to select the SRES A1B max (0.69 m) and 1.0 meter rise by 2100. By quartering these rates, these scenarios will represent about 0.17 m and 0.25 m for the SRES A1B max and 1.0 meter rise scenarios by 2025.

Calvert County Watersheds

The smallest scale study I explored estimated changes at the 12-digit scale watersheds in Calvert County, Maryland. A 12-digit watershed scale is the smallest hydrologic unit classification used by the U.S. Geological Survey and it represents the subwatershed scale. The local county government uses this scale of watershed (i.e. 12-digit subwatershed) to develop WIPs to meet the required county reductions for nitrogen, phosphorus, and sediment TMDLs for the

Chesapeake Bay (MDE 2012). Similarly to the criteria selection for the basin study, I selected the scenario for this study based upon restoration goals for Calvert County and the projected rate of SLR for Maryland. The Calvert County WIP (Calvert County (2013) provides nitrogen loading goals for the 22 Calvert County watersheds by 2020. Therefore, I selected the 2025 SLR simulation for SRES A1B max (0.17 m) and 0.25 m by 2025.

Spatial Analyses:

Chesapeake Bay

In addition to truncating the simulation scenarios of interest for my study, it was also necessary to narrow the areas covered by the simulation. As previously mentioned, the original simulations included the Chesapeake Bay, Delaware Bay, and coastal lagoons. I was only interested in analyzing tidal wetlands in the Chesapeake Bay. I imported the raster-based SLAMM files into ArcGIS (version 10; ESRI 2010). Using the ArcMap Spatial Analyst extension, raster cells were extracted using a vector shapefile of the Chesapeake Bay watershed boundary (ftp://ftp.chesapeakebay.net/pub/Geographic/ChesapeakeBay/). I repeatedly performed this process for each of the scenarios (i.e. 0.69 m, 1.0 m, and 1.5 m) and years (i.e. 1996, 2025, 2050, 2075, and 2100) of interest until all extractions were complete. Because each raster cell was defined as having a 30 by 30 m area, areas of each tidal wetland type could be computed by multiplying the number of cells found for each wetland category by the area of the raster cells.

Maryland Basin

GIS shapefiles providing boundaries for the major TMDL Maryland basins were obtained from the Maryland Department of the Environment (www.mde.maryland.gov). To determine the wetland coverage found in each basin for each scenario and simulation year, I applied spatial analyst tools in ArcMap to scale each raster file to the basin of interest. As in the Chesapeake Bay–wide analysis, total hectares for each wetland type were then computed.

Calvert County Watersheds

Calvert County 12-digit watershed shapefiles for this portion of the study were provided by a member of the Calvert County Phase II WIP team (Dr. Brownlee, personal communication). Predicted nitrogen loads and targets for each of the 22 watersheds are reported in the Calvert County portion of Phase II of the WIP (MDE 2012). I used these smaller scale watershed shapefiles for Calvert County to narrow the focus of the study from the SLAMM Chesapeake Bay projections down to the Calvert County scale following the same methods used for the other study scales.

Tidal Wetland Computations:

Upon completing the extractions for all three spatial scales involved in this study, the attribute tables were exported for calculations of changes in wetland area, denitrification, and N burial in comparison to the reference conditions for each scale, scenario, and year. The 1996 reference year produced by Glick et al. (2008) in the SLAMM model application were used as a "time zero" from which I computed percent changes in wetland area and nitrogen removal ecosystem

services. I eliminated many of the 26 land categories originally incorporated in the SLAMM simulation and focused on tidal wetlands, combining similar categories into three broad categories of tidal fresh (i.e. tidal fresh marsh, tidal fresh swamp), salt (i.e. salt marsh, transitional marsh), and brackish wetlands.

Nitrogen removal

I conducted a literature review to find denitrification and nitrogen burial rates for each of the broad types of tidal wetlands (Table 1). As much as possible, rate measurements for these processes were collected from studies that took place in the Chesapeake Bay region. All units were converted to g N m^{-2} yr^{-1} for ease of computation. Nitrogen removal services were calculated for each scenario and year by multiplying the wetland area by the removal rate derived from literature corresponding to that particular type of tidal wetland. These calculations were repeated for all scales, scenarios, and years. I computed the estimated percent change in tidal wetland area (or nitrogen removal services) for the SLR projections.

Maryland Basin and Calvert County Watersheds

In addition to the analysis outlined above, I also compared the nitrogen removal services performed by the tidal wetlands under the projected SLR scenarios by 2025 to the corresponding restoration goals (i.e. nitrogen loadings) provided by the TMDLs for the five Basins (EPA 2010) and the WIP for the 22, 12-digit county watersheds (MDE 2012). For the basins, this was done by computing the loss of denitrification or N burial for all the tidal wetlands under the two SLR scenarios (i.e. 0.17 m and 0.25 m) from the reference scenario for a

given basin. Denitrification and nitrogen burial losses were summed for a cumulative computation of total nitrogen removal. These calculations were performed for all basins and all scenarios (0.17 m and 0.25 m). For the county watersheds, I computed the ratio of total nitrogen removal by all tidal wetlands for both 2025 SLR scenarios to the WIP nitrogen loading goal for the given watershed. This was performed for all watersheds and all scenarios (reference, 0.17 m and 0.25 m). The units for the nitrogen loading goals for both the TMDLs (EPA 2010) and the WIP (MDE 2012) were converted from lbs yr^{-1} to g yr^{-1}, for ease of computation.

Maps and Graphs:

I created tidal wetland area maps in ArcMap for the three scenarios by 2100 to compare to the reference wetland area for the Chesapeake Bay. I also created tidal wetland area maps for the Maryland basins, though I only mapped two scenarios (0.17 m and 0.25 m) by 2025. Similarly, a reference map of tidal wetland area was created for the basins. Lastly, I created maps for the Calvert County WIP watersheds for the reference scenario to illustrate which watersheds have the most wetlands, and as a result, are particularly important as normalized to incoming loads and where the largest wetland nitrogen removals are occurring in the county. Graphs were created using Microsoft Excel, to show percent change from the reference for each scenario.

RESULTS AND DISCUSSION

The largest sources of nitrogen to the Bay are attributed to agriculture (38%), atmospheric deposition (21%), sewage and industry (19%), and stormwater (16%; CBF 2012). The Chesapeake Bay watershed covers ~172,000 km^2 and the Susquehanna River drains an area of ~71, 200 km^2, making the Susquehanna the largest freshwater input from the Bay watershed (Hagy et al. 2004). With future climate change, there is an expectation that the annual discharge from the Susquehanna River will increase by ~24% (Hagy et al. 2004). Given the large contribution the Susquehanna River makes to the Chesapeake Bay watershed, ~41% (Hagy et al. 2004), an increase in annual discharge will likely lead to increase in nitrogen loading to the Bay.

Tidal marshes act as nitrogen sinks, helping to buffer the Chesapeake Bay watershed against some of the negative effects of eutrophication via processes such as denitrification and nitrogen burial in marsh sediments (Seitzinger 1988, Kemp et al. 2005, Boynton et al. 2008). Land conversion from forest to agriculture in the 18^{th} century led to a large pulse of sediment into streams and creeks in the Bay watershed, which contributed to the growth of tidal marshes, particularly tidal fresh and brackish marshes in the 19^{th} century (Kemp et al. 2005). By the late 20^{th} century, there was growing concern about whether the tidal marshes in the Bay would be able to accrete enough sediment to keep pace with accelerated SLR (Kearney et al. 2002, Kemp et al. 2005). Along with the loss of many tidal wetlands in the Bay, there has been a loss in the capacity of the

remaining marshes to perform nutrient removal services (Kemp et al. 2005). What does the future hold for the Chesapeake Bay?

Chesapeake Bay

To answer this question, I examined the projected change in Chesapeake Bay tidal wetlands for each of the SLR scenarios over the 21st century. Overall, total tidal wetland area (ha) is estimated to decrease by 2100 (Table 2; Figure 2) for all SLR scenarios (0.69, 1.0, and 1.5 m). By 2025, no substantial change is estimated for total tidal wetland area for any of the three scenarios (Table 2). There is a more evident change in projected wetland area by 2050, with the most estimated loss (about 16%; Table 2) seen in the 1.5 m scenario. Interestingly, by 2075 the estimated loss of tidal wetland area in both the 1.0 and 1.5 m SLR scenarios are about the same (30%) and by 2100 the estimated loss of wetland area in the 1.0 m scenario is greatest (43%), surpassing even the 1.5 m scenario (39%; Table 2).

In order to better understand what contributes to this change in total tidal wetlands, it is helpful to examine the trends for tidal fresh, brackish, and salt marshes separately. The estimated loss of tidal fresh wetland area is consistent throughout all years, with the greatest loss occurring in the 1.5 m scenario (70%; Table 3; Figure 3). Brackish marsh loss is similar to that of tidal fresh, showing a consistent decreasing trend by 2100 and the greatest estimated loss in the 1.5 m scenario (89%; Table 4; Figure 4). However, the loss does not appear to be linear, as was the case with the tidal fresh marshes, and by 2075 all three SLR scenarios converge, with only a difference of about 5% between SLR scenarios by 2100

(Table 4; Figure 4). Unlike tidal fresh and brackish marshes, salt marsh area increases with SLR, particularly under the 1.5 m projection. By 2050, the estimated gain in salt marsh area reaches a peak (267%; Table 5) under the 1.5 m scenario. Predicted salt marsh area, while still greater than existing areal extent, starts to decline by 2075 (Figure 5). Future studies, when feasible, should consider projections into the 22nd century to see if salt marsh fate will be similar to that of tidal fresh and brackish marshes in the 21st century. To further illustrate the estimated loss of total tidal wetland area expected in the Bay by the end of the 21st century, I provide maps for each of the simulation scenarios and reference conditions of wetland coverage in Figures 6-9. There is an overall decline in tidal wetlands, particularly tidal fresh and brackish marshes, and the biggest changes are seen on the Eastern shore of the Bay.

For nitrogen removal services, estimated denitrification (i.e. absolute values and percent change) provided by tidal wetlands declined under the SLAMM projections of changed wetland coverage in the 21st century, especially under higher SLR scenarios (Table 2; Figure 10). By 2100, there is an estimated loss in denitrification services by about 77% under the 1.5 m scenario (Table 2). Predicted nitrogen burial (i.e. absolute values and percent change) follows a similar trend (Table 2; Figure 11), with about 68% loss in burial services by 2100 under the 1.5 m scenario (Table 2). I also considered how the individual types of wetlands contributed to these results and found similar trends as seen previously for tidal wetland area, a not unexpected result given the way that these removal processes are estimated using multipliers to represent denitrification and burial

rates. Tidal fresh and brackish marshes show a consistent decline in nitrogen removal services, with the greatest estimated loss occurring by 2100 under the 1.5 m rise scenario (70%; Table 3 and 89%; Table 4, respectively). As estimated salt marsh area increases with increasing SLR so does estimated denitrification and nitrogen burial services. Again, there is a peak by 2050 in projected denitrification and nitrogen burial (Table 5), followed by a decline (though still positive) in estimated nitrogen removal services in salt marshes, though this increase does not offset losses of nitrogen removal in lower salinity marshes. These results present some interesting wetland responses leading to the question: Why is there an overall decrease in tidal wetland area and nitrogen removal services when salt marshes are increasing in the Bay with long term SLR? To answer this, it is useful to compare the nitrogen removal rates for tidal fresh, brackish, and salt marshes. Recall that nitrogen removal services in salt marshes occur at lower rates compared to brackish and tidal fresh marshes (Table 1). Salinity influences the nitrogen cycling in marsh sediments. For instance, absorption of ammonium is dependent upon salinity (Seitzinger et al. 1991, Giblin et al. 2010) and the availability of ammonium is necessary for coupled nitrification/denitrification to occur. Under low salinities (i.e. tidal freshwater sediments), ammonium is stored in sediments and available for nitrification, whereas, under high salinities (i.e. salt marshes) ammonium is released from sediments (Seitzinger et al. 1991, Giblin et al. 2010). Furthermore, sulfide concentrations tend to be higher in salt marshes compared to tidal freshwater marshes, which can inhibit nitrification (Giblin et al. 2010). Lastly, DNRA has been shown to compete with denitrification for nitrate

in high salinity environments (Giblin et al. 2010). So, while predicted salt marsh area and nitrogen removal services are expected to increase, likely due to the conversion of brackish or tidal fresh wetlands, salt marshes are less efficient when it comes to denitrification and nitrogen burial, removing only about 4.1% and 18%, respectively, of the nitrogen that a tidal fresh marsh does.

To understand why salt marshes are predicted to increase while brackish and tidal fresh wetlands are predicted to decrease it is valuable to consider features of the SLR modeling approach. SLAMM incorporates a salinity algorithm to model salt-water intrusion with long-term SLR (Craft et al. 2009). Salt-water intrusion into estuaries and groundwater is a growing concern associated with future SLR (Hilton et al. 2008). Modeling studies suggest increases in SLR will also lead to an increase in salinity, which will have an impact on salinity sensitive species, such as tidal fresh and brackish marshes (Hilton et al. 2008). One modeling study in the Delaware Bay estimates an increase in salinity of 0.4 associated with an increase in SLR by 0.13 m when stream discharge is seasonally low (Hilton et al. 2008). Salt-water intrusion into the estuary and tidal creeks is likely to displace brackish and, particularly, tidal fresh wetland species. In oligohaline marshes, it has been found that an increase in salinity accompanied by an increase in flooding can lead to a decrease in seedling recruitment and germination for many plant species, particularly annual species (Baldwin et al. 1996, Baldwin et al. 2001). If there are no barriers to landward migration, these species may move further up into the estuary; however,

given the intense pressure from urban encroachment around the Bay, there may be limits to migration.

Maryland River Basins

The U.S. EPA developed TMDLs for the Chesapeake Bay that require Delaware, Maryland, New York, Pennsylvania, Virginia, West Virginia, and the District of Columbia to each develop WIPs for pollutant reductions to meet the TMDL restoration goal for the Chesapeake Bay. Of these restoration goals, the total nitrogen allocations, or allowable loadings, from these jurisdictions to the Chesapeake Bay is 84 billion g yr^{-1} by 2025(USEPA 2010).

Focusing on TMDLs for an individual state is important, especially given the findings from the previous section, which suggest that certain parts of the Bay (e.g. Eastern Shore, Figures 6-9) will be more vulnerable to long term SLR than others. As a result, I focused on the Maryland tidal basins (Figure 1) to assess the vulnerability of tidal wetland area and nitrogen removal services to SLR by 2025, when TMDL restoration goals are required to be met. The total nitrogen allocation for Maryland is 18 billion g yr^{-1} by 2025 (USEPA 2010).

In the five Maryland basins, tidal wetland area is estimated to increase slightly, ~ 1% (Figure 12) by 2025 under the 0.25 m rise scenario. I also examined the change in tidal wetland area for the individual basins. Overall, this slight increasing trend in tidal wetland area (ha) is seen in the Eastern Shore, Western Shore, and Susquehanna River basins (Table 6). The greatest positive and negative changes are predicted to occur under the 0.25 m rise scenario. By 2025, the Eastern and Western shore basins and the Susquehanna basin are

estimated to have tidal wetland gains of about 1%, 5%, and 6%, respectively, under the 0.25 m scenario (Figure 13). In comparison, the Patuxent and Potomac River basins are predicted to have a decrease in tidal wetland area (Table 6), losses of about 2% and 4%, respectively, under the 0.25 m scenario (Figure 13). I also examined the types of wetland changes occurring within each basin. For instance in the Eastern and Western shore basins, salt marsh area is estimated to double and quadruple (Tables 7 and 8, respectively) and in the Susquehanna, tidal fresh marshes are estimated to increase slightly and brackish marshes are expected to develop (Table 9) from the reference to the 0.25 m scenario. Very little change is predicted in the Patuxent River basin (Table 10) and in the Potomac River basin gains in salt marsh area, accompanied by losses in tidal fresh and brackish marsh are estimated by 2025 under the 0.25 m rise scenario (Table 11).

Despite the slight increase in tidal wetlands under the 0.25 m scenario, I estimate a loss of denitrification and nitrogen burial potential by ~ 15% and 11% (Figure 12), respectively, as a result of converting fresh and brackish wetlands to salt marsh habitat. Estimated losses in denitrification services in the individual basins are ~ 16% and 10% for the Eastern and Western shore basins, respectively, by 2025 (Figure 14) under the 0.25 m scenario. Similarly, losses of about 2% and 13% are estimated for the Patuxent and Potomac River basins, respectively (Figure 14). Finally, a gain in denitrification, estimated to be ~ 7%, is expected in the Susquehanna River basin under both 0.17 m and 0.25 m rise scenarios (Figure

14). The trends for nitrogen burial are similar to those described above for denitrification (Figure 15).

For absolute values of nitrogen removal see Table 6. Total estimated nitrogen removal, summed for the Maryland basins, is ~ 31 billion g N yr^{-1} and 30 billion g N yr^{-1} under the 0.17 and 0.25 m rise scenarios, respectively, by 2025. In comparison, the total nitrogen allocation for the Maryland basins is 18 billion g N yr^{-1} (USEPA 2010). The estimated ratio of total nitrogen removal to load allocation for the Maryland Basins is ~ 1.8 and 1.7 for the 0.17 and 0.25 m scenarios, respectively. These estimates suggest that tidal wetlands are removing more nitrogen than the load allocations required by restoration goals established for the Maryland basin by 2025. This highlights the importance of tidal wetlands, as the protection and restoration of these ecosystems will aid in reaching restoration goals.

In comparison to the results computed for the entire Chesapeake Bay watershed through the 21st century, the absolute values and percent change for tidal wetlands in the Maryland basins by 2025 is small, overall. However, there are some indications that change is expected to occur, particularly, the conversion of tidal fresh and brackish marshes into salt marshes, with the exception of the Susquehanna River basin, which is expected to gain some tidal fresh and brackish marshes by 2025 under the 0.25 m rise scenario (Tables 7-11). Despite this slight increase in tidal fresh and brackish marshes in the Susquehanna basin, there is expected to be an overall loss in nitrogen removal services in the basins. This is likely due to salt-water intrusion, resulting in the conversion of tidal fresh and

brackish marshes to salt marshes, which are less efficient when it comes to nitrogen removal (Table 1). It should also be noted that, given more time, the changes in these basins should be more prominent, as seen in the Bay by 2100; however, given that the TMDLs for nitrogen loadings are restoration goals set to be achieved by 2025, I focused on the same time frame for this study. Future studies should examine longer time scales to see if these trends continue beyond 2025. Changes in wetlands in Maryland, due to SLR, will likely not play an important role in TMDLs by 2025 but future SLR will likely be more significant.

Calvert County Watersheds

Calvert County lies within the Patuxent River basin, which is estimated to have a slight decline in tidal wetlands of about 2% by 2025 (Figure 13). The average load of nitrogen to the Patuxent River basin is about 15.8 g N m^{-2} yr^{-1}, with diffuse sources being the most prevalent, contributing about 51-70% of the total nitrogen (Boynton et al. 2008). Tidal wetlands are critical to the Patuxent River basin (Boynton et al. 2008, Williams et al. 2006) and, consequently, to Calvert County watersheds. As with the TMDL restoration goals for the basin study, the restoration goals for the WIP are set for the short-term, 2020. County governments are required to meet WIPs; however, the WIP implementation costs are often an impediment to reaching target load reductions (Calvert County 2013). For instance, the Maryland state government recommended Calvert County meet its required load reductions via upgrades to septic systems and stormwater management, which are quite costly to both the county and private property owners (Calvert County 2013). Furthermore, septic systems contribute about 4%

of the nitrogen pollution to the Bay (CBF 2012). Given the small contribution septic systems make to overall nitrogen pollution in the Bay and the costs associated with septic upgrades, this may not be the best way to meet restoration goals. The alignment of WIP nitrogen reduction goals with the nitrogen removal services naturally provided by tidal wetlands in the County might help reach the target load reductions. Furthermore, the protection and restoration of tidal wetlands within the County might be more cost effective when compared with septic upgrades and stormwater management.

The basis for my examination of the 22 Calvert County watersheds (Figure 16) was twofold. Firstly, I wanted to identify where in the county tidal wetlands are most prevalent, and, therefore, have the greatest potential to provide a natural buffer to nitrogen removal. Secondly, I wanted to compare the county watersheds with the most removal potential to the WIP restoration goals for nitrogen loading for the individual watersheds. While I performed the removal calculations for all the watersheds and the two SLR scenarios for 2025, I will only report the reference watershed results here. The reason for this is due to the small change seen in tidal wetland area by 2025. Given my results in the Maryland basin study, this is not surprising, as it appears a longer time step is necessary to see more substantial changes in wetland area resulting from SLR using the SLAMM modeling approach. The WIP restoration goals are set for 2020, which is why this study was originally focused on SLR scenarios for 2025. This analysis can still apprise county resource managers by identifying watersheds where wetlands have a particularly large contribution to nitrogen removal services,

essentially providing a natural nitrogen removal buffer, and normalizing those estimates to watershed based loads to help inform future restoration goals of where wetlands are most important for mediating land based loads.

The Calvert County WIP provides nitrogen reduction goals for each of the twenty-two 12-digit watersheds (Calvert County 2013). The highest nitrogen reduction goals (~ 25,000 – 48,000 kg N yr^{-1}) are set for Hunting, Fishing, St. Leonard, Mill, and Hall Creeks followed by Plum Point and Grays Creeks (~ 16,000 – 25,000 kg N yr^{-1}) (Figure 17). It is important to consider which of the twenty-two 12-digit watersheds have the natural capacity, via tidal wetlands, to remove nitrogen from the tidal creeks and, consequently, help with these reduction goals. The 12-digit watersheds providing the highest estimated nitrogen removal (i.e. ~ 40,000 - 69, 000 kg N yr^{-1}) are Hall, Fishing, Tyverne, Hunting, and St. Leonard Creeks, followed by Parkers, Ramsey, and Island Creeks, which are estimated to remove between 33, 000 and 39,000 kg N yr^{-1} (Figure 18). These watersheds have tidal wetlands estimated to remove high levels of nitrogen (~ 33, 000 to 69,000 kg N yr^{-1}), thus providing a natural buffer to the Bay (Figure 18). In contrast, Grays, Calvert Beach Run, and Plum Point Creeks, are a few of the county watersheds estimated to provide the lowest nitrogen removal services (~ 0 - 4845 kg N yr^{-1}). Of these 12-digit watersheds investigated thus far, Plum Creek and Grays Creek may potentially have unrealistically high nitrogen reduction goals, given the small amount of tidal wetlands present. Finally, I combined the above data to develop a ratio for estimated nitrogen removal to nitrogen loading (Figure 19). Interestingly, many of the watersheds with the

highest ratio of removal to loading are not the watersheds that I expected. For instance, Ramsey and Tyverne Creeks are estimated to have the highest ratio, between 2.9 to 4.0, whereas, Island, South, and Kings Branch Creeks are estimated to have the next highest ratio of removal to loading, between 2.3 to 2.8 (Figure 19). Buzzard, Graham, Tuckers, Lyons, Fishing, and Parkers Creeks have a ratio between 1.3 to 2.2 (Figure 19), which is a higher ratio of removal to loading when compared to the watersheds with the most tidal wetlands and highest estimated nitrogen removal services. I expected Hall, Hunting, and St. Leonard Creeks to have the highest ratio of nitrogen removal to loading, given the high estimates of nitrogen removal from the tidal wetlands present in these 12-digit watersheds (Figure 18). It is surprising, that these 12-digit watersheds have a nitrogen removal to loading ratio between 0.5 to 1.2 (Figure 19).

These estimates, while not providing predictions for the change in tidal wetland area for the Calvert County watershed under future SLR scenarios, do provide estimates of the 12-digit watersheds where wetlands are particularly important as normalized to incoming nitrogen loads. Furthermore, these data provide insight into where the largest nitrogen removals are occurring in county wetlands. I unexpectedly discovered that the watersheds with the most wetlands and the highest estimated nitrogen removal were not the watersheds with the highest ratios of nitrogen removal to loading. Tidal wetlands located at the boundary between the Calvert County 12-digit watersheds and estuarine receiving waters are also exposed to tidal sources of nitrogen, some of which may be sourced to distant rivers such as the Susquehanna and Patuxent as well as other,

adjacent counties, which have fewer wetlands to attenuate the loads. As a result, these contributions from outside the county watersheds could be contributing to the unexpectedly low ratios of removal to loading for our county watersheds with more wetlands and higher estimates of nitrogen removal.

Subtidal Estimates

There is much uncertainty as to what happens to tidal marshes that become submerged. Do they continue to provide nitrogen removal services after submergence? I did not conduct a full-scale subtidal analysis, but I did make several estimates based on subtidal nitrogen removal rates from the literature (Table 12; Boynton et al. 2008, Nixon et al. 1996, Green 2005). With the assumption that tidal wetland loss is a conversion to subtidal sediments, I computed a subtidal estimate of nitrogen removal for the Chesapeake Bay under the 0.69 m SLR scenario for 2050 (Table 13).

Considering a tidal wetlands loss of ~ 5.31×10^7 m^2, I estimated subtidal denitrification and nitrogen burial as ~ 228, 000 kg N yr^{-1} and 398,000 kg N yr^{-1}, respectively, using rates of nitrogen removal reported in literature for subtidal sediments (Table 12). In contrast to the subtidal nitrogen removal estimates, the tidal wetland denitrification and nitrogen burial estimates are ~ 16 million kg N yr^{-1} and 31 million kg N yr^{-1}, respectively, for the Chesapeake Bay by 2050 under the 0.69 m SLR scenario. The gains in estimated subtidal nitrogen removal for Bay sediments are small compared to those of tidal wetlands in the Bay, which suggests the possible gain in subtidal nitrogen removal will not offset the loss of tidal wetlands, particularly tidal freshwater wetlands.

The computed subtidal sediment estimates (Table 13) are within the same magnitude, though slightly lower, as those reported for Patuxent River denitrification (540, 000 kg N yr^{-1}) and nitrogen burial (511,000 kg N yr^{-1}) by Boynton et al. (2008). Similarly, According to Boynton et al. (2008), estimated nitrogen losses are less precise when compared to inputs and, as such, subtidal denitrification and burial rates are considered accurate to within 15% and 20%, respectively. These caveats are likewise true for my estimates of wetland nitrogen losses. However, it must be emphasized that very little research has been done to explore the biogeochemistry of submerged wetland soils and how erosion and submergence will affect the nutrient removal processes these sediments provide.

Assumptions and Uncertainty

SLAMM Shortcomings:

As with most modeling tools, SLAMM has advantages and disadvantages. SLAMM is an ecosystem-based model, which replicates general wetland processes (i.e., loss, conversion, salt-water intrusion, etc.) that are associated with long-term SLR at a large spatial scale (Fagherazzi et al. 2012). In order to accomplish this, SLAMM gives up the mechanistic complexity common in smaller-scale models, which focus on a single point in the marsh (Fagherazzi et al. 2012). Ecosystem models can simulate simple feedback mechanisms between vegetation and the environment, such as sedimentation and hydrodynamics, either directly, in one time step, or indirectly, in multiple time steps (Fagherazzi et al. 2012). As an indirect calculation model, SLAMM makes it easier to run

simulations in a timely manner even as the simplicity of the model prohibits simulating complex feedback mechanisms (Fagherazzi et al. 2012). Other modeling tools (Leonard and Luther 1995, Temmerman et al. 2005, Mudd et al. 2009) incorporate multiple feedback mechanisms (e.g. canopy structure, hydrodynamics, sedimentation, and species interactions, etc.) that may influence wetland stability at any given time. The added model complexity associated with incorporating these feedback mechanisms slows down simulation run time (Fagherazzi et al. 2012).

It is also worthwhile, when interpreting the simulation outputs from SLAMM, to consider additional shortcomings. For instance, there is no accounting for the mass balance of solids. In the model, as wetlands become submerged and erosion occurs, the marsh platform and its sediments simply disappear. Furthermore, since SLAMM is not a hydrological model, it does not incorporate factors such as evapotranspiration, precipitation, and water velocity, which we know to be important influences on wetland habitat productivity and stability. The large spatial extent that SLAMM is capable of simulating comes at the cost of these simplifying assumptions. For instance, seasonal and annual variability is ignored and accretion and subsidence rates are assumed to be constant. In reality, tidal wetlands are influenced by, and often constrained by, interacting parameters on multiple sales, such as, diurnal (tidal cycles), seasonal (growing seasons, streamflow), and annual (mean precipitation and temperatures), in addition to extreme events (e.g. storms, droughts, etc.). Finally, SLAMM incorporates a simplifying assumption about localized rates of subsidence and

accretion. SLAMM assumes these rates are linear and do not change over time (Glick et al. 2008). Accretion rates used in the SLAMM dataset were tidal fresh (6.1 mm yr-1), brackish (4.8 mm yr-1), and salt (4.0 mm yr-1), which were compiled from 58 marsh studies (Glick et al. 2008). When taking into consideration restoration goals associated with sediment reduction and the projected loss and conversion of wetlands in the Bay (i.e. reduced sediment capture potential), this assumption is not realistic.

As a first step to selecting and applying a model to a scientific question, it is imperative to identify the goals of a research project to match detail in mechanistic process, temporal, and spatial resolution to the task at hand. Despite the shortcomings and assumptions associated with SLAMM, it is a useful and accessible tool, and is often used by scientists and managers due to its simplicity and ease of use (Fagherazzi et al. 2012). Furthermore, when SLAMM simulations are combined with wetland specific measurements (e.g. nitrogen removal) preliminary predictions can be made as to how long term SLR will influence these wetland functions and services (Fagherazzi et al. 2012).

Nitrogen Removal and SLR Assumptions:

There are some assumptions I made to calculate the nitrogen removal estimates for tidal wetlands. For instance, I made the assumption that rates of denitrification and nitrogen burial are constant spatially, given a particular type of wetland, and temporally. Boynton et al. (2008) found that rates of nitrogen removal varied depending on the spatial scale and, more specifically, removal services decreased from high to low marsh elevations. Additionally, Boynton et

al. (2008) report temporal variations in nitrogen removal services, such as a decrease in nitrogen removal from early spring through fall. I also made the assumption that nitrogen removal rates, taken from literature, were consistent throughout the Bay for that particular type of wetland (i.e. tidal fresh, brackish, or salt marsh). Again, we know this is not necessarily the case, as each individual wetland has specific hydrological and climatic processes and nutrient loading that interact to create a particular wetland community. However, I did constrain my literature review to nitrogen removal studies in Chesapeake Bay tidal wetlands. These nitrogen removal rates are comparable to rates reported outside the Chesapeake Bay. Morris (1991) reported denitrification rates for salt and tidal fresh marshes in Massachusetts, which range between 0.4-14.3 g N m^{-2} yr^{-1}. The low end of this range is comparable to the salt marsh denitrification rates reported by Thomas and Christian (2001; Table 1) and the high end of this range is comparable to the tidal freshwater marsh rate reported by Greene (2005; Table 1). In another Massachusetts study, White and Howes (1994) nitrogen burial (3.7-4.1 g N m^{-2} yr^{-1}) rates for salt marshes, which are comparable to the rates reported by Thomas and Christian (2001; Table 1).

I expect, given the uncertainty of climate change effects on wetlands and the prevalence of eutrophication in the Bay, that the nitrogen removal rates taken from literature values (Table 1) reported over the past decade and extrapolated over the next century, may overestimate my removal estimates. Tidal wetlands serve as ecotones in the landscape, providing a natural buffer between terrestrial uplands and coastal waters. As such, tidal wetlands are well situated to remove

excess nutrients and sediments before these pollutants make it to the Bay. It is likely that extreme nutrient enrichment may alter these natural buffering processes (Kemp et al 2005) and the capacity for long-term nitrogen removal may be reduced. If this is indeed the case, these "current" values extrapolated through the 21st century may lead to an overestimate of nitrogen removal given the projected wetland loss expected. However, the purpose here is to simply provide a broad scale estimate of how tidal wetlands might respond to long term SLR and how this may effect nitrogen removal services.

It is also important to note the uncertainty associated with nitrogen removal rates for specific types of wetlands with future SLR. Salt marshes, located farther from nitrogen sources, are typically nitrate limited (Baldwin 2013) and conversion to dinitrogen gas typically depends on coupled nitrification-denitrification. As salt marshes migrate further up the Bay and nitrate sources become more readily available, direct denitrification (i.e. the conversion of nitrate directly to di-nitrogen gas) could increase salt marsh denitrification rates. It is unlikely that salt marsh denitrification rates will get as high as tidal fresh rates but they may increase over current rates given increased nitrogen inputs.

Finally, my use of the pre-existing SLAMM 5.0.2 dataset for estimating the loss of tidal wetland area may produce underestimates of wetland loss. The dataset incorporated SRES SLR scenarios taken from IPCC's Fourth Assessment Report (AR4; IPCC 2007). The AR4 estimates did not include ice sheet melting, which is now thought to contribute ~ 0.9-1.1 mm yr^{-1} to the global average SLR (Miller et al. 2013), which could make the SLAMM 5.0.2 projections

underestimate tidal wetland loss by the end of the century. Furthermore, the conversion of wetland to subtidal habitat may also result in a release of nitrogen that cannot be accounted for here. However, given the uncertainty associated with climate change, SLR, and how tidal wetlands will respond to both, it is difficult to predict the long-term effects of SLR.

Conclusions and Recommendations

These nitrogen removal analyses, though broad in scale and utilizing "back of the envelope" calculations, provide estimates of potential Chesapeake Bay tidal wetland response to short term and long term SLR. Examining multiple scales promotes sound, science-based management. For instance, conducting a case study, such as with the Calvert County 12-digit watersheds, allows a finer scale look at the nitrogen removal role of tidal wetlands, which can then be extrapolated to larger scales. Tidal wetlands play an important role in pollution reduction in the Bay, as they often serve as nutrient sinks, effectively removing these pollutants from further degradation of Bay water quality (Seitzinger et al. 1988, Boynton et al. 2008). In some cases, the inability to accrete sediments with increasing SLR rates can convert the tidal wetlands into a source of nutrients and sediments, as is the case with about 50% the tidal marshes in the Chesapeake Bay (Boynton et al. 2008, Kemp et al. 2005). High rates of marsh loss on the Maryland Eastern shore have been correlated to interior pond formation, which coalesce over time to create large open water areas (Kearney et al. 1988). To further exacerbate the situation, these marshes are constrained by adjacent land use, which effectively creates a barrier to marsh migration (Kearney et al. 1988).

As shown in this work on various scales, tidal wetlands provide a natural buffer against nitrogen pollution. On the state scale, estimates suggest Maryland tidal wetland area will change very little by 2025 due to projected SLR. Consequently, these natural buffers should help Maryland meet 2025 restoration goals. On the county scale, there can often be a disproportionate amount of wetlands and, consequently, naturally occurring nitrogen removal potential within a watershed. When considering nitrogen load reductions at a county scale, it is important to realize that the local tidal wetlands are not just processing local nitrogen. Tidal creeks receive nitrogen inputs from estuarine and large riverine sources, which could be attenuated by tidal wetlands within the county. The alignment of restoration goals with tidal wetland protection can be extrapolated to larger scales. Tidal wetlands may not fare as well under long term SLR, as seen with the Chesapeake Bay study. There is already concern regarding the potential negative effects of salt-water intrusion on species not accustomed to higher salinity ranges (Baldwin et al. 1996, Hilton et al. 2008, Weston et al. 2011). Another concern is that tidal wetlands may not be able to migrate landward, due to urbanization pressures. As such, tidal wetlands should be considered when resource managers are developing restoration goals to reduce pollutants to the Bay. Managers should consider these issues and attempt to restore and protect tidal wetlands, particularly tidal freshwater wetlands, which have higher nitrogen removal rates, as much as possible to help maintain these ecosystem services into the future.

FIGURES

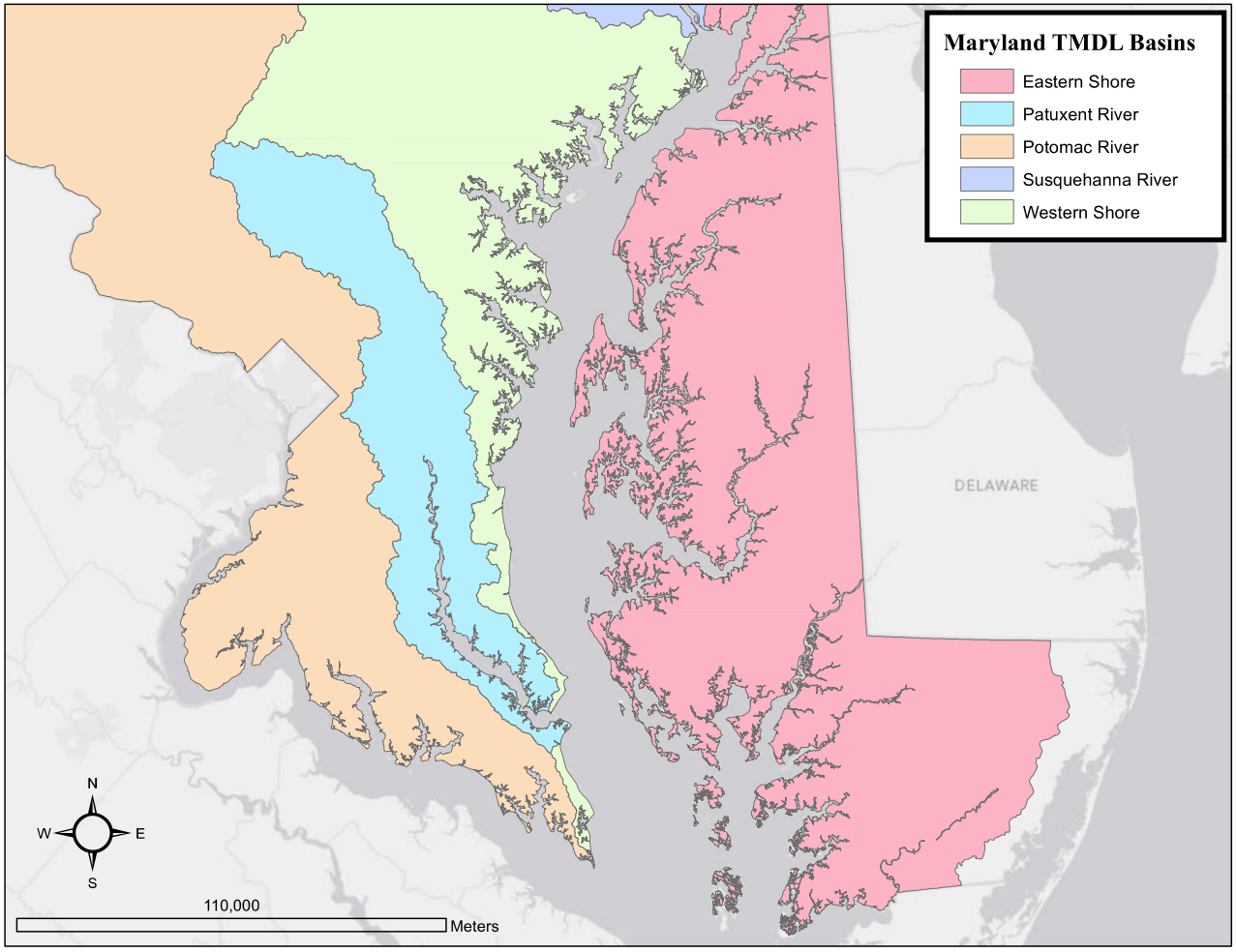

Figure 1 Reference map of the Maryland major river basins. Map based on Maryland basin TMDLs.

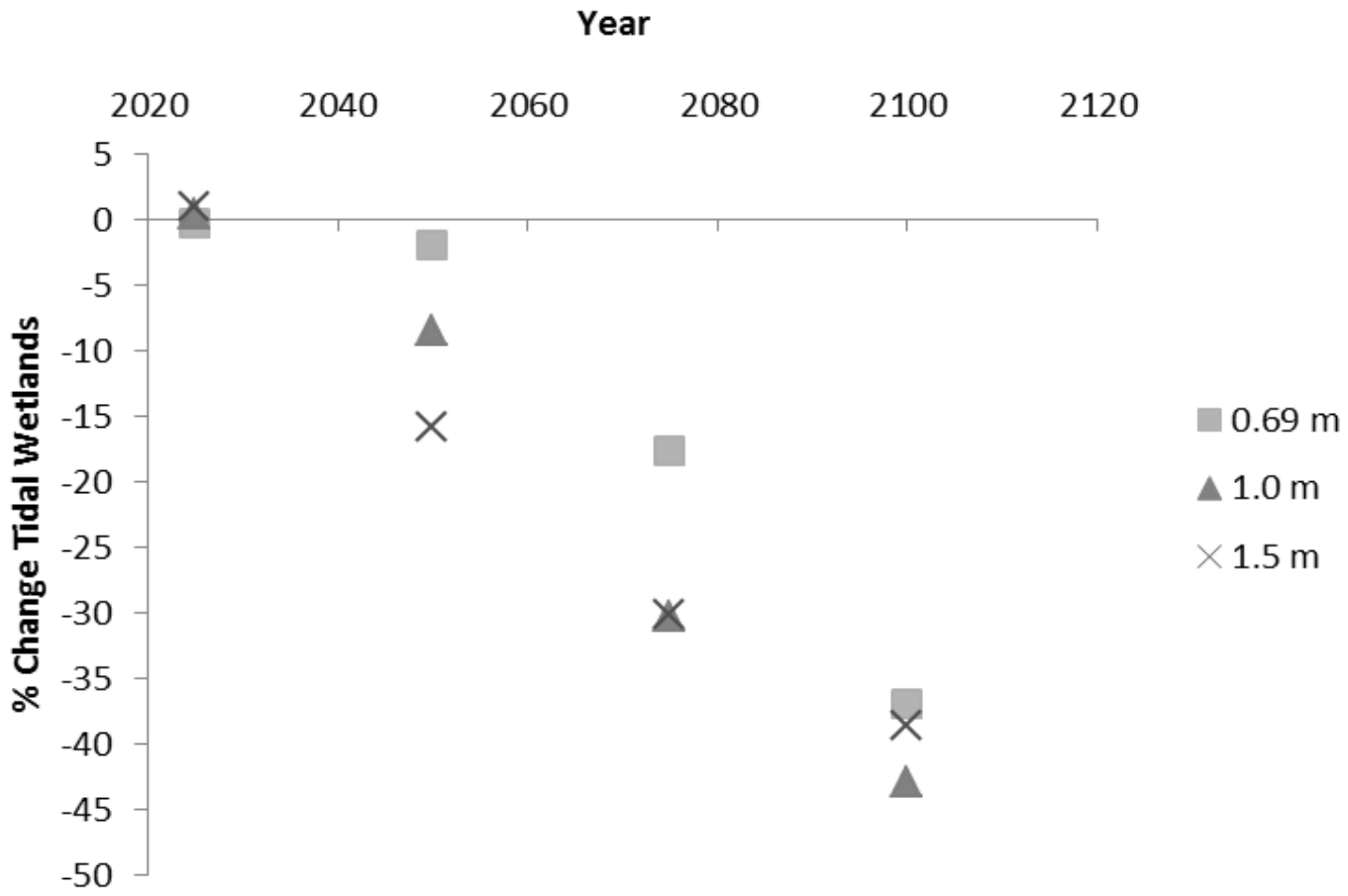

Figure 2 Percent change of all Chesapeake Bay tidal wetland area over the 21st century, based on projections using 0.69, 1.0, and 1.5 meter SLR scenarios.

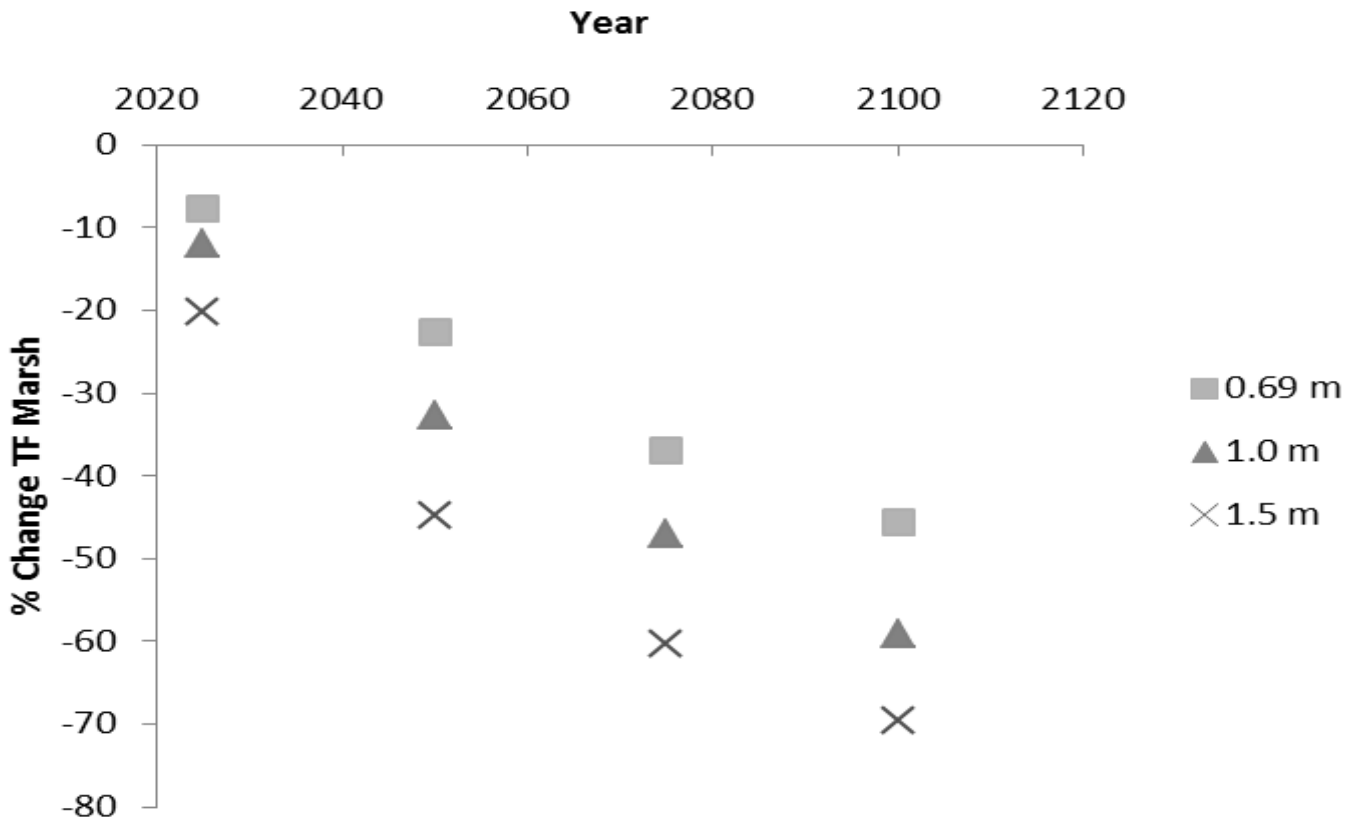

Figure 3 Percent change of tidal fresh wetland area over the 21st century, based on projections using 0.69, 1.0, and 1.5 meter SLR scenarios. TF = Tidal Fresh.

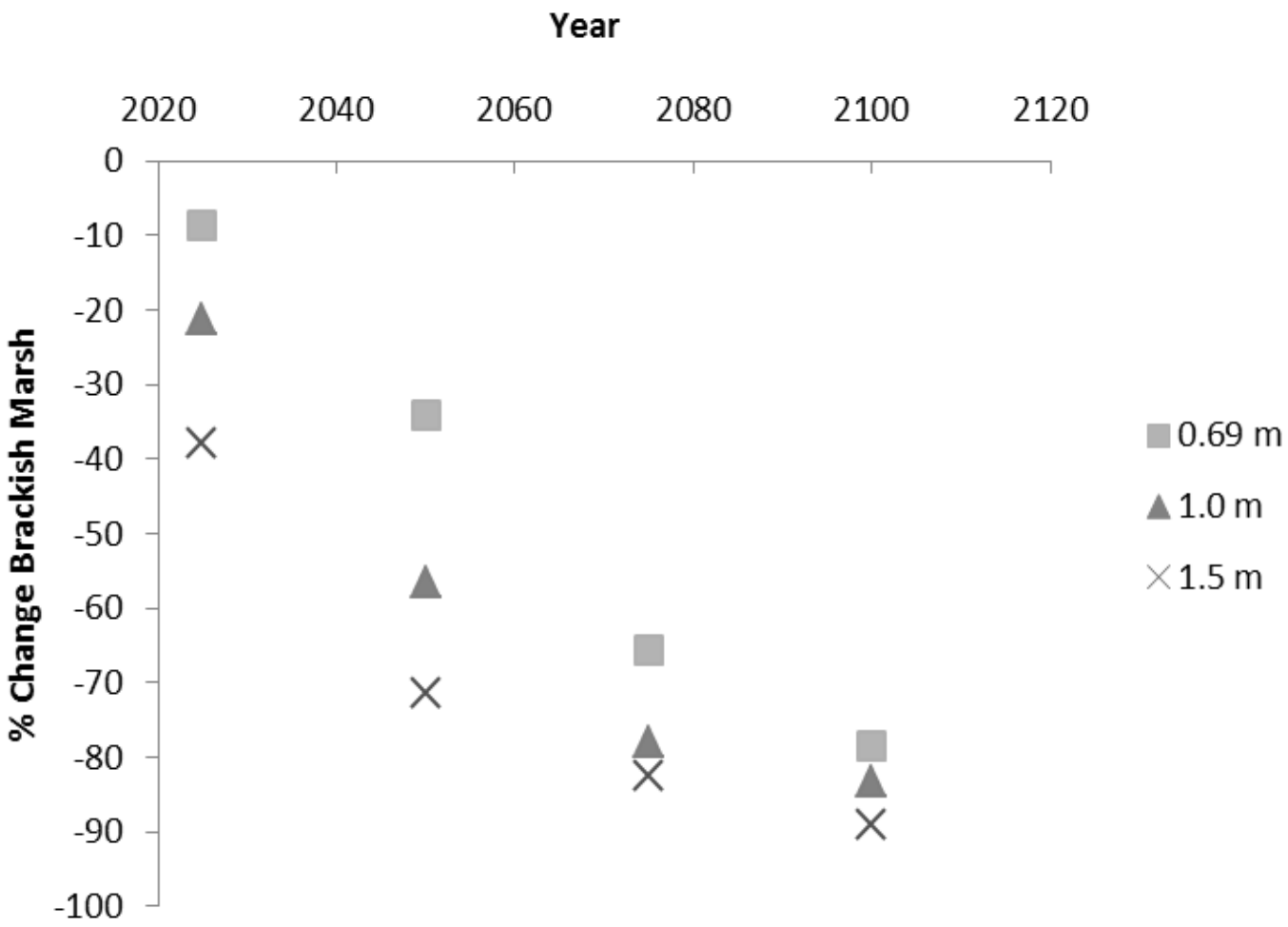

Figure 4 Percent change of brackish marsh area over the 21st century, based on projections using 0.69, 1.0, and 1.5 meter SLR scenarios.

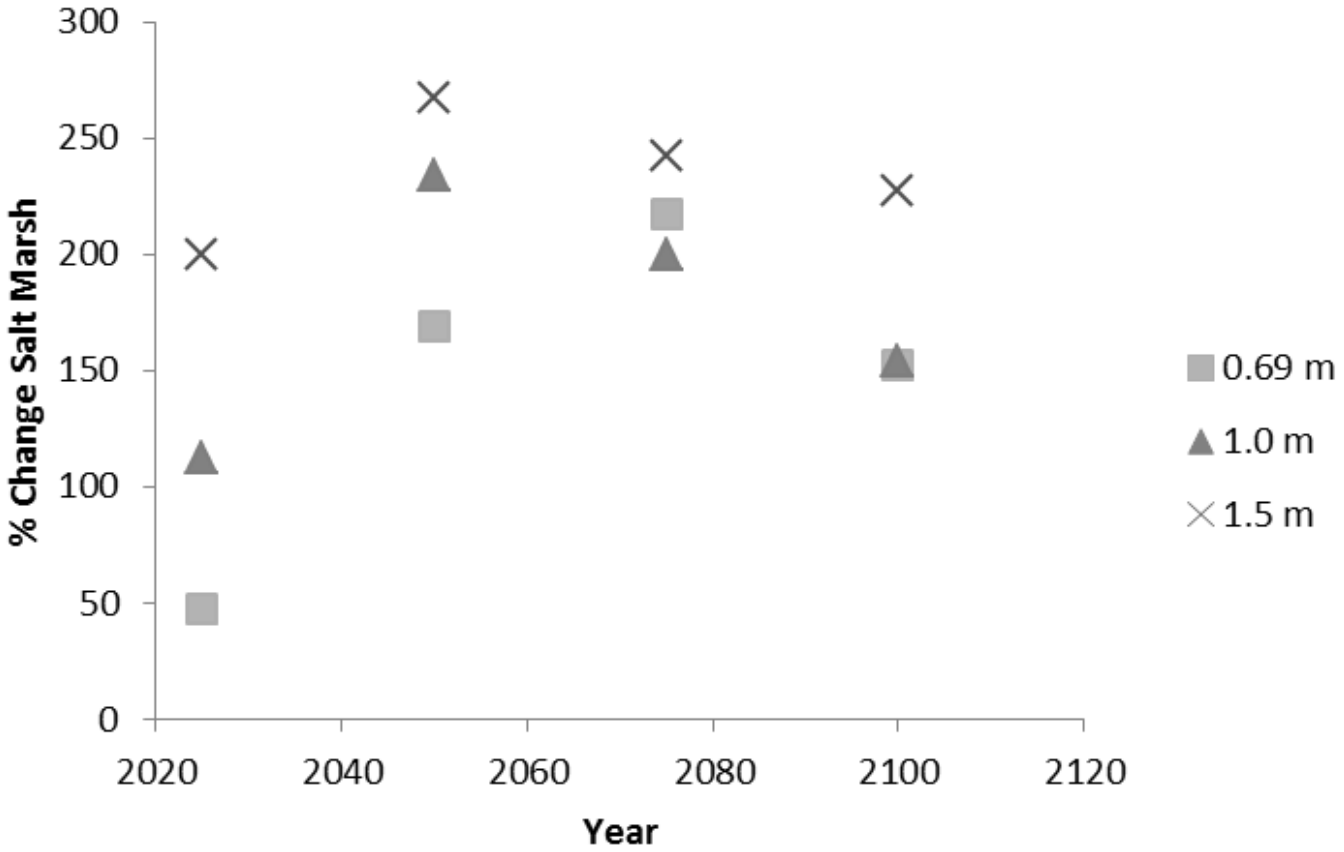

Figure 5 Percent change of salt marsh area over the 21st century, based on projections using 0.69, 1.0, and 1.5 meter SLR scenarios.

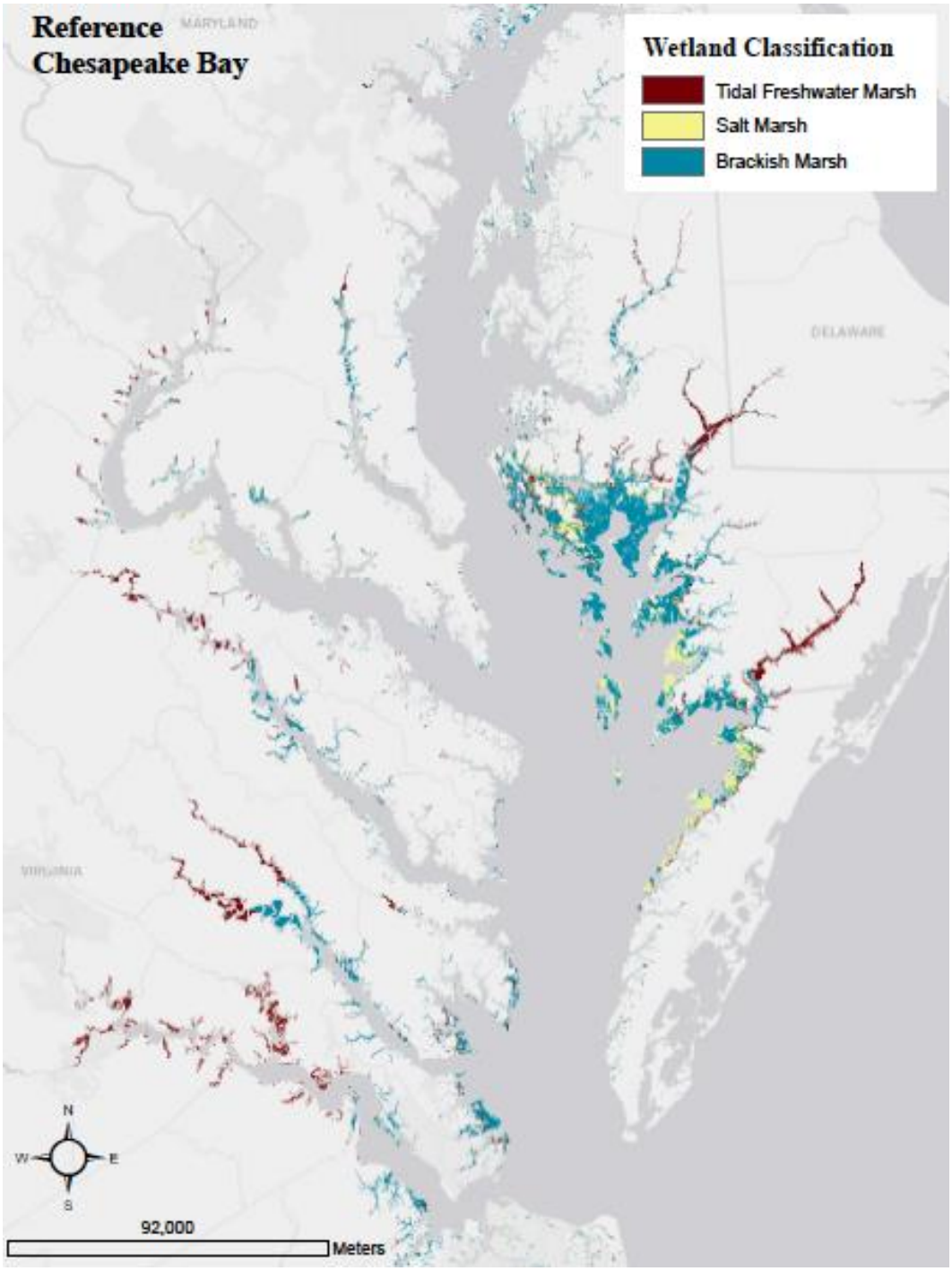

Figure 6 Reference map showing tidal wetland area in the Chesapeake Bay. Map based upon SLAMM 5.0 simulation of initial conditions.

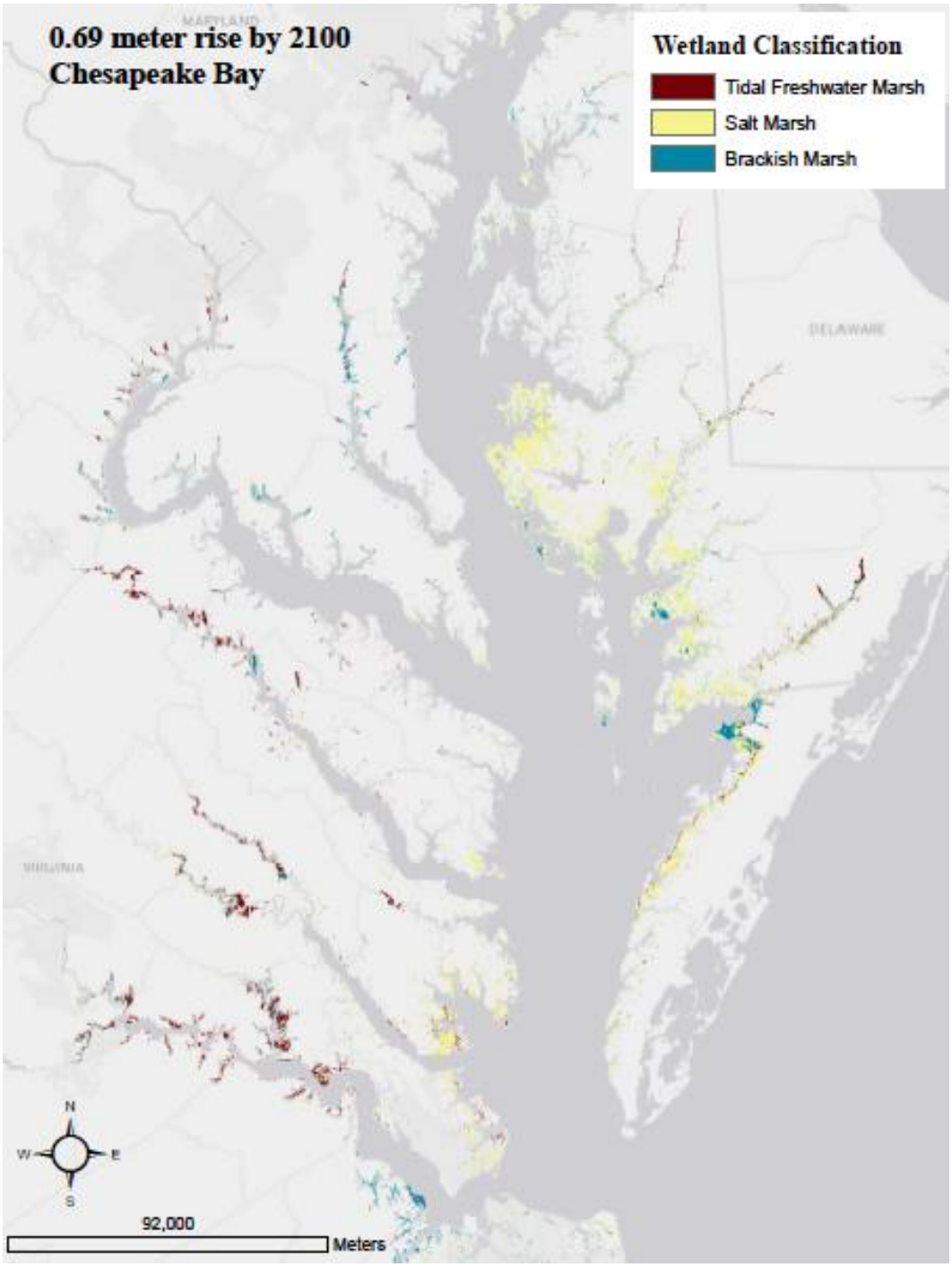

Figure 7 Map showing tidal wetland area in the Chesapeake Bay by 2100 under the 0.69 meter SLR scenario. Map based upon SLAMM 5.0 SLR projections.

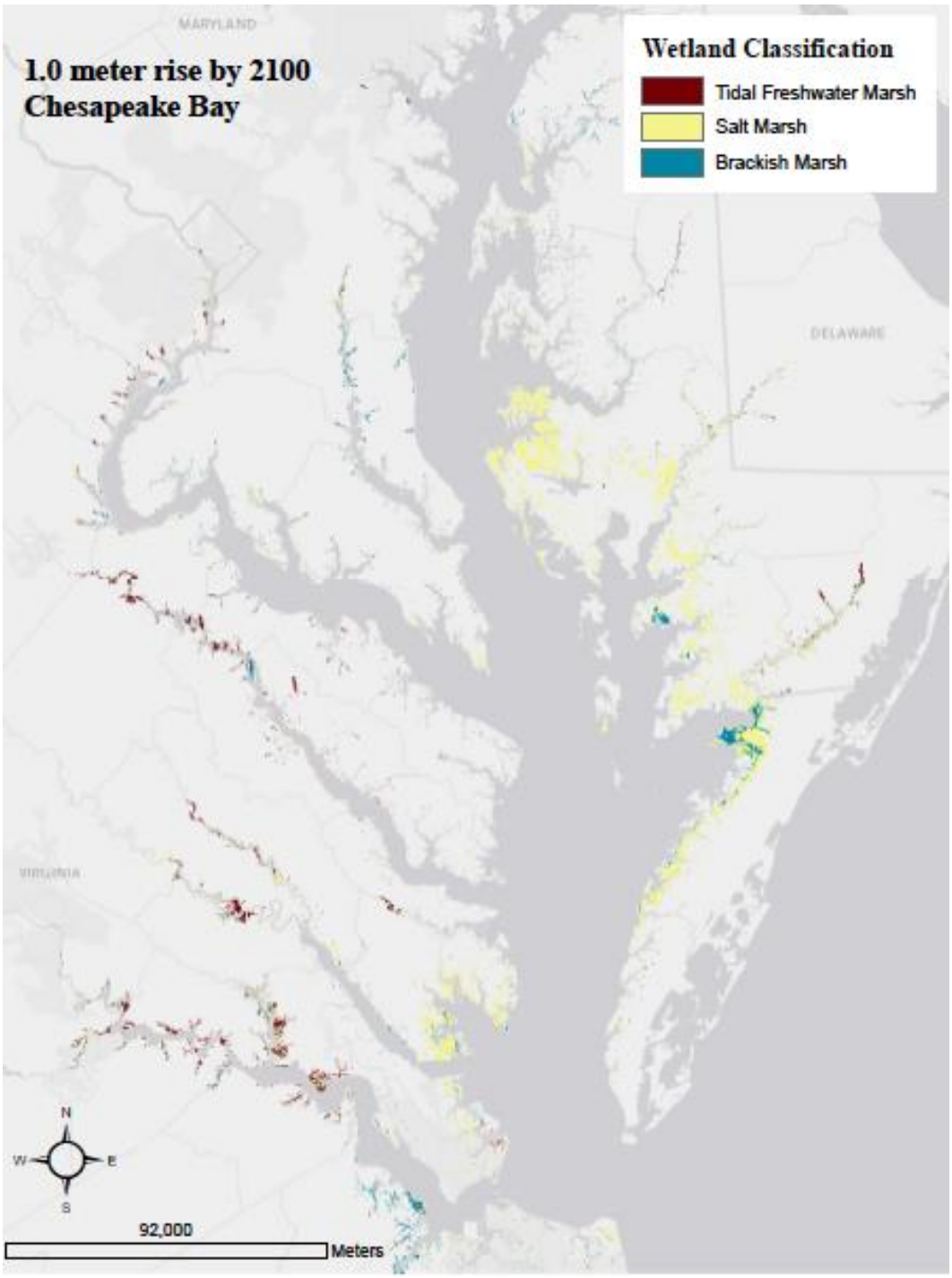

Figure 8 Map showing tidal wetland area in the Chesapeake Bay by 2100 under the 1.0 meter SLR scenario. Map based upon SLAMM 5.0 SLR projections.

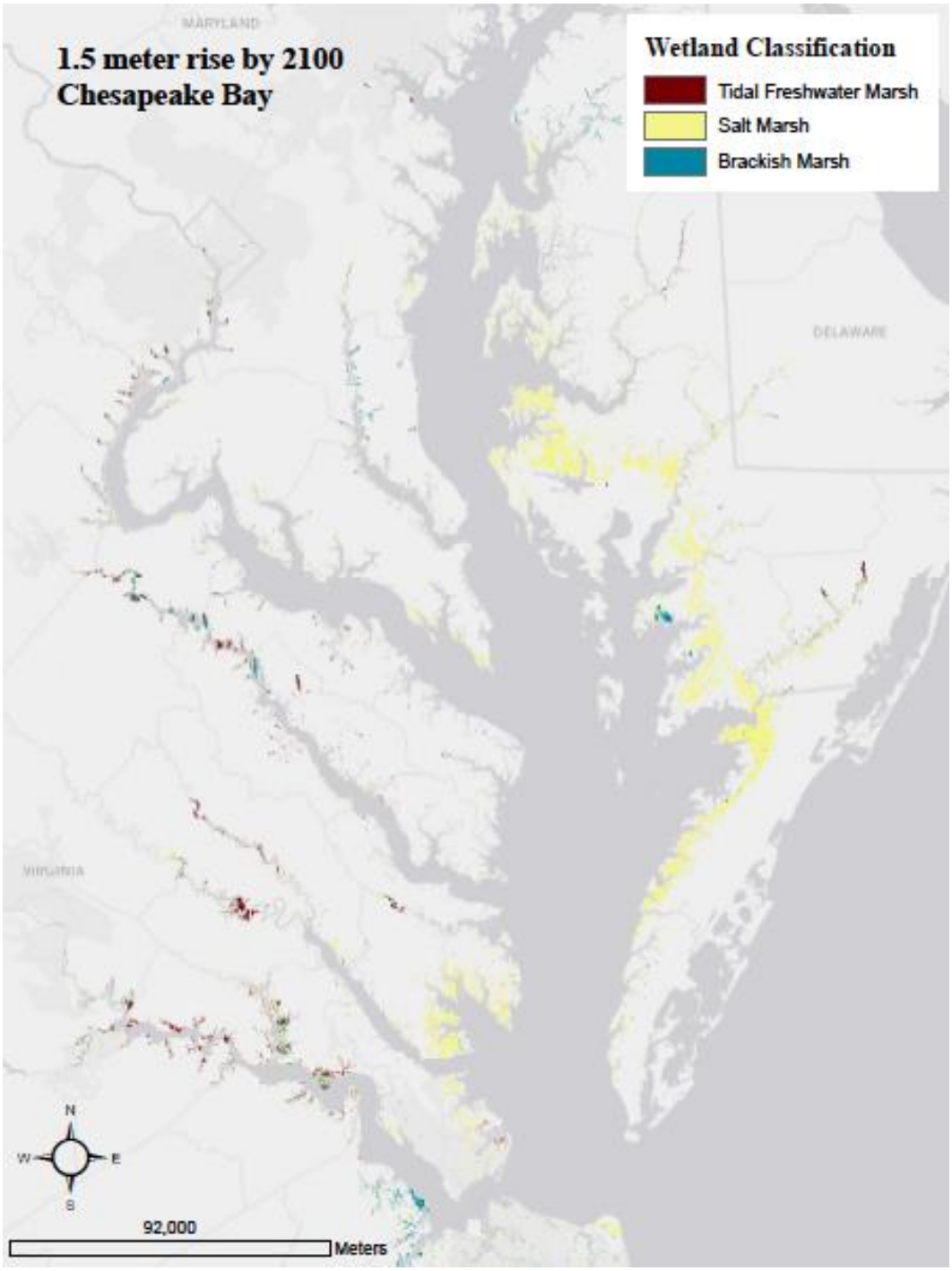

Figure 9 Map showing tidal wetland area in the Chesapeake Bay by 2100 under the 1.5 meter SLR scenario. Map based upon SLAMM 5.0 SLR projections.

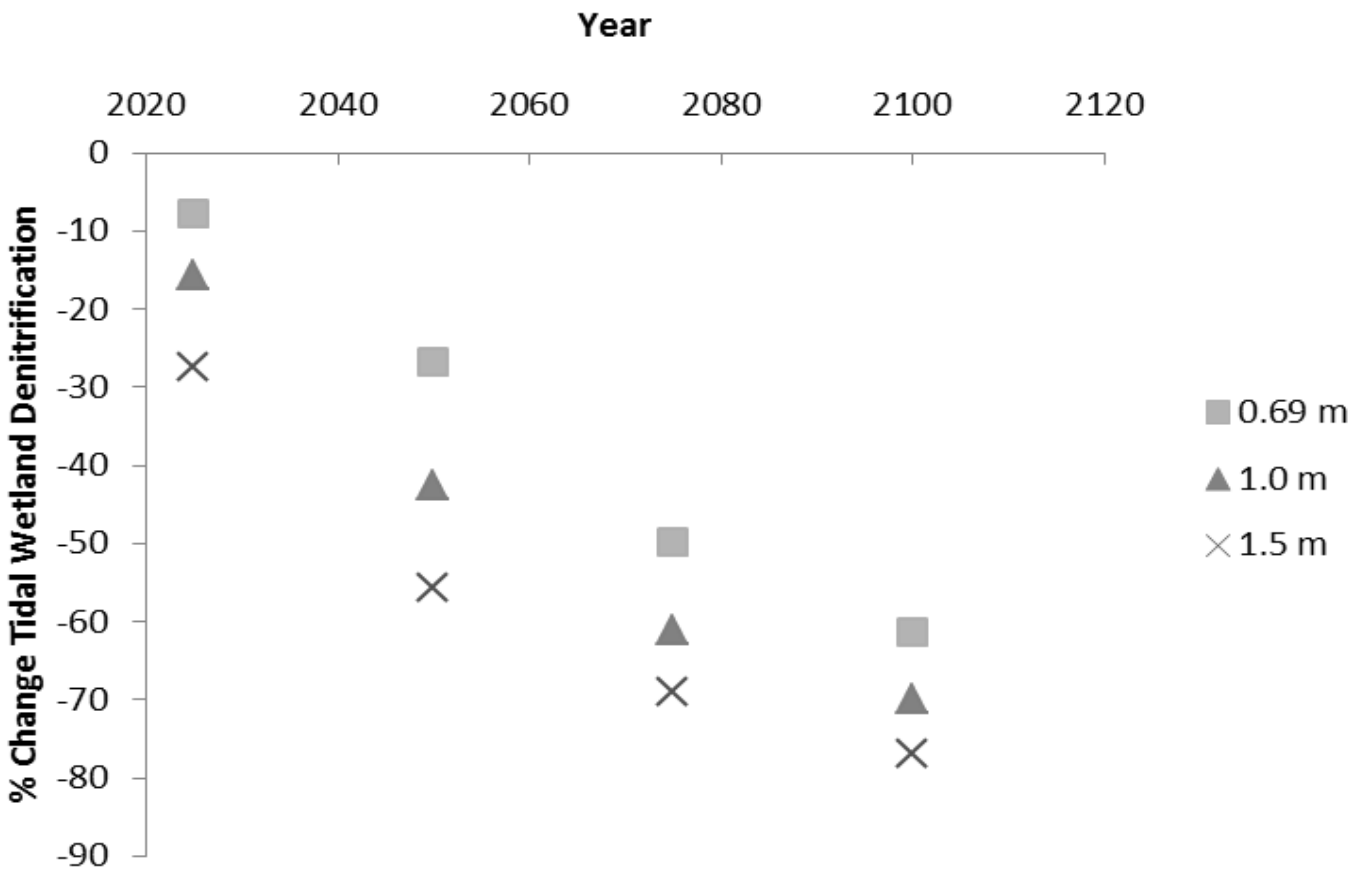

Figure 10 Percent change in denitrification for all Chesapeake Bay tidal wetlands over the 21st century, based on projections using 0.69, 1.0, and 1.5 meter SLR scenarios.

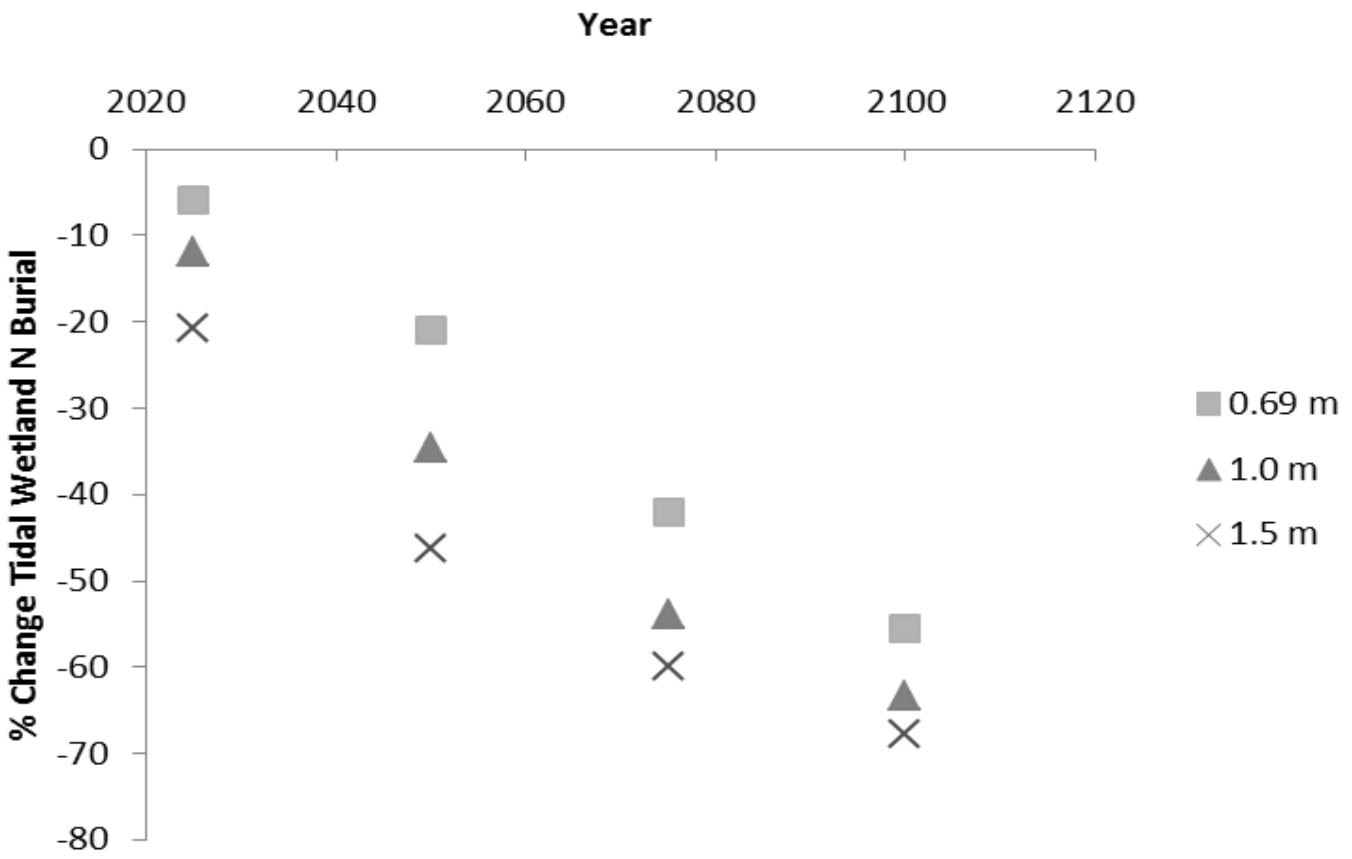

Figure 11 Percent change in nitrogen burial for all Chesapeake Bay tidal wetlands over the 21st century, based on projections using 0.69, 1.0, and 1.5 meter SLR scenarios.

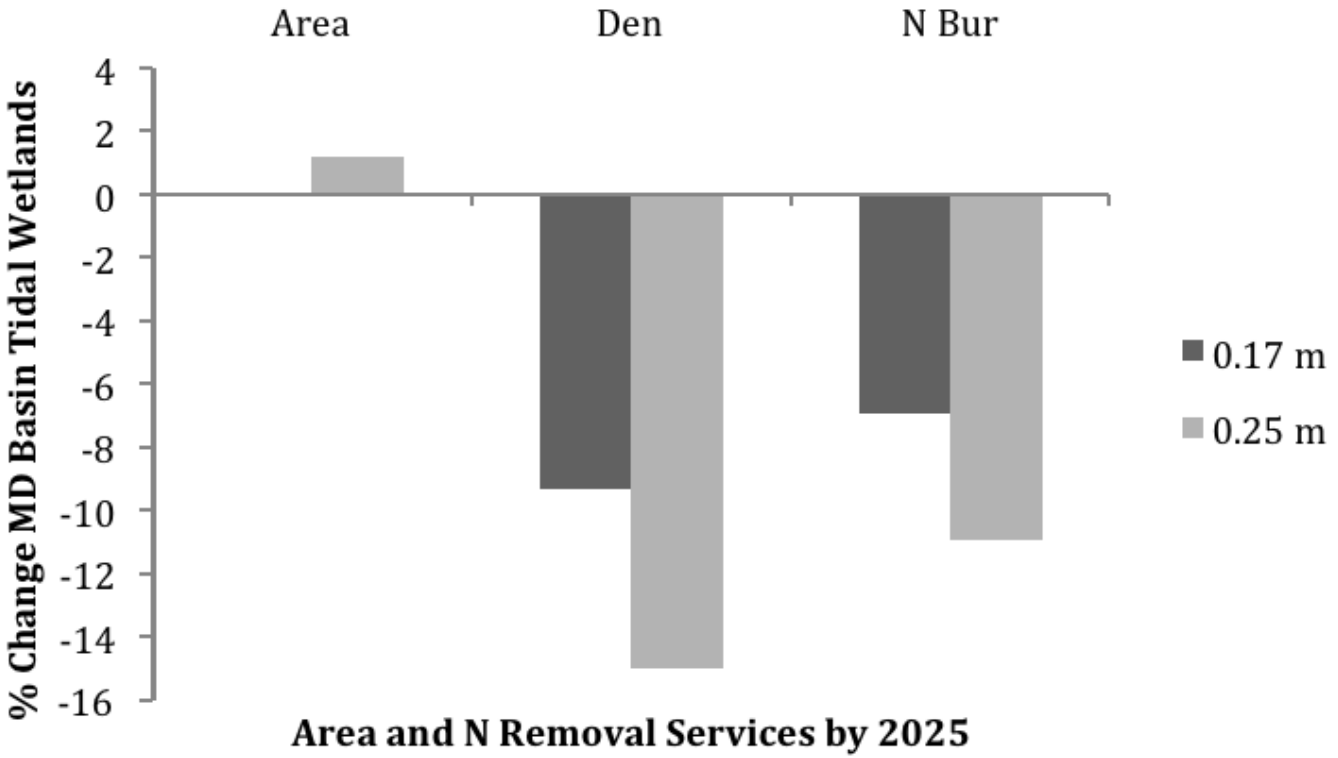

Figure 12 Percent change in tidal wetland area and nitrogen removal services for all the Maryland major river basins, based upon projections of 0.17 and 0.25 meter SLR scenarios by 2025. Den = denitrification and N Bur = nitrogen burial.

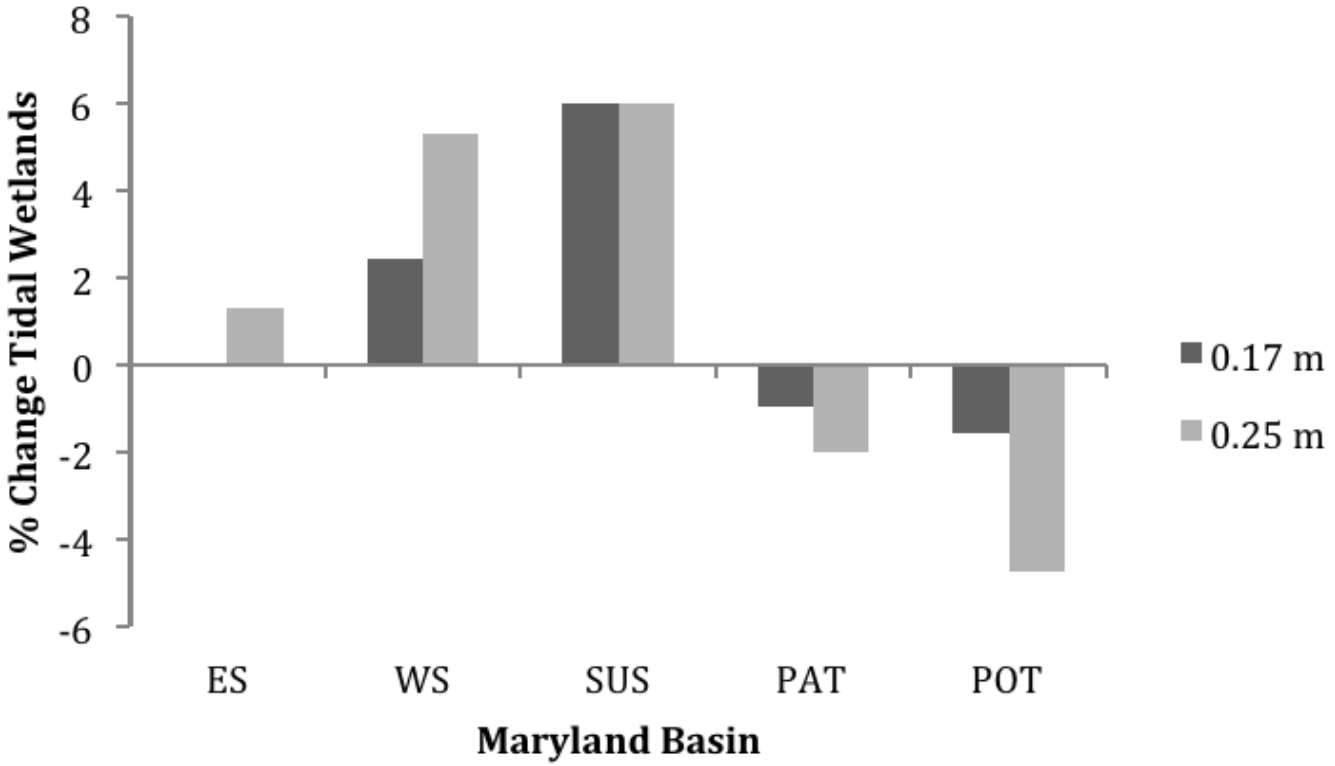

Figure 13 Percent change in tidal wetlands for each of the Maryland major river basins, based upon projections of 0.17 and 0.25 meter SLR scenarios by 2025. ES = Eastern Shore, WS = Western Shore, SUS = Susquehanna River, PAT = Patuxent River, POT = Potomac River.

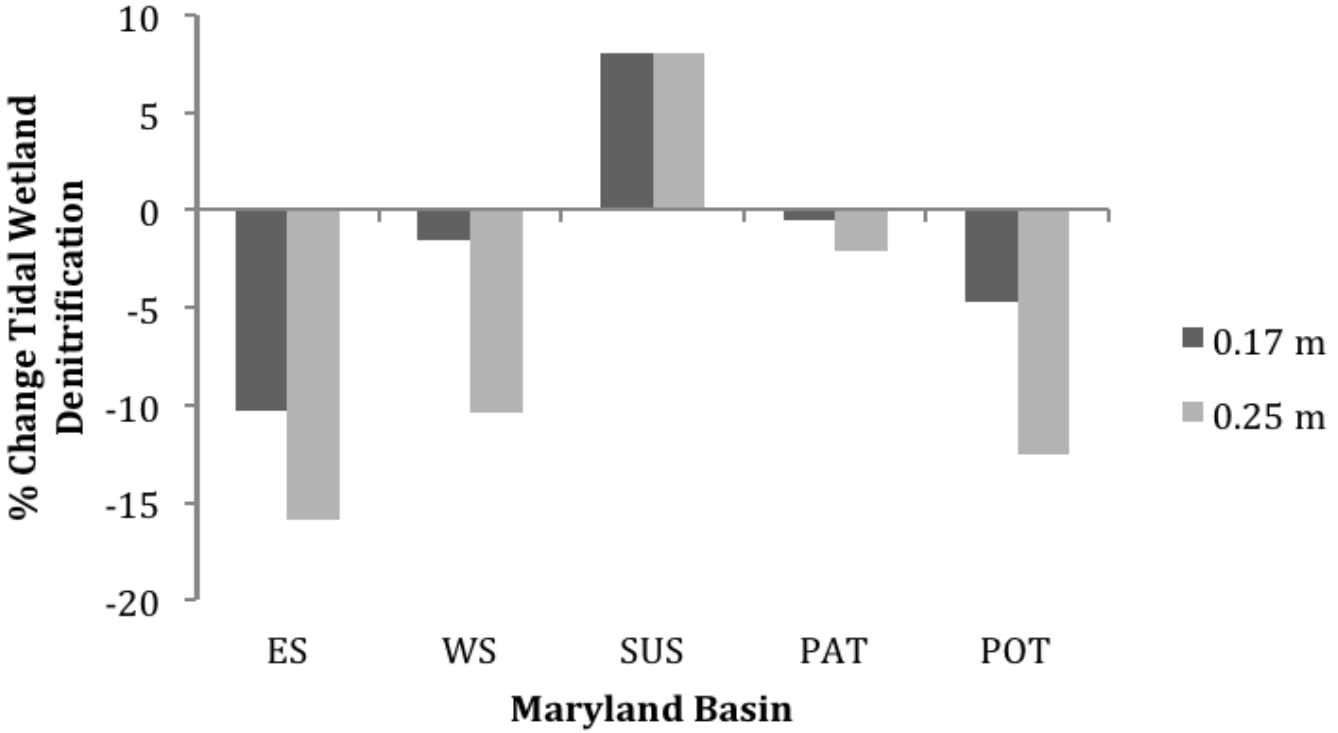

Figure 14 Percent change in tidal wetland denitrification for each of the Maryland major river basins, based upon projections of 0.17 and 0.25 meter SLR scenarios by 2025. ES = Eastern Shore, WS = Western Shore, SUS = Susquehanna River, PAT = Patuxent River, POT = Potomac River.

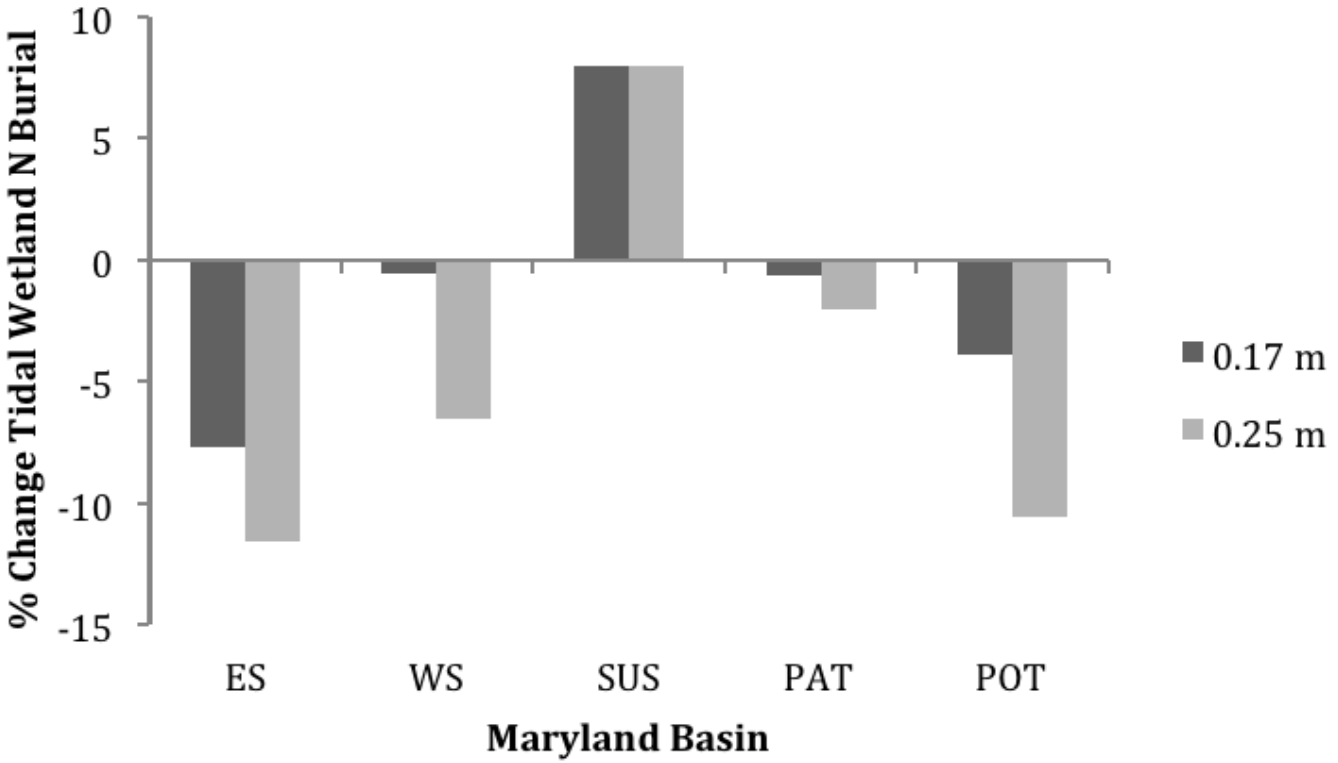

Figure 15 Percent change in tidal wetland nitrogen burial for each of the Maryland major river basins, based upon projections of 0.17 and 0.25 meter SLR scenarios by 2025. ES = Eastern Shore, WS = Western Shore, SUS = Susquehanna River, PAT = Patuxent River, POT = Potomac River.

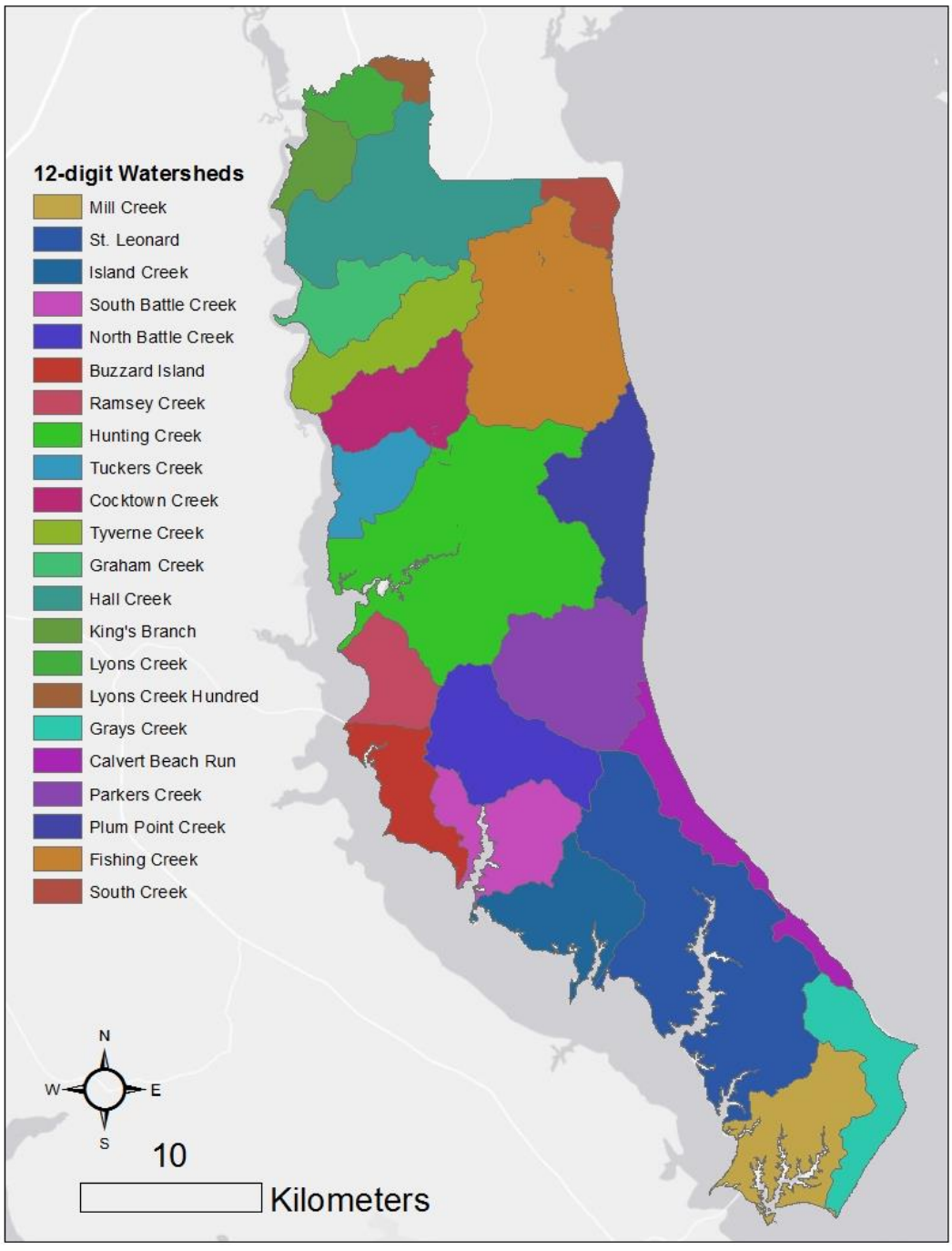

Figure 16 Map showing the 22 Calvert County 12-digit watersheds**.**

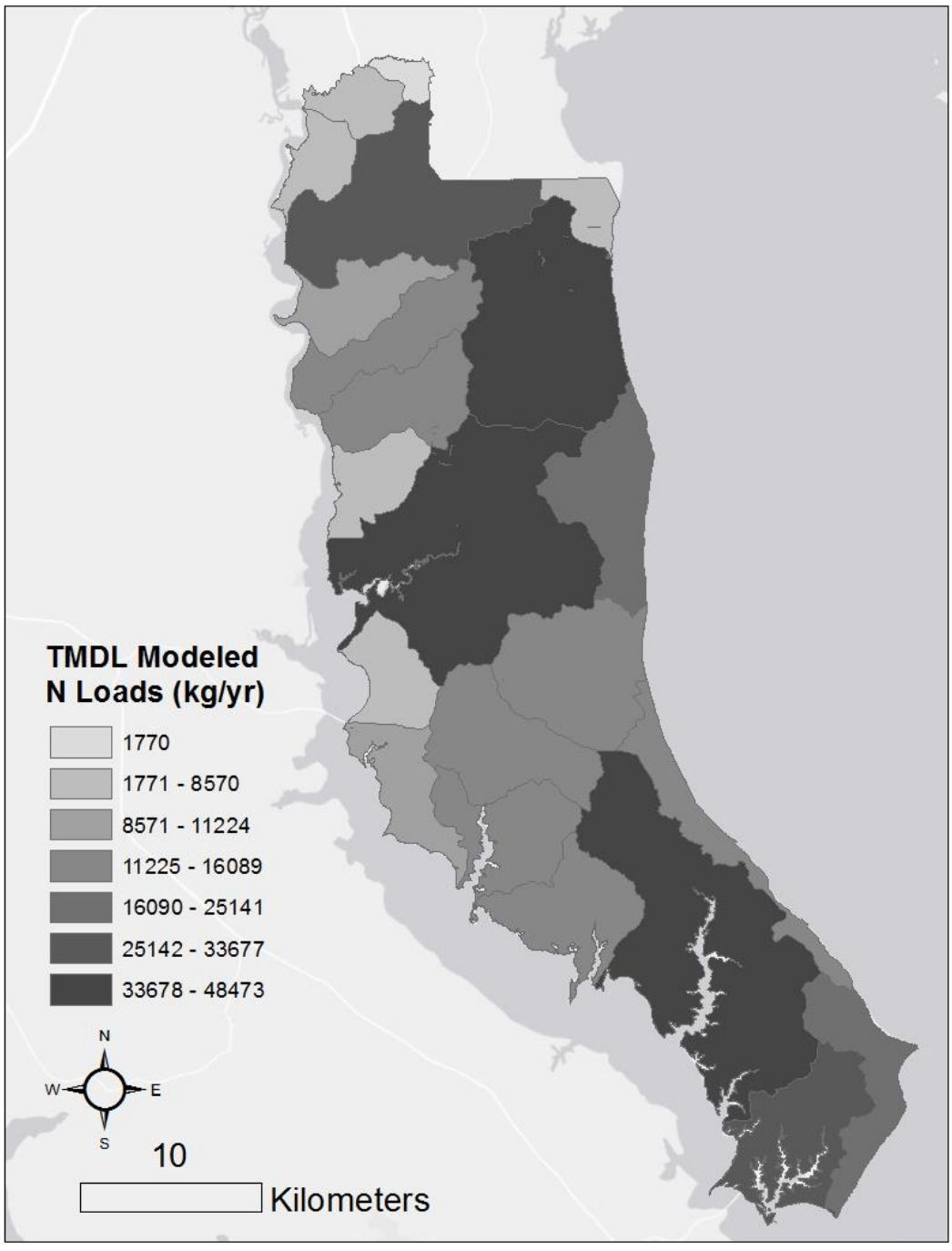

Figure 17 Map showing the 22 Calvert County 12-digit watersheds and the associated TMDL nitrogen load allocation for 2025. Nitrogen loads provided by Dr. David Brownlee (personal communication).

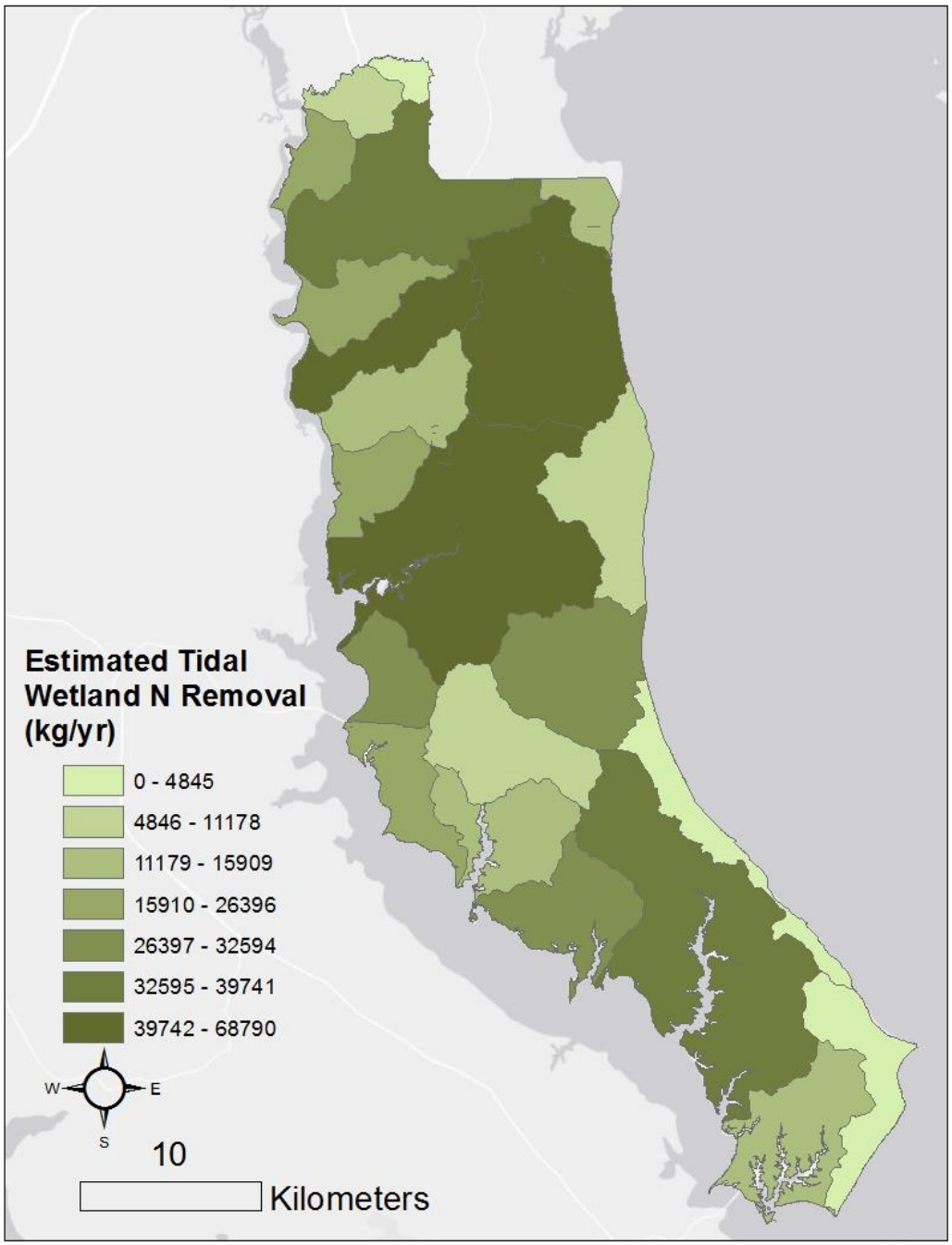

Figure 18 Map illustrating the estimated nitrogen removal in Calvert County, Maryland tidal wetlands for the 12-digit watersheds.

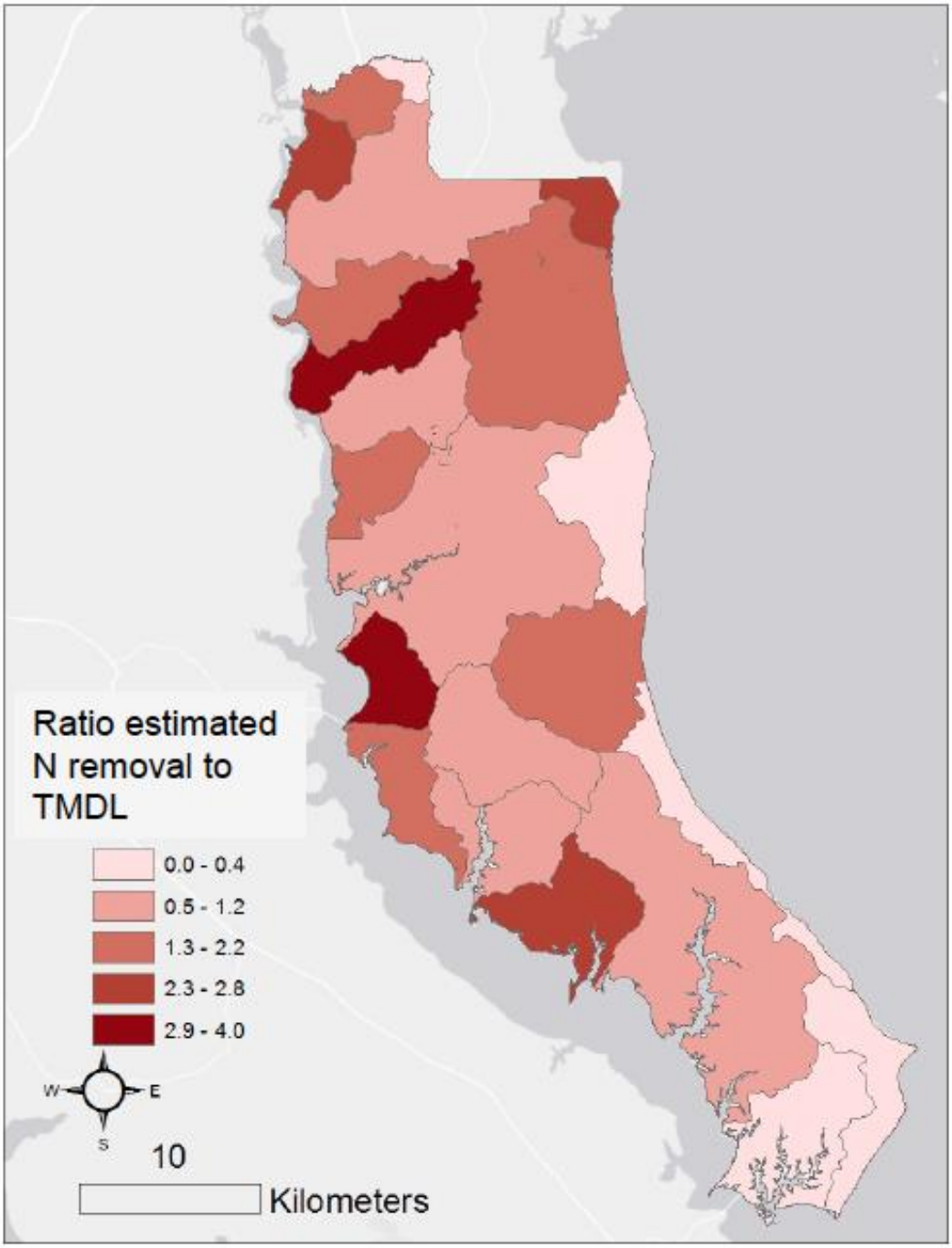

Figure 19 Map illustrating the ratio of estimated nitrogen removal in the Calvert County, Maryland 12-digit watershed tidal wetlands to nitrogen load allocations.

TABLES

Table 1 N Removal Literature Review: Summary of literature review denitrification and nitrogen burial rates used in estimates of nitrogen removal for tidal wetlands.

Wetland Category	Nitrogen Removal Services	Source
	Denitrification ($g\ N\ m^{-2}\ yr^{-1}$)	
Tidal Fresh	14.7	Greene 2005
Brackish	7.4	Kemp 2006
Salt	0.6	Thomas & Christian 2001
	Nitrogen Burial ($g\ N\ m^{-2}\ yr^{-1}$)	
Tidal Fresh	23.4	Merrill & Cornwell 2000
Brackish	13.6	Merrill & Cornwell 2000
Salt	4.3	Thomas & Christian 2001

Table 2 Bay Tidal Wetlands: Summary of estimated wetland area, denitrification, nitrogen burial, and corresponding percent change values for all tidal wetlands in the Chesapeake Bay based upon reference, 0.69, 1.0, and 1.5 meter SLR projections over the 21st century.

Total Tidal						
Year	**Wetland Area (ha)**	**Denitrification (x 10^6 g N yr^{-1})**	**N Burial (x 10^6 g N yr^{-1})**	**% Change Wetland Area**	**% Change Denitrification**	**% Change Burial**
			Reference			
1996	267520	22077	39464			
			0.69 m rise			
2025	266584	20390	37135	0	-8	-6
2050	262212	16159	31218	-2	-27	-21
2075	220447	11105	22853	-18	-50	-42
2100	168662	8561	17562	-37	-61	-55
			1.0 m rise			
2025	268375	18618	34781	0	-16	-12
2050	244676	12663	25831	-9	-43	-35
2075	186665	8572	18214	-30	-61	-54
2100	152818	6663	14430	-43	-70	-63
			1.5 m rise			
2025	270026	16029	31310	1	-27	-21
2050	225248	9773	21212	-16	-56	-46
2075	186967	6817	15846	-30	-69	-60
2100	164301	5084	12693	-39	-77	-68

Table 3 Tidal Fresh**:** Summary of estimated wetland area, denitrification, nitrogen burial, and corresponding percent change values for tidal fresh wetlands in the Chesapeake Bay based upon reference, 0.69, 1.0, and 1.5 meter SLR projections over the 21st century.

Tidal Fresh						
Year	Wetland Area (ha)	Denitrification (x 10^6 g N yr^{-1})	N Burial (x 10^6 g N yr^{-1})	% Change Wetland Area	% Change Denitrification	% Change Burial
Reference						
1996	67873	9991	15882			
0.69 m rise						
2025	62597	9214	14648	-8	-8	-8
2050	52497	7728	12284	-23	-23	-23
2075	42835	6305	10023	-37	-37	-37
2100	36966	5441	8650	-46	-46	-46
1.0 m rise						
2025	59717	8790	13974	-12	-12	-12
2050	45696	6726	10693	-33	-33	-33
2075	35903	5285	8401	-47	-47	-47
2100	27827	4096	6512	-59	-59	-59
1.5 m rise						
2025	54104	7964	12660	-20	-20	-20
2050	37531	5525	8782	-45	-45	-45
2075	26956	3968	6308	-60	-60	-60
2100	20607	3033	4822	-70	-70	-70

Table 4 Brackish Marsh: Summary of estimated wetland area, denitrification, nitrogen burial, and corresponding percent change values for brackish wetlands in the Chesapeake Bay based upon reference, 0.69, 1.0, and 1.5 meter SLR projections over the 21st century.

Brackish						
Year	Wetland Area (ha)	Denitrification (x 10^6 g N yr^{-1})	N Burial (x 10^6 g N yr^{-1})	% Change Wetland Area	% Change Denitrification	% Change Burial
Reference						
1996	161069	11855	21905			
0.69 m rise						
2025	147211	10835	20021	-9	-9	-9
2050	106117	7810	14432	-34	-34	-34
2075	55244	4066	7513	-66	-66	-66
2100	34462	2536	4687	-79	-79	-79
1.0 m rise						
2025	126865	9337	17254	-21	-21	-21
2050	70156	5163	9541	-56	-56	-56
2075	35250	2594	4794	-78	-78	-78
2100	26879	1978	3655	-83	-83	-83
1.5 m rise						
2025	100136	7370	13618	-38	-38	-38
2050	46178	3399	6280	-71	-71	-71
2075	27945	2057	3800	-83	-83	-83
2100	17582	1294	2391	-89	-89	-89

Table 5 Salt Marsh: Summary of estimated wetland area, denitrification, nitrogen burial, and corresponding percent change values for salt marshes in the Chesapeake Bay based upon reference, 0.69, 1.0, and 1.5 meter SLR projections over the 21st century.

Salt						
Year	Wetland Area (ha)	Denitrification (x 10^6 g N yr^{-1})	N Burial (x 10^6 g N yr^{-1})	% Change Wetland Area	% Change Denitrification	% Change Burial
Reference						
1996	38578	231	1676			
0.69 m rise						
2025	56776	341	2467	47	47	47
2050	103598	622	4501	169	169	168
2075	122368	734	5317	217	217	217
2100	97234	583	4225	152	152	152
1.0 m rise						
2025	81792	491	3554	112	112	112
2050	128824	773	5597	234	234	234
2075	115513	693	5019	199	199	199
2100	98112	589	4263	154	154	154
1.5 m rise						
2025	115786	695	5031	200	200	200
2050	141539	849	6150	267	267	267
2075	132066	792	5738	242	242	242
2100	126112	757	5480	227	227	227

Table 6 Maryland Basin Tidal Wetlands: Summary of estimated wetland area, denitrification, and nitrogen burial values for the Maryland Basins based upon reference, 0.17, and 0.25 meter SLR projections by 2025.

Tidal Wetlands			
Scenario	**Area (ha)**	**Denitrification (x 10^6 g N yr^{-1})**	**N Burial (x 10^6 g N yr^{-1})**
Eastern Shore Basin			
Reference	138485	10626	19360
0.17 m	138496	9530	17869
0.25 m	140320	8937	17127
Western Shore Basin			
Reference	7683	603	1094
0.17 m	7871	594	1088
0.25 m	8089	541	1023
Susquehanna River Basin			
Reference	19	3	5
0.17 m	21	3	5
0.25 m	21	3	5
Patuxent River Basin			
Reference	5267	423	761
0.17 m	5217	421	757
0.25 m	5162	414	746
Potomac River Basin			
Reference	5911	435	801
0.17 m	5818	415	770
0.25 m	5632	381	717

Table 7 Eastern Shore**:** Summary of estimated wetland area, denitrification, and nitrogen burial values for the Eastern Shore Basin, Maryland based upon reference, 0.17, and 0.25 meter SLR projections by 2025.

Eastern Shore Basin			
Scenario	**Area (ha)**	**Denitrification (x 10^6 g N yr^{-1})**	**N Burial (x 10^6 g N yr^{-1})**
Tidal Fresh			
Reference	24459	3600	5723
0.17 m	20972	3087	4907
0.25 m	19153	2819	4482
Salt			
Reference	20211	121	878
0.17 m	32645	196	1418
0.25 m	41418	249	1800
Brackish			
Reference	93815	6905	12759
0.17 m	84879	6247	11544
0.25 m	79748	5869	10846

Table 8 Western Shore: Summary of estimated wetland area, denitrification, and nitrogen burial values for the Western Shore Basin, Maryland based upon reference, 0.17, and 0.25 meter SLR projections by 2025.

Western Shore Basin			
Scenario	**Area (ha)**	**Denitrification (x 10^6 g N yr^{-1})**	**N Burial (x 10^6 g N yr^{-1})**
Tidal Fresh			
Reference	917	135	214
0.17 m	905	133	212
0.25 m	903	133	211
Salt			
Reference	442	3	19
0.17 m	770	5	33
0.25 m	1794	11	78
Brackish			
Reference	6324	465	860
0.17 m	6196	456	843
0.25 m	5392	397	733

Table 9 Susquehanna: Summary of estimated wetland area, denitrification, and nitrogen burial values for the Susquehanna River Basin, Maryland based upon reference, 0.17, and 0.25 meter SLR projections by 2025.

Susquehanna River Basin			
Scenario	**Area (ha)**	**Denitrification (x 10^6 g N yr^{-1})**	**N Burial (x 10^6 g N yr^{-1})**
Tidal Fresh			
Reference	19.3	2.8	4.5
0.17 m	20.7	3.0	4.8
0.25 m	20.7	3.0	4.8
Brackish			
0.17 m	0.36	0.03	0.05
0.25 m	0.36	0.03	0.05

Table 10 Patuxent: Summary of estimated wetland area, denitrification, and nitrogen burial values for the Patuxent River Basin, Maryland based upon reference, 0.17, and 0.25 meter SLR projections by 2025.

Patuxent River Basin			
Scenario	**Area (ha)**	**Denitrification (x 10^6 g N yr^{-1})**	**N Burial (x 10^6 g N yr^{-1})**
Tidal Fresh			
Reference	1189	175	278
0.17 m	1173	173	274
0.25 m	1155	170	270
Salt			
Reference	773	5	34
0.17 m	732	4	32
0.25 m	751	5	33
Brackish			
Reference	3305	243	450
0.17 m	3312	244	450
0.25 m	3256	240	443

Table 11 Potomac: Summary of estimated wetland area, denitrification, and nitrogen burial values for the Potomac River Basin, Maryland based upon reference, 0.17, and 0.25 meter SLR projections by 2025.

Potomac River Basin			
Scenario	**Area (ha)**	**Denitrification (x 10^6 g N yr^{-1})**	**N Burial (x 10^6 g N yr^{-1})**
Tidal Fresh			
Reference	1178	173	276
0.17 m	1088	160	255
0.25 m	1049	154	246
Salt			
Reference	1277	8	55
0.17 m	1383	8	60
0.25 m	1644	10	71
Brackish			
Reference	3456	254	470
0.17 m	3346	246	455
0.25 m	2939	216	400

Table 12 Subtidal Literature Review**:** Summary of literature review subtidal denitrification and nitrogen burial rates. Units were converted for ease of comparison.

Subtidal Denitrification ($g\ N\ m^{-2}\ yr^{-1}$)	Subtidal Burial ($g\ N\ m^{-2}\ yr^{-1}$)	Literature Source
4.3	7.6	Boynton et al. 2008
3.4	4.6	Nixon et al. 1996
4.9	n/a	Greene 2005

Table 13 Subtidal Estimates: Summary of Chesapeake Bay subtidal nitrogen removal estimates for 0.69 m SLR scenario by 2050. Literature source corresponding to the rate used for each estimate is also included.

Subtidal Denitrification ($g\ N\ m^{-2}\ yr^{-1}$)	Subtidal Burial ($g\ N\ m^{-2}\ yr^{-1}$)	Literature Source
227872	398135	Boynton et al. 2008
182089	243033	Nixon et al. 1996
260425	n/a	Greene 2005

REFERENCES

Anten, N.P.R., Casado-Garcia, R., and Nagashima, H. 2005. Effects of Mechanical Stress and Plant Density on Mechanical Characteristics, Growth, and Lifetime Reproduction of Tobacco Plants. *The American Naturalist*, 166, 650-660.

Baldwin, A.H. 2013. Nitrogen and Phosphorus Differentially Affect Annual and Perennial Plants in Tidal Freshwater and Oligohaline Wetlands. *Estuaries and Coasts*, 36: 547-558.

Baldwin, A.H., McKee, K.L., and Mendelssohn, I.A. 1996. The Influence of Vegetation, Salinity, and Inundation on Seed Banks of Oligohaline Coastal Marshes. *American Journal of Botany*, 83: 470-479.

Baldwin, A.H., Eganotovich, M.S., and Clarke, E. 2001. Hydrologic change and vegetation of tidal freshwater marshes: field, greenhouse, and seed-bank experiments. *Wetlands*, 21: 519-531.

Baldwin, A.H., Kangas, P.J., Megonigal, J.P., Perry, M.C., and Whigham, D.F. 2012. Coastal wetlands of Chesapeake Bay (Chapter 3). In D.P. Batzer and A.H. Baldwin [ed.], Wetland Habitats of North America: Ecology and Conservation Concerns. University of California Press.

Barbier, E.B., Hacker, S.D., Kennedy, C., Koch, E.W., Stier, A.C., and Silliman, B.R. 2011. The value of estuarine and coastal ecosystem services. *Ecological Monographs*, 81: 169-193.

Barbosa, S.M. and Silva, M.E. 2009. Low-frequency sea-level change in Chesapeake Bay: Changing seasonality and long-term trends. *Estuarine, Coastal and Shelf Science*, 83: 30-38.

Boesch, D.F., L.P. Atkinson, W.C. Boicourt, J.D. Boon, D.R. Cahoon, R.A. Dalrymple, T. Ezer, B.P. Horton, Z.P. Johnson, R.E. Kopp, M. Li, R.H. Moss, A. Parris, C.K. Sommerfield. 2013. Updating Maryland's Sea-level Rise Projections. Special Report of the Scientific and Technical Working Group to the Maryland Climate Change Commission, 22 pp. University of Maryland Center for Environmental Science, Cambridge, MD.

Boumans, R., Ceroni, M., Burdick, D., Cahoon, D., and Swarth, C. 2002. Sediment Elevation Dynamics in Tidal Marshes: Functional Assessment of Accretionary Biofilters. CICEET Final Report for the period 8/15/1999 through 8/15/2002. University of Vermont, Gund Institute for Ecological Economics.

Boynton, W.R., Hagy, J.D., Cornwell, J.C., Kemp, W.M., Greene, S.M., Owens, M.S., Baker, J.E., and Larsen, R.K. 2008. Nutrient Budgets and Management Actions in the Patuxent River Estuary, Maryland. *Estuaries and Coasts*, 31:623-651.

Calvert County. 2013. Draft Calvert County Phase II Watershed Implementation Plan: 2-Year Milestone Report**.** http://www.mde.state.md.us/programs/Water/TMDL/TMDLImplementation/Pages/MD_Milestone_Goals_2012-2013.aspx

CBF. 2012. www.cbf.org

Church, J.A. and White, N.J. 2006. A 20th Century Acceleration in Global Sea-Level Rise. *Geophysical Research Letters*, 33: 1-4.

Clough, J.S. and Park, R.A. 2008. SLAMM 5.0.2. Technical Documentation.

Costanza, R., R. d'Arge, R. de Groot, S. Farber, M. Grasso, B. Hannon, K. Limburg, S. Naeem, R.V. O'Neill, J. Paruelo, R. G. Raskin, P. Sutton, and van den Belt, M. 1997. The value of the world's ecosystem services and natural capital. *Nature*, 387: 253-260.

Craft, C., Clough, J., Ehman, J., Joye, S., Park, R., Pennings, S., Guo, H. and Machmuller, M. 2009. Forecasting the Effects of Accelerated Sea-Level Rise on Tidal Marsh Ecosystem Services. *Frontiers in Ecology and the Environment*, 7: 73-78.

Data Basin. 2013. Conservation Biology Institute. http://databasin.org/ Site accessed February 2013.

EO. 2009. Executive Order 13508: Chesapeake Bay Protection and Restoration. Federal Register Vol 74, No. 93.

ESRI. 2010. http://www.esri.com/

Fagherazzi, S., Kirwan, M.L., Mudd, S.M., Guntenspergen, G.R., Temmerman, S., D'Alpaos, A., van de Koppel, J., Rybczyk, J.M., Reyes, E., Craft, C., and Clough, J. 2012. Numerical Models of Salt Marsh Evolution: Ecological, Geomorphic, and Climatic Factors. *Reviews of Geophysics*, 50: 1-28

Fox, J. and Weisberg, S. 2011. An {R} Companion to Applied Regression, Second Edition. Thousand Oaks CA: Sage. URL: http://socserv.socsci.mcmaster.ca/jfox/Books/Companion

Glick, P., Clough, J., and Nunley, B. 2008. Sea-Level Rise and Coastal Habitats in the Chesapeake Bay Region: Technical Report. National Wildlife Federation.

Greene, S.E. 2005. Nutrient Removal by Tidal Fresh and Oligohaline Marshes in a Chesapeake Bay Tributary. Thesis. University of Maryland, College Park, Maryland.

Gross, J. and Ligges, U. 2012. Nortest: Tests for Normality. R package version 1.0-2. http://CRAN.R-project.org/package=nortest

Hagy, J.D., Boynton, W.R., Keefe, C.W., and Wood, K.V. 2004. Hypoxia in Chesapeake Bay, 1950-2001: Long-Term Change in Relation to Nutrient Loading and River Flow. *Estuaries*, 27: 634-658.

Hansson, L-A., Bronmark, C., Nilsson, P.A., and Abjornsson, K. 2005. Conflicting demands on wetland ecosystem services: nutrient retention, biodiversity or both? *Freshwater Biology*, 50: 705-714.

Harley, C.D.G and Bertness, M.D. 1996. Structural Interdependence: An Ecological Consequence of Morphological Responses to Crowding in Marsh Plants. *Functional Ecology*, 10, 654-661.

Hayhoe, K., Wake, C.P., Huntington, T.G., Luo, L., Schwartz, M.D., Sheffield, J., Wood, E., Anderson, B., Bradbury, J., DeGaetano, A., Troy, T.J., and Wolfe, D. 2007. Past and future changes in climate and hydrological indicators in the US Northeast. *Climate Dynamics*, 28:381-407.

Hilton, T.W., Naffan, R.G., Zhong, L., and Li, M., 2008. Is there a signal sea-level rise in Chesapeake Bay salinity? *Journal of Geophysical Research*, 113, doi: 10.1029/2007JC004247.

Hothorn, T., Bretz, F., and Westfall, P. 2008. Simultaneous Inference in General Parametric Models. *Biometrical Journal* 50, 346--363.

Hussein, A.H. and Rabenhorst, M.C. 2002. Modeling of Nitrogen Sequestration in Coastal Marsh Soils. *Soil Sci. Soc. Am. J*., 66: 324-330.

IPCC, 2007: Summary for Policymakers. In: Climate Change 2007: The Physical Science Basis. Contribution of Working Group I to the Fourth Assessment Report of the Intergovernmental Panel on Climate Change [Solomon, S., D. Qin, M. Manning, Z. Chen, M. Marquis, K.B. Avery, M.Tignor and H.L. Miller (eds.)]. Cambridge University Press, Cambridge, United Kingdom and New York, NY, USA.

Kearney, M.S., Grace, R.E., and Stevenson, J.C**.** 1988. Marsh Loss in Nanticoke Estuary, Chesapeake Bay. *Geographical Review*, 78: 205-220.

Kearney, M.S., Rogers, A.S., Townsend, J.R.R.G., Rizzo, E., Stutzer, D., Stevenson, J.C., and Sundberg, K.L. 2002. Landsat imagery shows decline of coastal marshes in Chesapeake and Delaware Bays. *EOS*, 3: 173-178.

Kellogg, M.L., Cornwell, J.C., Owens, M.S., Paynter, K.T. 2013. Denitrification and nutrient assimilation on a restored oyster reef. *Marine Ecology Progress Series*, 480: 1-19.

Kemp, W.M., Sampou, P., Caffrey, J. and Mayer, M. 1990. Ammonium recycling versus denitrification in Chesapeake Bay sediments. *Limnology and Oceanography*, 35: 1545-1563.

Kemp, W.M., Boynton, W.R., Adolf, J.E., Boesch, D.F., Boicourt, W.C., Brush, G., Cornwell, J.C., Fisher, T.R., Glibert, P.M., Hagy, J.D., Harding, L.W., Houde, E.D., Kimmel, D.G., Miller, W.D., Newell, R.I.E., Roman, M.R., Smith, E.M., and Stevenson, J.C. 2005. Eutrophication of Chesapeake Bay: historical trends and ecological interactions. *Marine Ecology Progress Series*, 303: 1-29

Kemp, W.M. 2006. Monie Bay NERR Site Literature Review and Synthesis: Final Report. NOAA Chesapeake Bay NERR-MD

Kirwan, M. and Temmerman, S. 2009. Coastal marsh response to historical and future sea-level acceleration. *Quarternary Science Reviews*, 28: 1801-1808.

Kirwan, M.L. and Guntenspergen, G.R. 2010a. Influence of tidal range on the stability of coastal marshland. *Journal of Geophysical Research*, 115.

Kirwan, M.L., Guntenspergen, G.R., D'Alpaos, A., Morris, J.T., Mudd, S.M. and Temmerman, S. 2010b. Limits on the adaptability of coastal marshes to rising sea level. *Geophysical Research Letters*, 37.

Kirwan, M.L. and Guntenspergen, G.R. 2012. Feedbacks between inundation, root production, and shoot growth in a rapidly submerging brackish marsh. *Journal of Ecology*, 100: 764-770.

Kirwan, M.L., Langley, J.A., Guntenspergen, G.R., and Megonigal, J.P. 2012. The impact of sea level rise on organic matter decay rates in Chesapeake Bay brackish tidal marshes. *Biogeosciences Discussions*, 9: 14689-14708.

Koop-Jakobsen, K. and Giblin, A.E. 2010. The effect of increased nitrate loading on nitrate reduction via denitrification and DNRA in salt marsh sediments. *Limnology and Oceanography*, 55: 789-802

Langley, J. A., Mozdzer, T.J., Shepard, K.A., Hagerty, S.B., and Megonigal, J.P. 2013. Tidal marsh plant responses to elevated CO2, nitrogen fertilization, and sea level rise. *Global Change Biolog*, doi: 10.1111/gcb.12147.

Leonard, L.A., Hine, A.C., and Luther, M.E. 1995a. Surficial sediment transport and deposition processes in a *Juncus roemerianus* marsh. *Journal of Coastal Research* 11: 322-336.

Leonard, L.A., Hine, A.C., and Luther, M.E. 1995b. Flow Hydrodynamics in Tidal Marsh Canopies. *Limnology and Oceanography* 40: 1474-1484.

Lightbody, A.F. and Nepf, H.M. 2006. Prediction of velocity profiles and longitudinal dispersion in emergent salt marsh vegetation. *Limnol. Oceanogr.*, 51: 218-228.

Lippson, A.J. and Lippson, R.L. 2006. Life in the Chesapeake Bay, 3rd Ed. The John Hopkins University Press. Baltimore.

Lopez, F. and Garcia, M. 1998. Open-channel flow through simulated vegetation: Suspended sediment transport modeling. *Water Resources Res*., 34: 2341-2352.

MDE. 2012. Final Maryland Phase II Watershed Implementation Plan for the Chesapeake Bay TMDL. http://www.mde.state.md.us

Merrill, J.Z. and J.C. Cornwell. 2000. The role of oligohaline marshes in estuarine nutrient cycling, p. 425-441. In M.P. Weinstein and D.A. Kreeger [ed.], Concepts and Controversies in Tidal Marsh Ecology. Kluwer Academic Publishers.

Miller, K.G., Kopp, R.E., Horton, B.P., Browning, J.V., and Kemp, A.C. 2013. A geological perspective on sea-level rise and its impacts along the U.S. mid-Atlantic coast. *Earth's Future,* doi:10.1002/2013EF000135.

Morris, J.T. 1991. Effects of Nitrogen Loading on Wetland Ecosystems with Particular Reference to Atmospheric Deposition. *Annual Review of Ecology and Systematics*, 22: 257-279.

Morris, J.T., Sundareshwar, P.V., Nietch, C.T., Kjerfve, B., and Cahoon, D.R. 2002. Responses of Coastal Wetlands to Rising Sea Level. *Ecology*, 83: 2869-2877.

Morris, J.T. 2004, Marsh Organ Construction. Retrieved 7/16/2011 from sitemason.vanderbilt.edu/files/dDGms0/marshorganassembly.pdf.

Morris, J.T. 2007a. Ecological engineering in intertidal saltmarshes. *Hydrobiologia*, 577: 161-168.

Morris, J.T. 2007b Estimating Net Primary Production of Salt Marsh Macrophytes. In: Principles and Standards for Measuring Primary Production. Fahey, T.J. and Knapp, A.K. (Eds.). Oxford University Press, New York, NY; pgs 106-119.

Mudd, S.M., Howell, S.M. and Morris, J.T. 2009. Impact of dynamic feedbacks between sedimentation, sea level rise, and biomass production on near-surface marsh stratigraphy and carbon accumulation. *Estaurine Coastal and Shelf Science*, doi:10.1016/j.ecss.2009.01.028.

Najjar, R.G., Walker, H.A., Anderson, P.J., Barron, E.J., Bord, R.J., Gibson, J.R., Kennedy, V.S., Knight, C.G., Megonigal, J.P., O'Connor, R.E., Polsky, C.D., Psuty, N.P., Richards, B.A., Sorenson, L.G., Steele, E.M., and Swanson, R.S. 2000. The potential impacts of climate change on the mid-Atlantic coastal region. *Climate Research*, 14: 219-233.

Najjar, R.G., Pyke, C.R., Adams, M.B., Breitburg, D., Hershner, C. Kemp, M., Howarth, R., Mulholland, M.R., Paolisso, M., Secor, D., Sellner, K., Wardrop, D., and Wood, R. 2010. Potential climate-change impacts on the Chesapeake Bay. *Estuarine, Coastal, and Shelf Science*, 86: 1-20.

Niklas, K.J. 1991. Bending Stiffness of Cylindrical Plant Organs with a 'Core-Rind' Construction: Evidence from Juncus effusus leaves. *American Journal of Botany*, 78: 561-568.

Niklas, K.J. 1992. Plant Biomechanics: An Engineering Approach to Plant Form and Function. The University of Chicago Press.

Niklas, K.J. 1994. Interspecific Allometries of Critical Buckling Height and Actual Plant Height. *American Journal of Botany*, 81: 1275-1279.

Niklas, K.J. 1995. Plant Height and the Properties of Some Herbaceous Stems. *Annals of Botany* 75:133-142

Nixon, S.W., Ammerman, J.W., Atkinson, L.D, Berounsky, V.M., Billen, G., Boicourt, W.C., Boynton, W.R., Church, T.M., Ditoro, D.M., Elmgren, R., Garber, J.H., Giblin, A.E., Jahnke, R.A., Owens, N.J.D., Pilson, M.E.Q., and Seitzinger. 1996. The Fate of Nitrogen and Phosphorus at the Land-Sea Margin of the North Atlantic Ocean. *Biogeochemistry*, 35: 141-180.

NOAA Tides and Currents. 2014. Station ID: 8851910, Reedy Point, DE. Website: http://tidesandcurrents.noaa.gov

Odum, W.E., Smith III, T.J., Hoover, J.K., and McIvor, C.C. 1984. The Ecology of Tidal Freshwater Marshes of the United States East Coast: A Community Profile. U.S. Fish and Wildlife Service. FWS/OBS-83/17.

Odum, W.E. 1988. Comparative Ecology of Tidal Freshwater and Salt Marshes. *Annual Review of Ecology and Systematics*, 19: 147-176.

Park, R.A., Trehan, M.S., Mausel, P.W., and Howe, R.C. 1989. The effects of sea level rise on U.S. coastal wetlands. Cooperative Agreement CR814578-01, final report U.S. Environmental Protection Agency, Washington DC.

Pasternack, G.B. and Brush, G.S. 2001. Seasonal Variations in Sedimentation and Organic Content in Five Plant Associations on a Chesapeake Bay Tidal Freshwater Delta. *Estuarine, Coastal and Shelf Science*: 53: 93-106.

Puijalon, S., Léna, Jean-Paul, N.R., Champagne, J.R., and Bornette, G. 2007. Phenotypic plasticity in response to mechanical stress: hydrodynamic performance and fitness of four aquatic plant species. *New Phytologist*, 177: 907-917.

R Core Team. 2013. R: A language and environment for statistical computing. R Foundation for Statistical Computing, Vienna, Austria. ISBN 3-900051-07-0, URL http://www.R-project.org/

Rahmstorf, S. 2007. A Semi-Empirical Approach to Projecting Future Sea-Level Rise. *Science*, 315: 368-370.

Reed, D.J. 1995. The response of coastal marshes to sea-level rise: survival or submergence? *Earth Surface Processes and Landforms*, 20: 39-48.

Reed, D.J., Bishara, D.A., Cahoon, D.R., Donnelly, J., Kearney, M., Kolker, A.S., Leonard, L.L., Orson, R.A. and Stevenson, J.C. 2008. Site-specific scenarios for wetlands accretion as sea level rises in the Mid-Atlantic region. Section 2.1 in: Background documents supporting climate change science program synthesis and assessment product 4.1. Eds: Titus, J.G. and Strange, E.M. EPA 430R07004. U.S. EPA, Washington, DC.

Rich, J.J., Dale, O.R., Song, B., Ward B.B. 2008. Anaerobic ammonium oxidation (Anammox) in Chesapeake Bay sediments. *Microbial Ecology*, 55: 311-320.

Sallenger, Jr., A.H., Doran, K.S., Howd, P.A. 2012. Hotspot of accelerated sea-level rise on the Atlantic coast of North America. *Nature Climate Change* 2: 884-888.

Seitzinger, S.P. 1988. Denitrification in freshwater and coastal marine ecosystems: Ecological and geochemical significance. *Limnology and Oceanography*, 33: 702-724.

Seitzinger, S.P., Gardner, W.S., and Spratt, A.K. 1991. The effect of salinity on ammonium sorption in aquatic sediments: Implications for benthic nutrient cycling. *Estuaries*, 14: 167-174.

SLAMM. 2008. http://www.warrenpinnacle.com/prof/SLAMM/

Stevenson, J.C., Kearney, M.S., and Koch, E.W. 2002. Impacts of Sea Level Rise on Tidal Wetlands and Shallow Water Habitats: A Case Study from Chesapeake Bay. *American Fisheries Society Symposium*, 32: 23-36.

Temmerman, S., Bouma, T.J., Govers, G., Wang, Z.B., De Vries, M.B., and Herman, P.M.J. 2005. Impact of vegetation on flow routing and sedimentation patterns: Three-dimensional modeling for a tidal marsh. *J. Geophys. Research*, F04019. doi: 10.0129/2005JF000301.

Thomas, C.R. and Christian, R.R. 2001. Comparison of nitrogen cycling in salt marsh zones related to sea-level rise. *Marine Ecology Progress Series*, 221: 1-16.

Titus, J.G. (Coordinating Lead Author), Anderson, K.E., Cahoon, D.R., Gesch, D.B., Gill, S.K., Gutierrez, B.T., Thieler, E.R., and Williams, S.J. (Lead Authors). 2009. Coastal Sensitivity to Sea-Level Rise: A Focus on the Mid-Atlantic Region. A report by the U.S. Climate Change Science Program and the Subcommittee on Global Change Research. U.S. Environmental Protection Agency, Washington D.C., USA, 320 pp.

USEPA. 2010. Chesapeake Bay Total Maximum Daily Load for Nitrogen, Phosphorus and Sediment. U.S. Environmental Protection Agency Region 3 Report.

Ward, L.G., Kearney, M.S., and Stevenson, J.C. 1998. Variations in sedimentary environments and accretionary patterns in estuarine marshes undergoing rapid submergence, Chesapeake Bay. *Marine Geology*, 151: 111-134.

Warren, R.S. and Niering, W.A. 1993. Vegetation Change on a Northeast Tidal Marsh: Interaction of Sea-Level Rise and Marsh Accretion. *Ecology*, 74: 96-103.

Weston, N.B., Dixon, R.E., Joye, S.B. 2006. Ramifications of increased salinity in tidal freshwater sediments: Geochemistry and microbial pathways of organic matter mineralization. *Journal of Geophysical Research*, 111: 1-14.

Weston, N.B., Vile, M.A., Neubauer, S.C., and Velinsky, D.J. 2011. Accelerated microbial organic matter mineralization following salt-water intrusion into tidal freshwater marsh soils. *Biogeochemistry*, 102: 135-151.

Whigham, D. and Simpson, R. 1977. Growth, Mortality, and Biomass Partitioning in Freshwater Tidal Wetland Populations of Wild Rice (*Zizania aquatica var aquatica*). *Bulletin of the Torrey Botanical Club*, 104: 347-351.

White, D.S. and Howes, B.L. 1994. Long-term ^{15}N-nitrogen retention in the vegetated sediments of a New England salt marsh. *Limnology and Oceanography*, 39: 1878-1892.

Williams, M.R., Fisher, T.R., Boynton, W.R. Cerco, C.F., Kemp, M.W., Eshleman, K.N., Kim, S-C., Hood, R.R., Fiscus, D.A., and Radcliffe, G.R. 2006. An integrated modeling system for management of the Patuxent River estuary and basin, Maryland, USA. *International Journal of Remote Sensing*, 27:3705-3726.

Yang, S.L. 1998. The role of *Scirpus* marsh in attenuation of hydrodynamics and retention of fine sediment in the Yangtze Estuary. *Estuarine Coastal and Shelf Science*, 47: 227-233